PRESSURE DROP AND PHASE FRACTION IN OIL-WATER-AIR VERTICAL PIPE FLOW

by

ARTHUR R. SHEAN

S.B., United States Military Academy

(1969)

SUBMITTED IN PARTIAL FULFILLMENT
OF THE REQUIREMENTS FOR THE
DEGREE OF

MASTER OF SCIENCE

at the

MASSACHUSETTS INSTITUTE OF TECHNOLOGY

(7 May 1976)

gnature of Author .. ..
Department of Mechanical Engineering, May 7, 1976

rtified by .....
Thesis Supervisor

cepted by .....
Chairman, Department Committee on Graduate Students

PRESSURE DROP AND PHASE FRACTION IN OIL-WATER-AIR VERTICAL PIPE FLOW

by

ARTHUR R. SHEAN

Submitted to the Department of Mechanical Engineering on May 7, 1976 in partial fulfillment of the requirements for the Degree of Master of Science.

ABSTRACT

The upward flow of oil-water-air and oil-water mixtures in a .75 inch I.D. tube is investigated. Flow pattern, volume fraction, and pressure loss data is presented for mixture velocities from 4 to 20 ft/sec and oil in liquid volume fraction from 0 to 1.0.

The drift flux method of Zuber and Findley is successfully extended from two phase flow to three phase flow in order to predict the air void while a new correlation method is presented to estimate the In Situ oil phase volume fraction. In addition, the oil-water flow regime-map of Govier is extended to three phase flow in order to predict the transition between liquid flow regimes.

Finally several friction pressure loss prediction methods from two phase flow are modified to three phase flow and compared to actual data. As a result, a scheme of several methods is recommended for use in preparing three phase flow pressure loss estimates.

Thesis Supervisor: Peter Griffith
Title: Professor of Mechanical Engineering

ACKNOWLEDGEMENTS

I would like to express my appreciation to my wife for her patience, understanding and endurance, without which this work may never have been completed. Further I thank my parents who originally implanted the seed of my academic curiosity which Professor Peter Griffith guided during this work. Finally, I thank the technicians of the Engineering Projects Laboratory for their assistance in my experimental effort.

TABLE OF CONTENTS

	Page
TITLE PAGE	1
ABSTRACT	2
ACKNOWLEDGEMENTS	3
TABLE OF CONTENTS	4
LIST OF TABLES	6
LIST OF FIGURES	7
LIST OF SYMBOLS	10
CHAPTER I: INTRODUCTION	12
CHAPTER II: TEST APPARATUS	16
CHAPTER III: EXPERIMENTAL PROCEDURE	20
CHAPTER IV: SUMMARY OF DATA	23
CHAPTER V: RESULTS AND DISCUSSION	24
CHAPTER VI: CONCLUSIONS	77
CHAPTER VII: SUGGESTIONS FOR FURTHER WORK	79
REFERENCES	80
APPENDICES	
A. FOREMAN AND WOODS DATA	82
B. GOVIER'S DATA AND ANALYSIS OF PROPERTY EFFECTS ON TWO PHASE FRICTION PRESSURE LOSS	84
C. FLOW REGIME VISUAL OBSERVATIONS	96
D. DERIVATION OF QUASI - ANNULAR FLOW PRESSURE DROP METHOD	101

	Page
E. FLUID CHARACTERISTICS	105
F. SAMPLE CALCULATIONS	106
G. DATA LISTING	110

LIST OF TABLES

	Page
PREDICTED Fo VERSUS ACTUAL Fo: TWO PHASE FLOW	45
PREDICTED Fo VERSUS ACTUAL Fo: THREE PHASE FLOW	66
PRESSURE LOSS METHOD COMPARISON: THREE PHASE FLOW	68
NUJOL AND WATER CONTACT ANGLES	75
FOREMAN AND WOODS VOID DATA	82
FOREMAN AND WOODS DATA REDUCTION	83
GOVIER TWO PHASE DATA	85

LIST OF FIGURES

	Page
DIAGRAM OF THE APPARATUS	17
INSETS TO DIAGRAM OF THE APPARATUS	18
CONTACT ANGLE TANK	22
THREE PHASE VOID FRACTION ZUBER-FINDLEY PLOTS	26
THREE PHASE VOID FRACTION VELOCITY AND CONCENTRATION DISTRIBUTION PLOTS	31
THREE PHASE VOID FRACTION OIL - WATER VELOCITY DIFFERENCE	33
PICTURE OF AIR SLUG	34
TEMPERATURE EFFECT ON THE OIL-WATER VELOCITY DIFFERENCE Fo .5	35
TEMPERATURE EFFECT ON THE OIL - WATER VELOCITY DIFFERENCE Fo .8	36
INSITU OIL PHASE VOLUME FRACTION VERSUS Fo: TWO PHASE FLOW	38
OIL-WATER VELOCITY DIFFERENCE: TWO PHASE FLOW	39
TOTAL PRESSURE LOSS: TWO PHASE FLOW	41
FRICTION PRESSURE LOSS: TWO PHASE FLOW	42
GOVIER'S FLOW REGIME MAP	43
GOVIER'S 20.1 cp OIL TOTAL PRESSURE DROP: TWO PHASE FLOW	44
ZUBER-FINDLEY PLOTS VARYING Fo: THREE PHASE FLOW	48
CONSOLIDATED ZUBER-FINDLEY PLOTS: THREE PHASE FLOW	49
AIR VOID, PREDICTED VERSUS ACTUAL: FOREMAN AND WOODS	52
AIR VOID, PREDICTED VERSUS ACTUAL: THREE PHASE VOID DATA	53

	Page
IN SITU OIL PHASE VOLUME FRACTION/IN SITU FLUID PHASE VOLUME FRACTION VERSUS F_o	54
INSITU OIL PHASE VOLUME FRACTION, PREDICTED VERSUS ACTUAL: THREE PHASE VOID DATA	56
INSITU OIL PHASE VOLUME FRACTION, PREDICTED VERSUS ACTUAL: FOREMAN AND WOODS	57
OIL-WATER VELOCITY DIFFERENCE VERSUS MIXTURE VELOCITY	59
OIL-WATER VELOCITY DIFFERENCE VERSUS Fo	60
FRICTION PRESSURE LOSS VERSUS Fo: THREE PHASE FLOW	61
TOTAL PRESSURE LOSS VERSUS Fo: THREE PHASE FLOW	62
IDEALIZED SLUG FLOW	64
GRAVITY PRESSURE LOSS, PREDICTED AND ACTUAL: 12 FT/SEC	71
FRICTION PRESSURE LOSS, PREDICTED AND ACTUAL: 12 FT/SEC	72
CONTACT ANGLE DEFINITION	74
TOTAL PRESSURE LOSS, PREDICTED AND ACTUAL: 12 FT/SEC	75
FRICTION PRESSURE LOSS, DIAMETER VARIED, 2 FT/SEC: TWO PHASE FLOW	89
FRICTION PRESSURE LOSS, DIAMETER VARIED, 3 FT/SEC: TWO PHASE FLOW	90
FRICTION PRESSURE LOSS, VISCOSITY VARIED, 2 FT/SEC: TWO PHASE FLOW	91
FRICTION PRESSURE LOSS, VISCOSITY VARIED, 3 FT/SEC: TWO PHASE FLOW	92
FRICTION PRESSURE LOSS, MIXTURE VELOCITY VARIED, 150 cp: TWO PHASE FLOW	93

	Page
FRICTION PRESSURE LOSS, MIXTURE VELOCITY VARIED, 20.1 cp: TWO PHASE FLOW	94
FRICTION PRESSURE LOSS, MIXTURE VELOCITY VARIED, .936 cp: TWO PHASE FLOW	95
TYPICAL FRICTION PRESSURE LOSS CURVE	97
FLOW REGIME DIAGRAM	98
FLOW REGIME DIAGRAM	98
FLOW REGIME DIAGRAM	100
FLOW REGIME DIAGRAM	100
SLUG - ANNULAR FLOW DIAGRAM	101
LINEAR INTERPOLATION OF THE FACTOR K	104

NOMENCLATURE

SYMBOL	Definition
A	Cross sectional area of tube
D	Diameter of tube
F	Introduced fluid in liquid volometric fraction
	i.e. $F_o = Qo/_{Qf} = \beta o/_{\beta f}$
f	Friction factor
G	Mass flux
go	Gravitational constant
j	Average volumetric flux density, i.e. = Q/A
L	Length of tube
p	Pressure
Δp	Pressure difference
Q	Volumetric flow rate introduced into the tube
R	Radius of tube
Re	Reynolds number
S	Phase velocity difference
V	Specific Volume
V_w	Superficial velocity ($Q_w/A.$)
v	Velocity
$\tilde{v}$	Weighted mean velocity, i.e. $\bar{v}_a = Q_a/\alpha_a A.$
W	Mass flow rate
x	Mass gas quality

Symbol	Definition
α	Insitu volumetric phase fraction
β	Volumetric flow concentration introduced into the tube, i.e. $\beta o = {}^{Q}o/Q_t$
ρ	Density
μ	Viscosity
Θ	Contact angle
ϕ^2	Friction multiplier

Subscripts

a	Air
b	Bubble
c	Critical
f	Fluid
F	Friction
g	Gas
m	Mixture
o	Oil
t	Total
w	Water
ρ	Density

CHAPTER I

INTRODUCTION

Three phase flows are being encountered in the petroleum industry more and more often. The emphasis on greater production has forced the exploitation of marginal oil wells, and forced the use of secondary recovery schemes. Two methods currently in use to achieve these goals are, oil field flooding and gas lift wells. Oil field flooding introduces water into the oil field in an effort to maintain natural liquid levels. The result is an oil-water mixture is taken out of the pipe. If, in addition, natural gas is present, which is not uncommon, a three phase flow appears in the well tubing. Gas lift wells on the other hand inject gas into the well to help lift the natural oil-water mixture to the surface. Again a three phase flow of oil, water and gas is encountered. Despite the frequency of appearance of the three phase flow, designers lack a complete knowledge of the flow, hence cannot properly design pipe sizes, production levels, pumping efforts, or optimal flow conditions. The major inadequacies are the inability to predict phase fractions, the density pressure losses, effective viscosities and friction pressure loss. Therefore, there is a need for an investigation of three phase flow.

The lack of knowledge on three phase flows stems mainly from the extremely limited number of published works on the subject. M. Rasin Tek[1] in 1961, Galyomov and Karpushin [2] in 1971 and Bacharov, Andriasov

and Sakharov [3] in 1972 have published papers on the subject three phase flows. Foreman and Woods [4] performed some work at M.I.T. and furnished an unpublished paper in 1975.

Conversely two phase flow, from which this work draws heavily has been intensely investigated. The works of Govier, Radford and Dunn [5], Govier, Sullivan and Wood [6], Zuber-Findley [7], Griffith and Wallis [8], Orkiszewski [9] and Singh and Griffith [10] in particular were used in this work. In addition, the correlations of Martinelli [11] and McAdams [11] were employed during comparison calculations.

M. Rasin Tek [1] in his work considered the two fluids as a single liquid with multiphase mixture properties. With this assumption he provided a correlation of oil well data which supplied satisfactory pressure loss predictions. His assumption, however, overlooked the various flow configurations encountered by the various phases. Hence, no insight into the true nature of the flows was gained from his work. The Russian researchers [2,3] examined the effects on the effective viscosity in horizontal pipes caused by the variation of liquid fraction, gas content, and turbulence of the flow. Their work did not provide a correlation, but did find that the three phase flows did vary significantly from two phase flows. Even more important they recorded the variation in effective viscosity of the fluid as a function of liquid fraction (this method is similar to the work of Govier on oil-water flows). Their works are significant in that they recognized all three

phases effect the nature of the flow. Foreman and Woods [4] continued the separated phase investigation by applying the work of Zuber and Findley to the gas phase of the flow. Their limited data indicated that the gas phase could be handled separately from the liquids. They, however, did not approach the question of pressure drop.

The approach of this current work is to attack the three phase flow first as a gas liquid two phase flow as suggested by Tek, then to examine the two fluids using a variation of the liquid fraction as suggested by the Russian investigators and Govier. In the two phase approximation the Zuber-Findley Drift Flux model will be applied as did Foreman and Woods.

To execute this approach, experimentation was conducted in a vertical .75" ID plexiglass tube using a mineral oil, water and air mixture system. The mineral oil was chosen because its density was less than that of water and its viscosity was much greater than water (see Appendix E) . These differences allowed for easier differentiation of the individual fluid effects on the flow. The separation was further enhanced by the fact the oil, because of its large viscosity, remained in laminar flow throughout the experiment. The experimentation was conducted in three parts: First three phase void fraction data was obtained to verify the Foreman-Woods conclusion that the gas could be treated by the drift Flux method; then two phase oil water data was obtained and combined with Goviers [6] data (Appendix B) to determine the

variation effects of various parameters on the flow characteristics, and finally three phase void and pressure drop data was obtained over a variety of mixture velocities to provide a correlation for the In Situ Oil Volume Phase Fraction and to check pressure drop predictions.

CHAPTER II

TEST APPARATUS

The three phase flow of mineral oil (Nujol), water and air was developed in a 282" by .75" ID vertical tube (Fig. 1). The oil and water were drawn by pumps from a separator tank (Inset C to Fig. 1) through flowrator tubes into the vertical tubes. The rates were adjusted by gate valves. The air flow was provided by a shop air system and was likewise metered by a flowrator and pressure gauge. The connection to the tube (Inset A to Fig. 1) started the air in the center of the vertical tube. All observations and measurements were taken approximately 200 L/D up the tube to allow for full developement of the flow.

The test section consisted of a piece of plexiglass tubing which was separated from the remaining vertical tube by a pair of quick acting valves. These valves were linked together and operated simultaneously. The section between the valves was 80.25" long. The plexiglass tubing had two purposes. First, the clear tubing allowed for visual observation. In some cases, especially in three phase flows, 35mm camera photographs were necessary to freeze the action for close observation. In order to differentiate between the fluids, red dye was added to the water. The Nujol although clear at rest, became milky white when worked. Both effects accentuated observation. The second purpose of the plexiglass was to measure the void and fluid fractions. When the quick acting valves were closed, the mixture settled out into

Fig. 1 Diagram of the Apparatus.

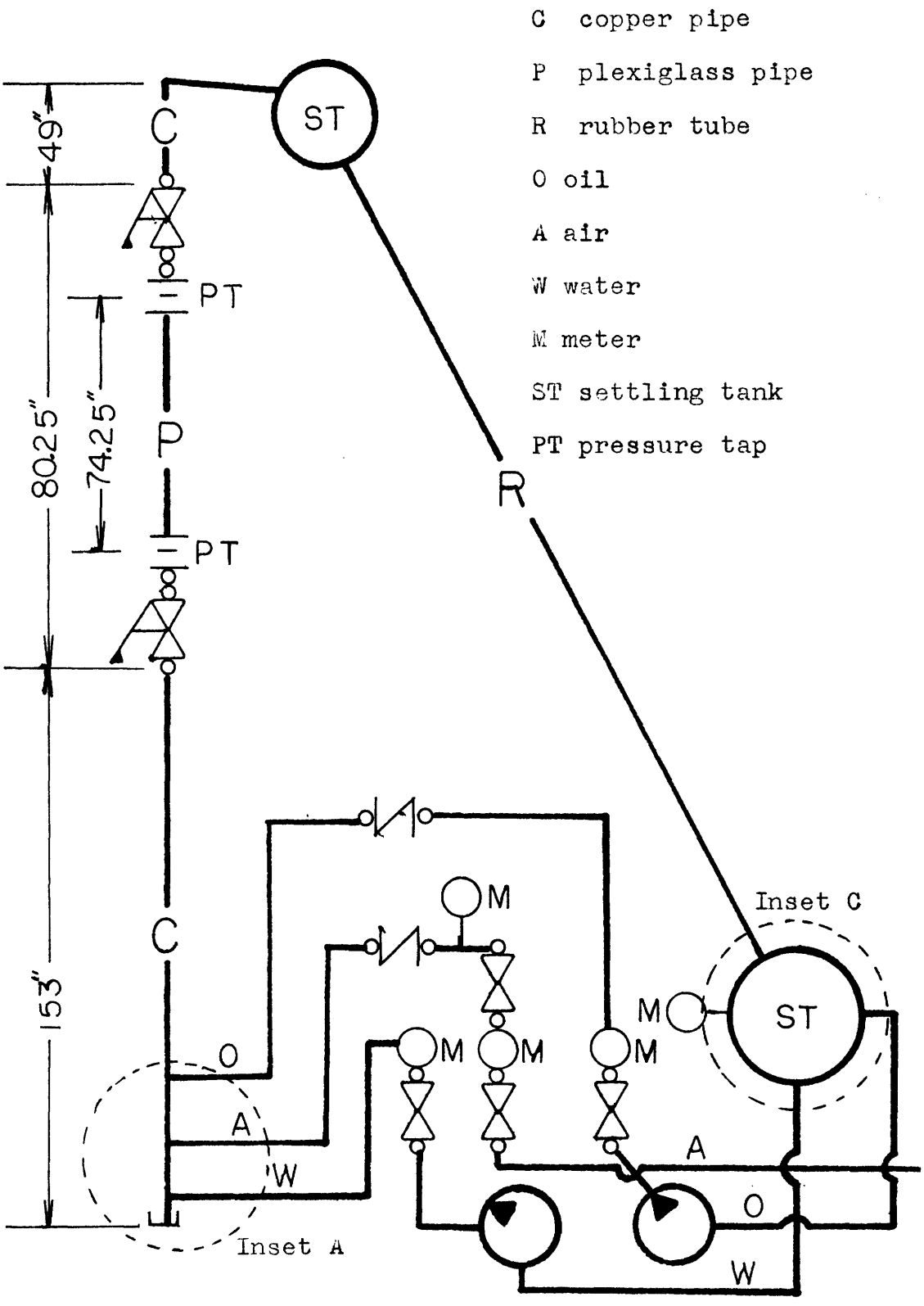

Fig. 2 Insets to Diagram of the Apparatus.

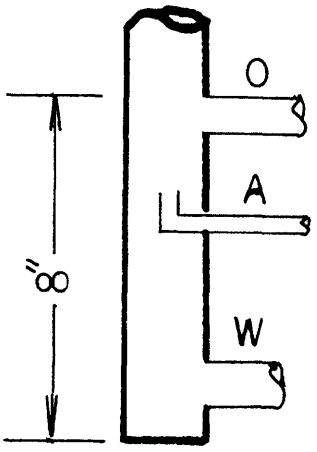

Inset A

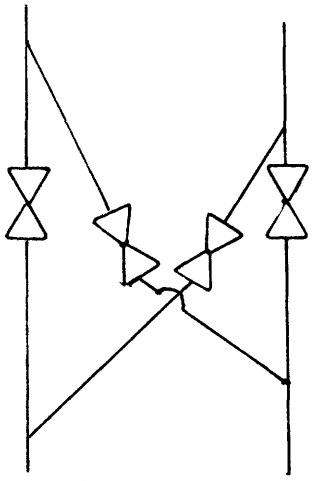

Inset B

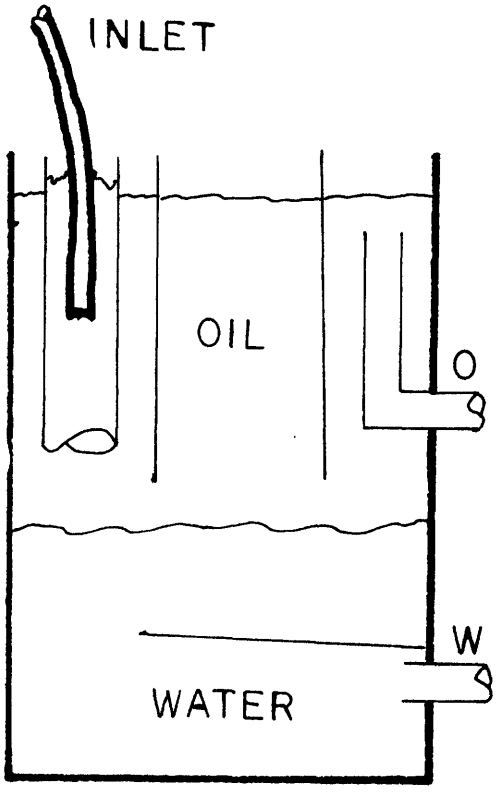

Inset C

its component parts. The volume averaged void and fluid fractions could then be measured. Also located between the quick closing valves were two pressure tapes 74.25 inches apart. These were used in measuring the pressure drop.

After departing the test section, the mixture traveled an additional 65 L/D up to an air separator and then back down to the fluid separator. The additional length beyond the test section was to avoid any end effects. A thermometer was inserted into the side of the fluid separator so that the temperature of the recycled fluids could be recorded.

In measuring the pressure drop across the test section, two sets of equipment were used. For the two phase Nujol and water data, the water filled pressure tubes were fed from the pressure taps to a differential pressure gauge which read in inches of water. A cross-over system (Inset B to Fig. 1) was needed because the water head was overtaken by friction losses under certain flow conditions causing negative meter readings. The pressure gauge system was sufficiently accurate because the pressure deviations across an oil bubble were relatively small. The three phase flow however had large pressure deviations over the air bubbles. Attempts to dampen out this effect fluidically were disappointing. Therefore, Statham pressure transducers and an R.C. circuit were utilized to dampen out the transient fluctuations in pressure. This system provided adequate average pressure data.

CHAPTER III

EXPERIMENTAL PROCEDURES

A. Three Phase Void Fraction Data:

During this test the void fraction was measured for a variety of oil in liquid volume fractions and varying mixture velocities. In a particular series of runs, the oil in fluid volume fraction was fixed and readings of the void were taken at 10% increments of the maximum air flow. The air variation provided the mixture velocity variation. In a particular run the specific procedure was as follows: The oil and water flow rates were calculated to produce the appropriate fluid volume fraction and be within the capacity of the apparatus. These flows were then established within the tube. The air flow was then adjusted to the appropriate increment of maximum flow. When the flow rates had stabilized, the air metering pressure, flow rates and separator tank temperature were read and recorded. Then the flow was visually observed and photographs, if appropriate, were taken. After observation the quick acting valves were closed and the mixture was allowed to separate. The void and fluid fractions were recorded using a ruler which was fastened to the tube supports. Each run was repeated at least three times and the data recorded. This repetition was essential because the inconsistency of the churn turbulent flow and the length of the slugs within the test section gave different results on any single run. This was found true in other tests which included air flow.

Normally the air flow was initiated at low volume rates and increased. With frequency of run, however, the separator tank temperature would rise due to friction loss and pump work. This temperature change affected the viscosity of both fluids. In order to avoid any data bias at the higher air flows, the progression was occasionally reversed. In later tests, each series of runs was completed prior to any repetition so that temperatures for a series would be more uniform.

B. Two Phase Liquid Flows:

During this test the total volume flow rate was held constant while the oil volume fraction was varied from zero to one. As before, the flows were calculated to provide the appropriate fraction and within the apparatus capacity. The flows were then introduced into the tube and allowed to stabilize. The flows, separator tank temperature, and pressure drop across the test section were recorded. The flow was then observed and the void data read and recorded as above. Various mixture velocities were obtained by varying the total volume flow rates. Again each run was repeated three times. Except as noted above, each series was completed prior to any repeats. This repetition was unnecessary in this test because the fluctuations were less without air flow.

C. Three Phase Pressure Loss and Void Tests:

In this test the fluid volume flow rate was held constant while the oil in liquid volume fraction was varied from zero to one. Air was introduced in varying amounts to obtain various mixture velocities.

Each series of runs was characterized by a different mixture velocity. The same procedure as the two phase oil water test above was utilized except air flow and metering pressure were recorded. Also the pressure at the top and bottom of the test section were recorded rather than the difference.

D. Contact Angle Measurements:

A glass fish tank was filled with red dye water and Nujol and allowed to settle. A flat plate of test material was introduced so that its midpoint was at the fluid interface. Observing the edge of the plate it was tilted until the fluid interface adjacent to the plate became parallel to the remainder of the interface (Fig. 3). At this point, the angle between the plate and interface was the contact angle for the fluids and material. A photograph was taken to record this angle. This measurement was repeated for several materials.

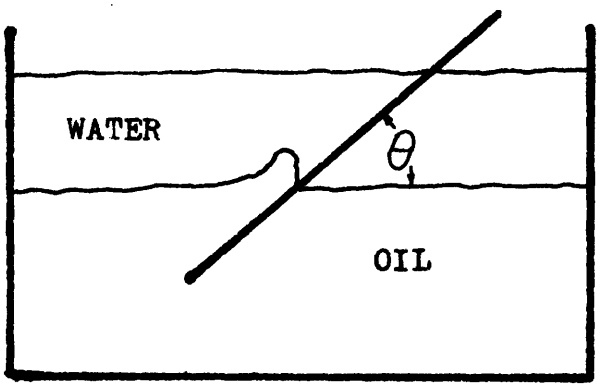

Figure 3

CHAPTER IV

See Appendix G: Data Listing

CHAPTER V

RESULTS AND DISCUSSION

A. Three Phase Void Fraction Test

Zuber and Findley predicted that in a two phase flow the gas velocity plotted as a straight line with the following equation:

$$\tilde{v}_a = C_o \tilde{v}_m + \tilde{v}_{aj} \tag{5.1}$$

where $\tilde{v}_{aj}$ is the bubble rise velocity. For turbulent slug flow in a vertical tube the suggested valves of Co varied between 1.0 and 1.5 while the $\tilde{v}_{aj}$ is of the order of .5 ft./sec.. All of the current tests were within this slug flow range and did indeed plot as straight lines. Figures 4a through 4e show the following quantities plotted versus the mixture velocity:

$$\tilde{v}_a = \frac{Qa}{\alpha_a A} \tag{5.2}$$

$$\tilde{v}_w = \frac{Q}{\alpha_w A} \tag{5.3}$$

$$\tilde{v}_o = \frac{Q}{\alpha_o A} \tag{5.4}$$

The Co for all air velocity curves ranged between 1.19 and 1.32 with $\tilde{v}_{aj}$ between .4 and .6 ft./sec.. The variation in Co showed no dependence on the oil in liquid volume fraction (Fo) or the velocity of the mixture or fluid components. Such close results indicate that the assumptions of

Tek and the conclusion of Foreman and Woods, that the air can be separately handled from the liquid, is reasonable. In addition, the methods of Zuber-Findley can be extended to three phase flow to perform this function.

Figure 4a through 4e show another interesting result. All the plots of $\tilde{v}_w$ and $\tilde{v}_o$, except for the Fo = .50 plot, cross. Likewise, the data of Foreman and Woods when similarly plotted show the same occurance. Zuber and Findley in their work ascribed a higher velocity to the air which was flowing in the center of the tube. This was based on assumed velocity and concentration profiles such as Fig. 5a. Fig. 7 illustrates this concentration profile. The fluid with higher concentration on the outside moved at a lower average velocity than that of the air at the center with a higher velocity profile. Similarly if the oil water concentration profile is divided as in Fig. 5b, then the average value of $\tilde{v}_o$ would be greater than $\tilde{v}_w$. If the two fluid concentration profiles are reversed, then the bulk of the oil would be on the outside of the tube where the velocity profile is the lowest. Therefore the average oil velocity would be lower. Conversly the bulk of the water would be more toward the center of the tube and the average water velocity would be higher. The result is a reversal of the oil water velocity difference. Comparison of observation with data verify this correspondence between the switching of position and velocity difference reversal. When the velocity reversal occurs, the fluid color changes from red to white indicating an increase in oil concentration next to the wall. A further

Figure 4a. Three Phase Void Fraction Zuber- Findley Plot.

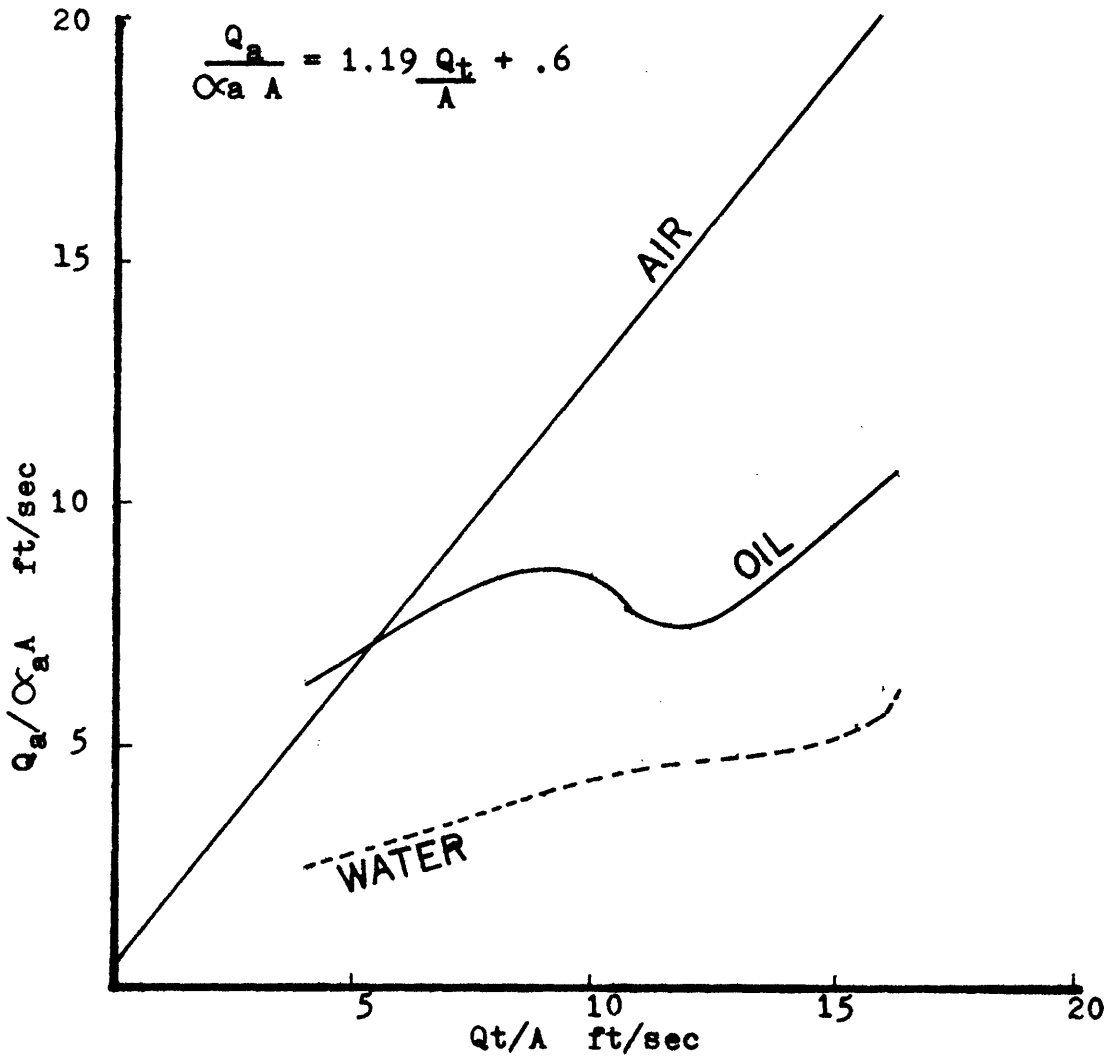

Figure 4b. Three Phase Void Fraction Zuber-Findley Plot.

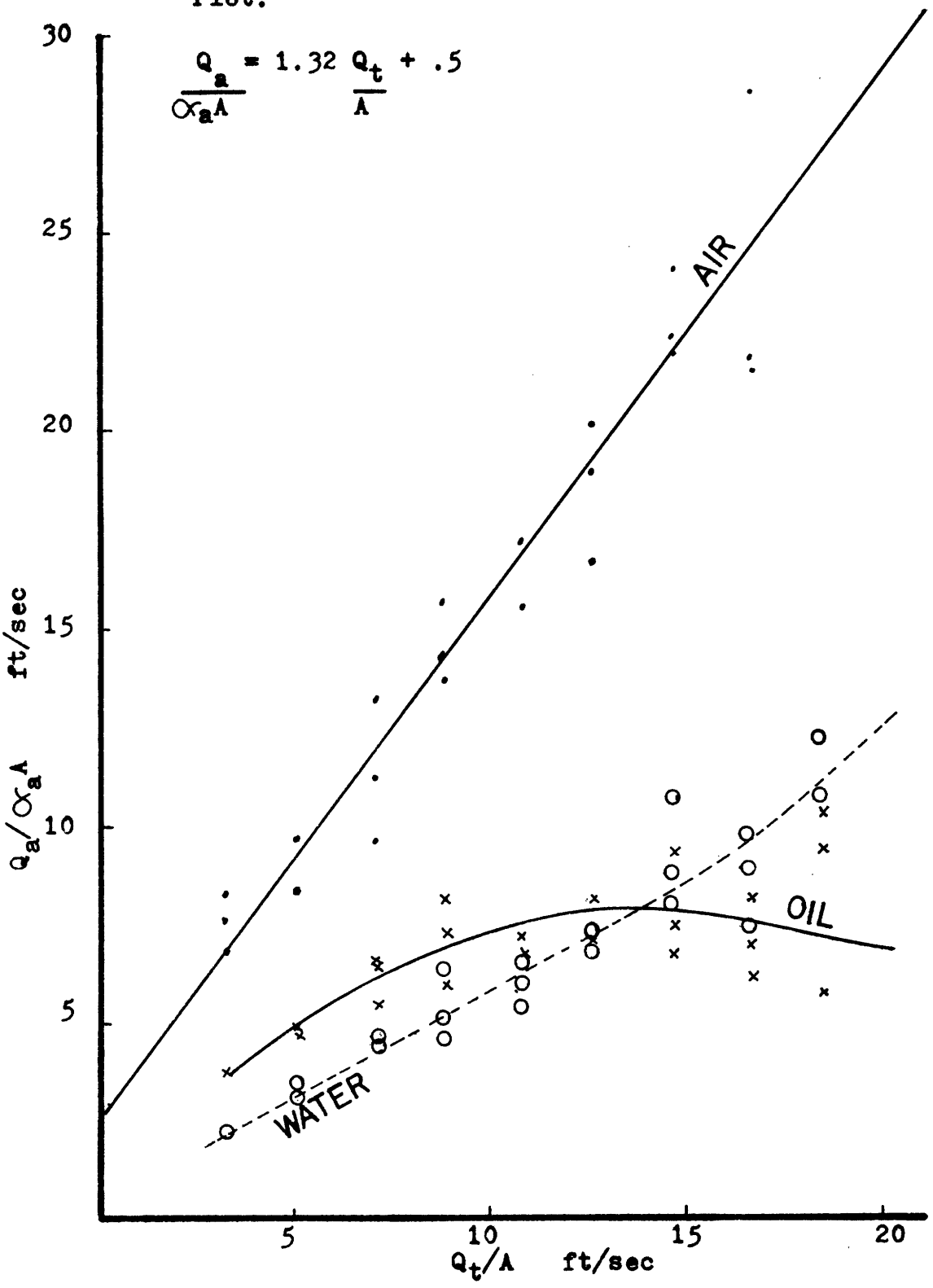

Figure 4c. Three Phase Void Fraction Zuber-Findley Plot.

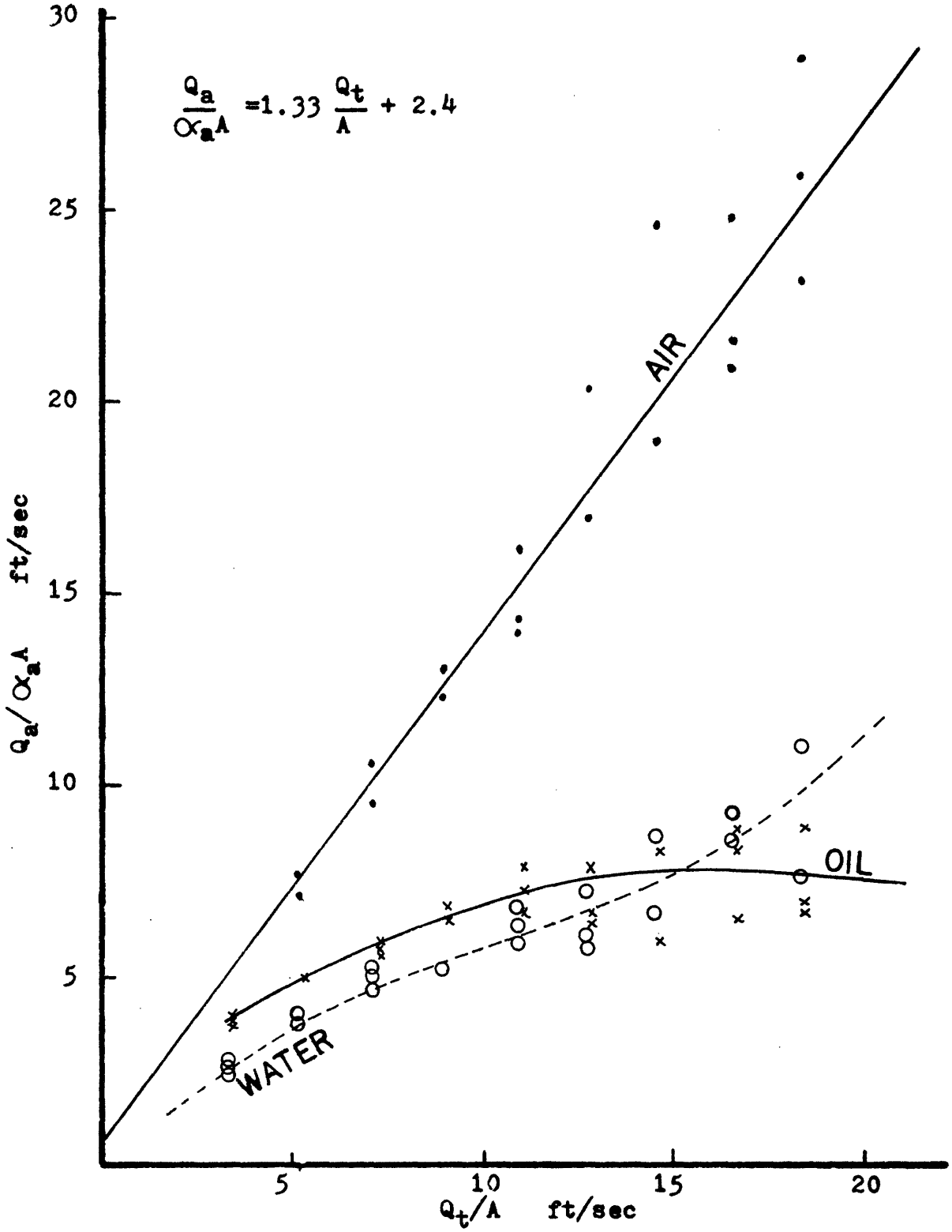

Figure 4d. Three Phase Void Fraction Zuber-Findley Plot.

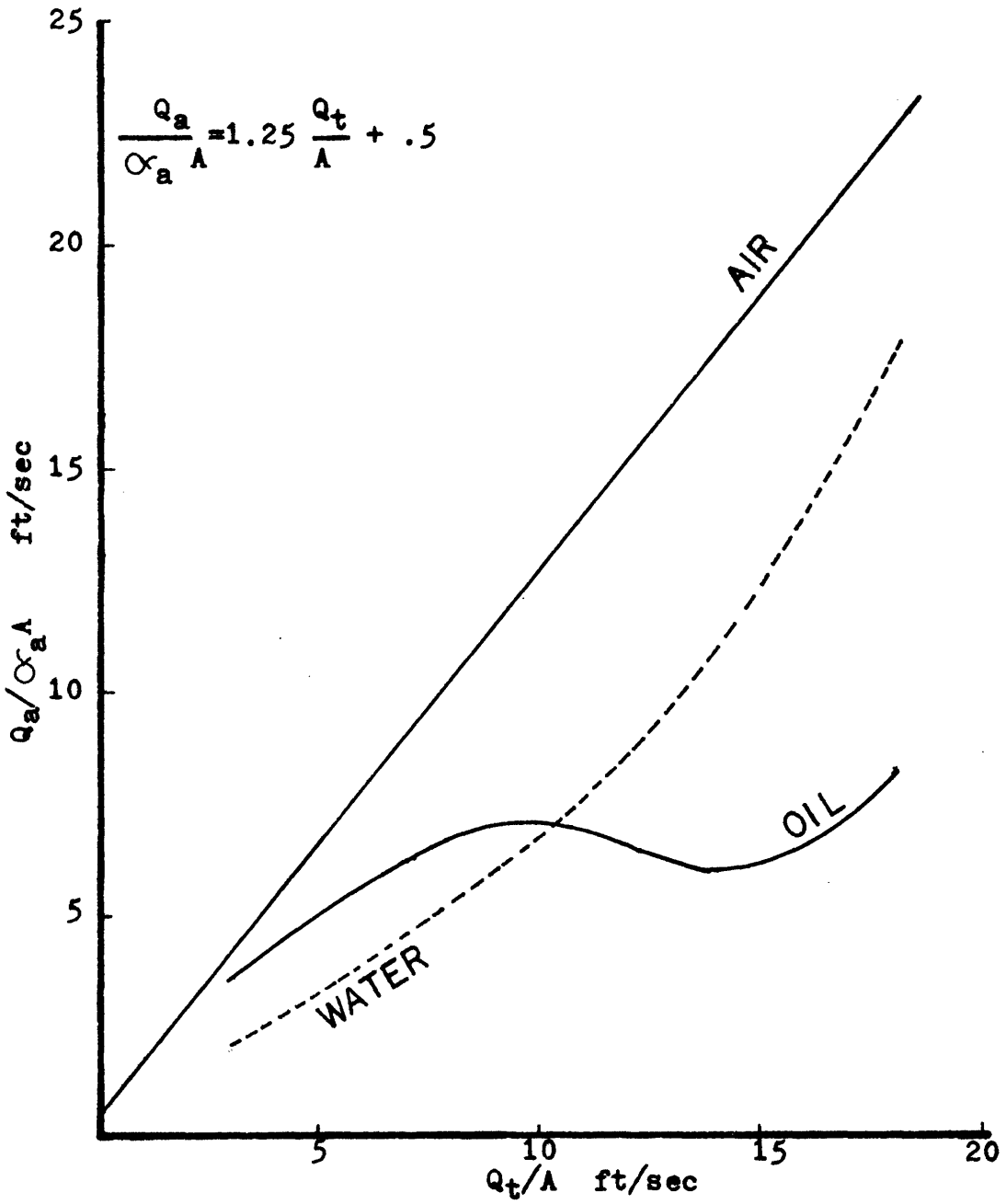

Figure 4e. Three Phase Void Fraction Zuber-Findley Plot.

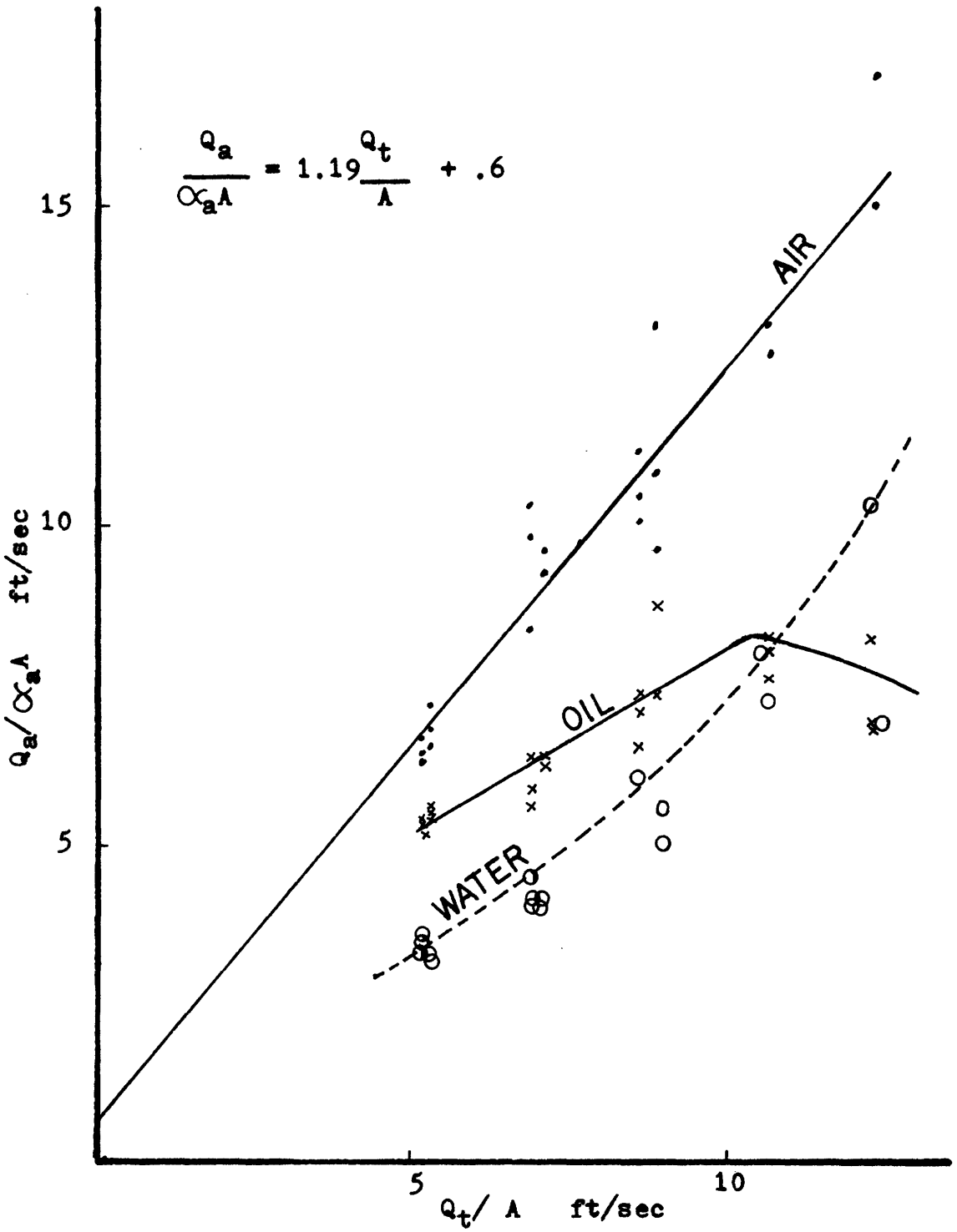

Figure 5. Three Phase Void Fraction Velocity and Concentration Distribution Plots.

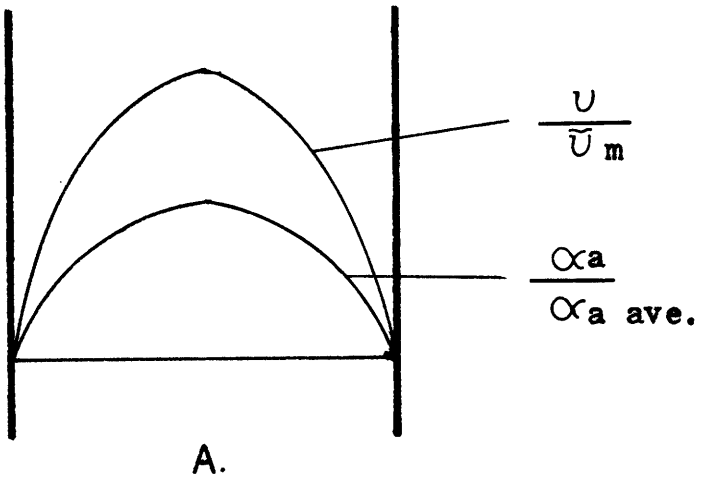

A.

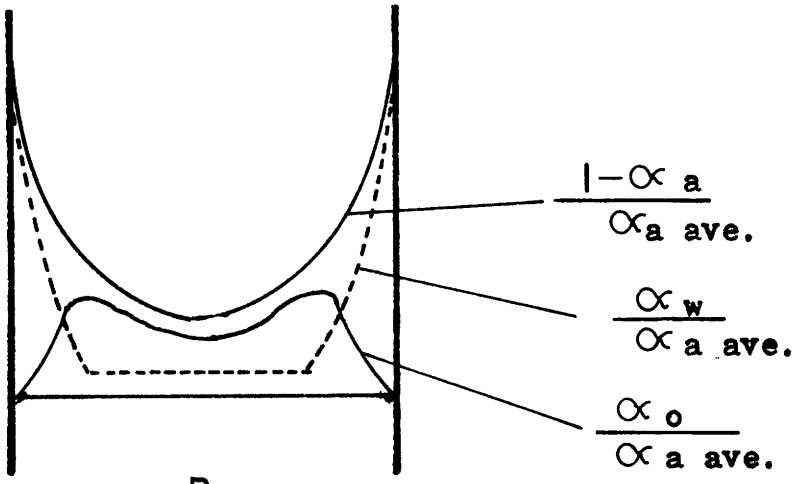

B.

FIG. 5.

demonstration of this switching can be seen in Figure 6, where the oil water velocity difference (Sow) is plotted against the mixture velocity. As the curves cross the zero line, the oil and water switch positions with relation to the wall. The location of the switching appears to be independent of the mixture velocity, however the .5 Fo curve indicates that the switch occurs only above a certain Fo. Later the boundry will be shown to be the Fo for the transition from oil bubbles in water to water bubbles in oil.

In addition to the oil water velocity change, a temperature effect was observed. During the experiment the temperature was not controlled but recorded. Figures 8 and 9 show the result of temperature deviations for Fo's of .5 and .8. A lower temperature indicated a higher velocity difference except at higher velocity were the difference reversed. A possible explanation is as follows: At lower velocities the flows are in the slug regime and the oil travels in bubbles within the water. If the bubbles were smaller, the distribution of oil would be better with a subsequent smaller Sow. Rohsenow and Choi [13] give an estimate of bubble diameter as:

$$D_b = C\Theta \frac{2g_o\sigma}{g\Delta\rho} \tag{5.5}$$

where C is a constant and Θ is the contact angle and a function of the surface tension. Although ρ and σ decrease with higher temperature, σ falls off more rapidly. Hence a higher temperature indicates a smaller bubble diameter with a lower expected velocity difference. At higher

Figure 6. Three Phase Void Fraction Oil- Water Velocity Difference.

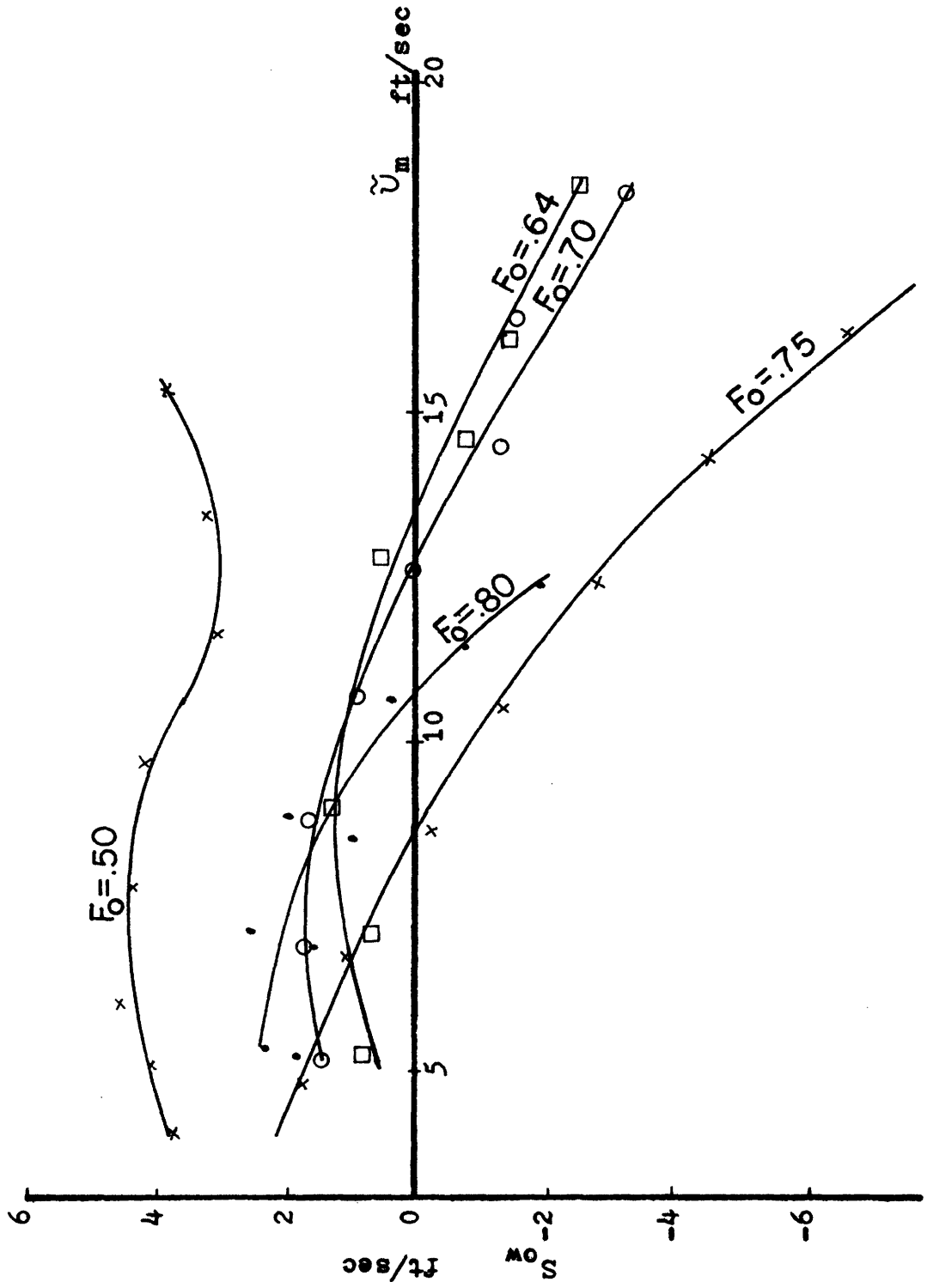

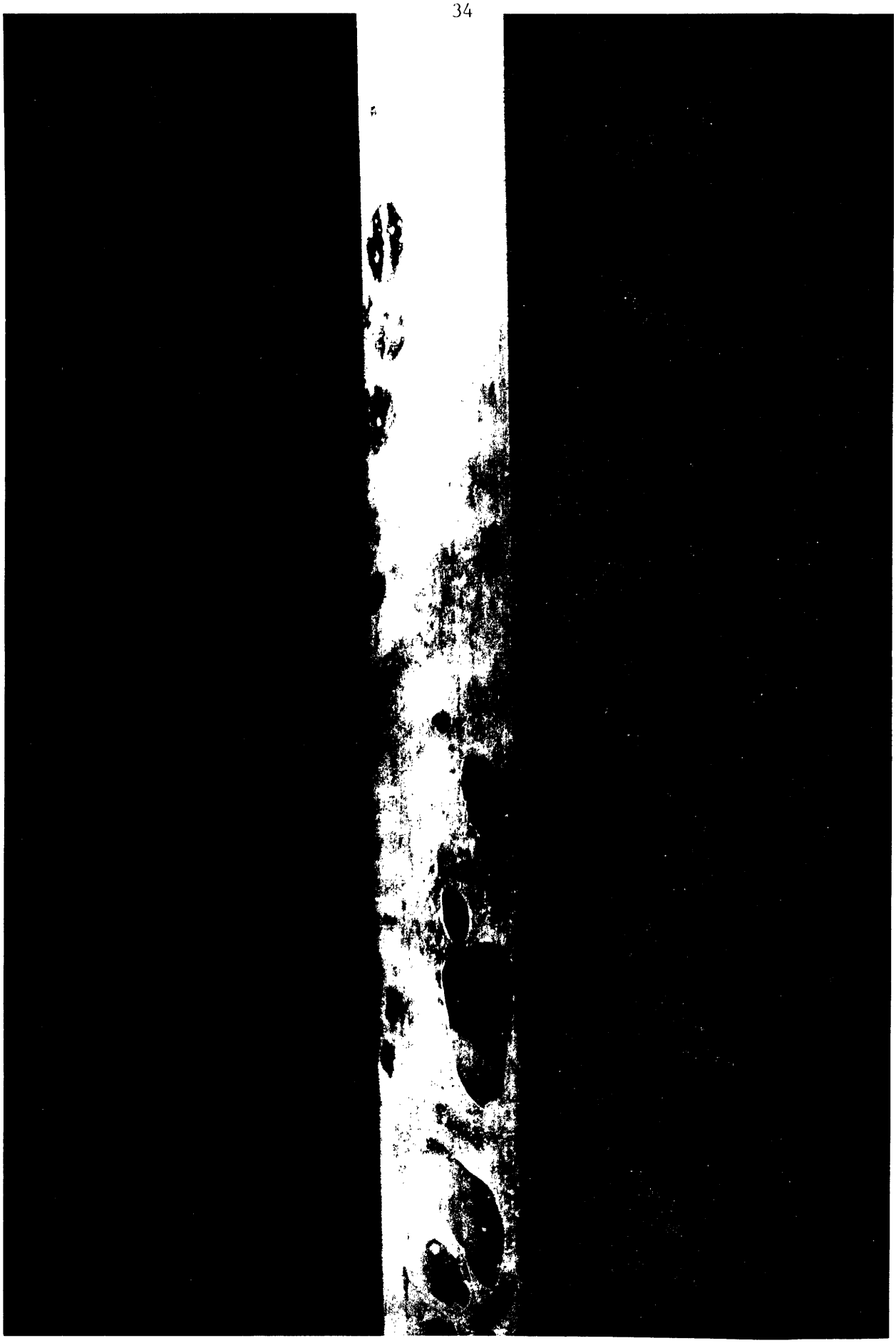

Fig 7

Figure 8. Temperature Effect on the Oil- Water Velocity Difference; $F_o = .5$

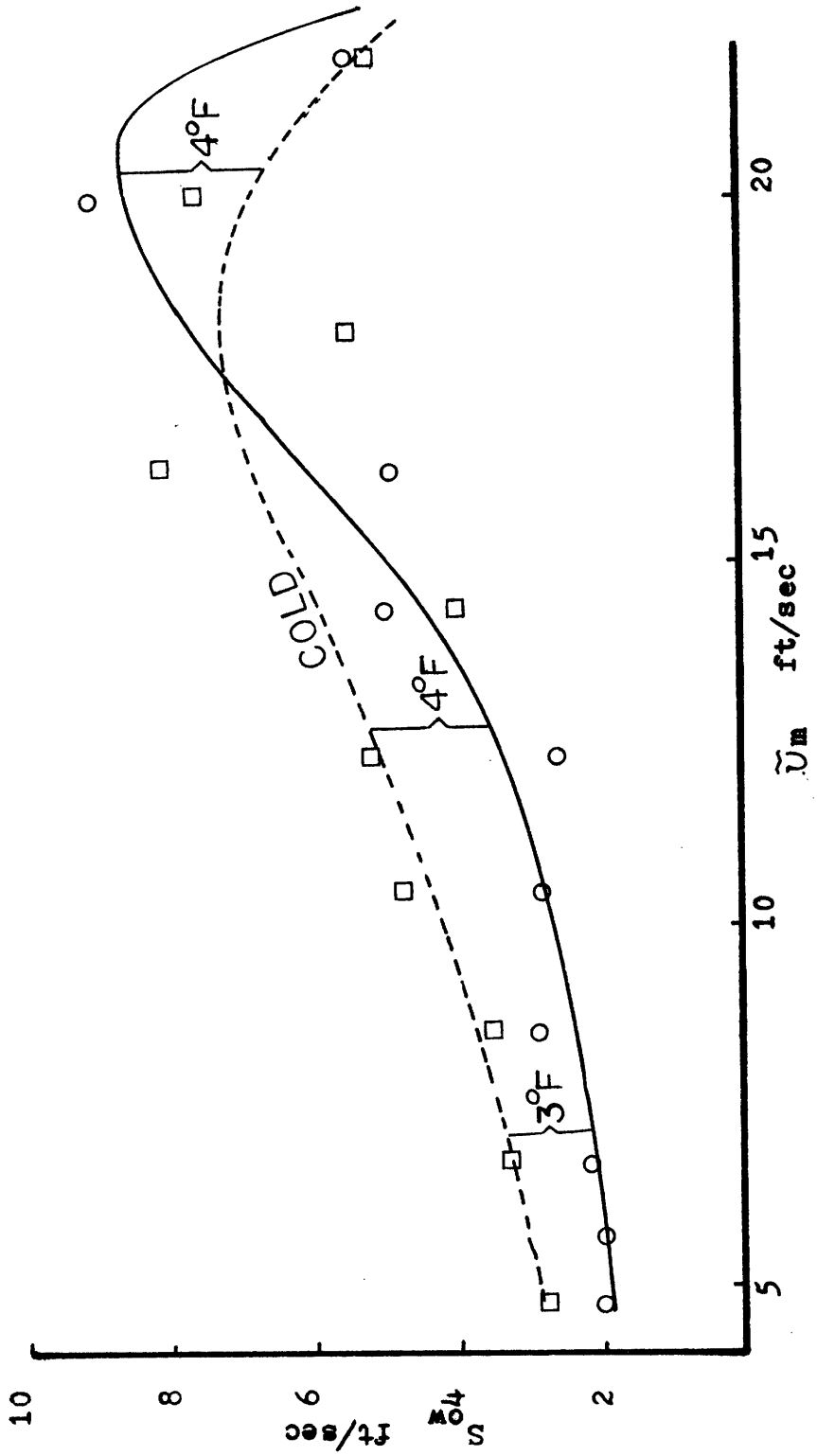

Figure 9. Temperature Effect on the Oil-Water Velocity Difference: F_o=.8.

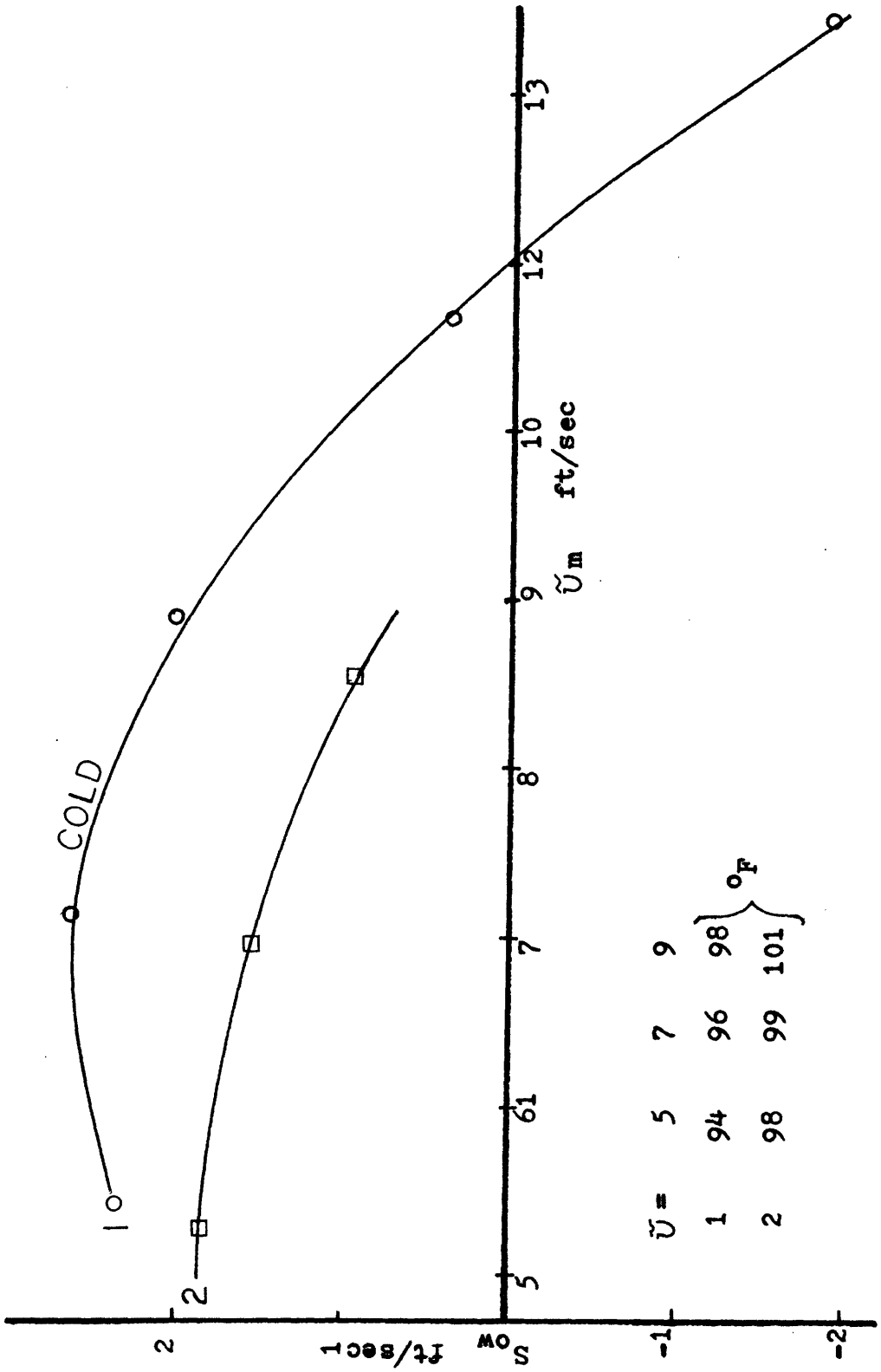

velocities the flow approaches an annular flow in which viscosities play a greater role. Viscosity again falls off with increasing temperature. Thus, lower temperature indicates a higher viscosity which retards the fluid flows reducing the Sow. In both cases illustrated, the temperature effect did not change the shape of the curves, just the relative locations. Also, the effect on the air data was minimal.

B. Two Phase Void Fraction and Pressure Drop Test

In the past, researchers have been successful in applying two phase information to three phase flow problems. For example, Zuber and Findley's approach worked well in part A while the Russian researchers employed the plotting technique of Govier[6]. Therefore, it seems logical to assume that two phase oil water information may be instrumental in separating the oil water portion of a three phase flow. This in fact appears to be true. The flow characteristics of the two phase flow turn out to be very similar to those of three phase flow and because of this, predictions of In Situ Phase Volume Fraction, critical oil in liquid volume fraction, and effective viscosity can be made from modified two phase flow information.

Figures 10 and 11 show the essential void fraction information of an oil-water mixture. The In Situ oil phase volume fraction and velocity difference show a marked crossover where the two liquids exchange places on the wall. During this test the switching became much more visible because the mixture velcoities were much lower than three phase flows.

Figure 10. In Situ Oil Phase Volume Fraction Versus F_o: Two Phase Flow.

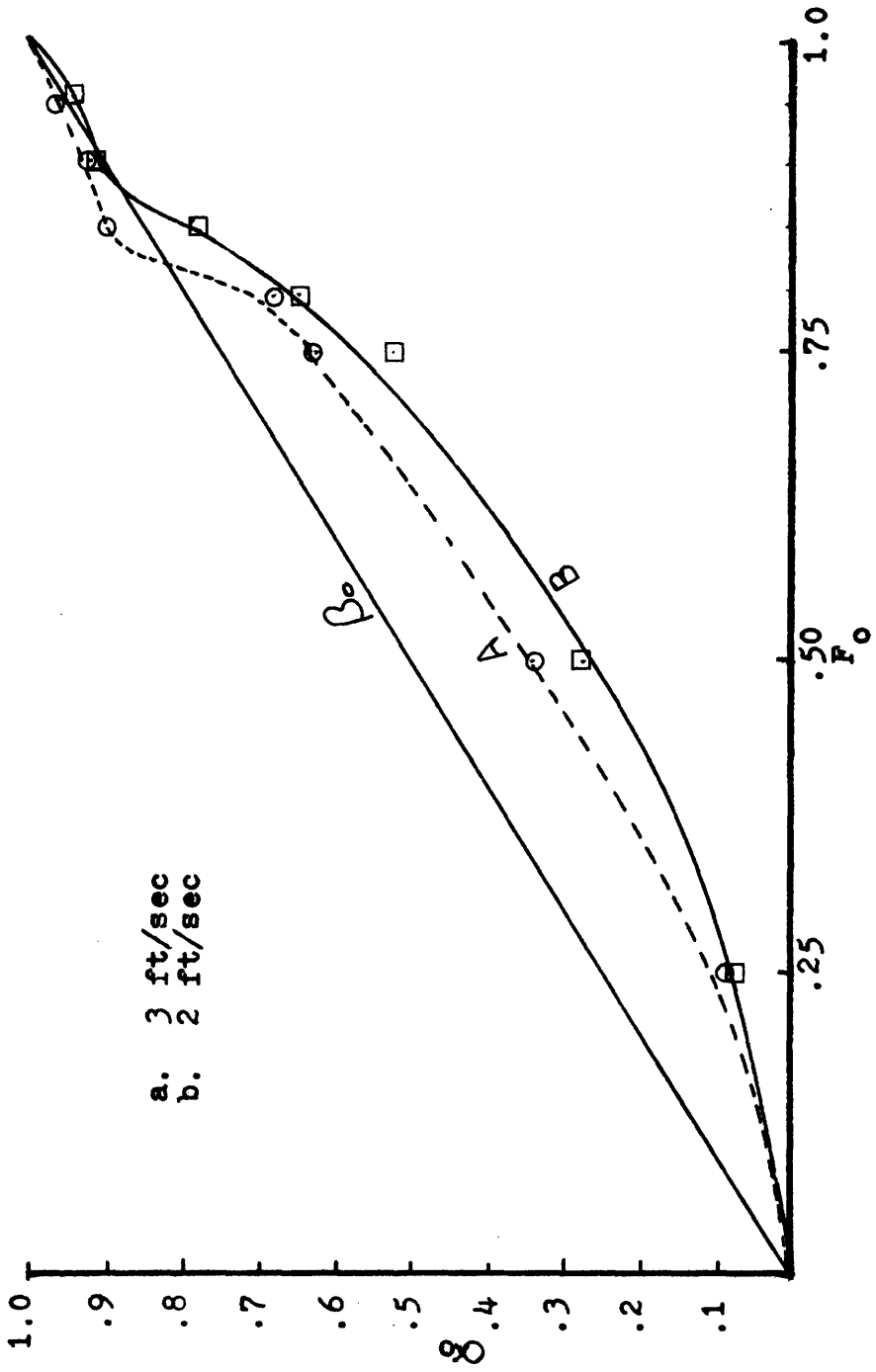

Figure 11. Oil-Water Velocity Difference: Two Phase Flow.

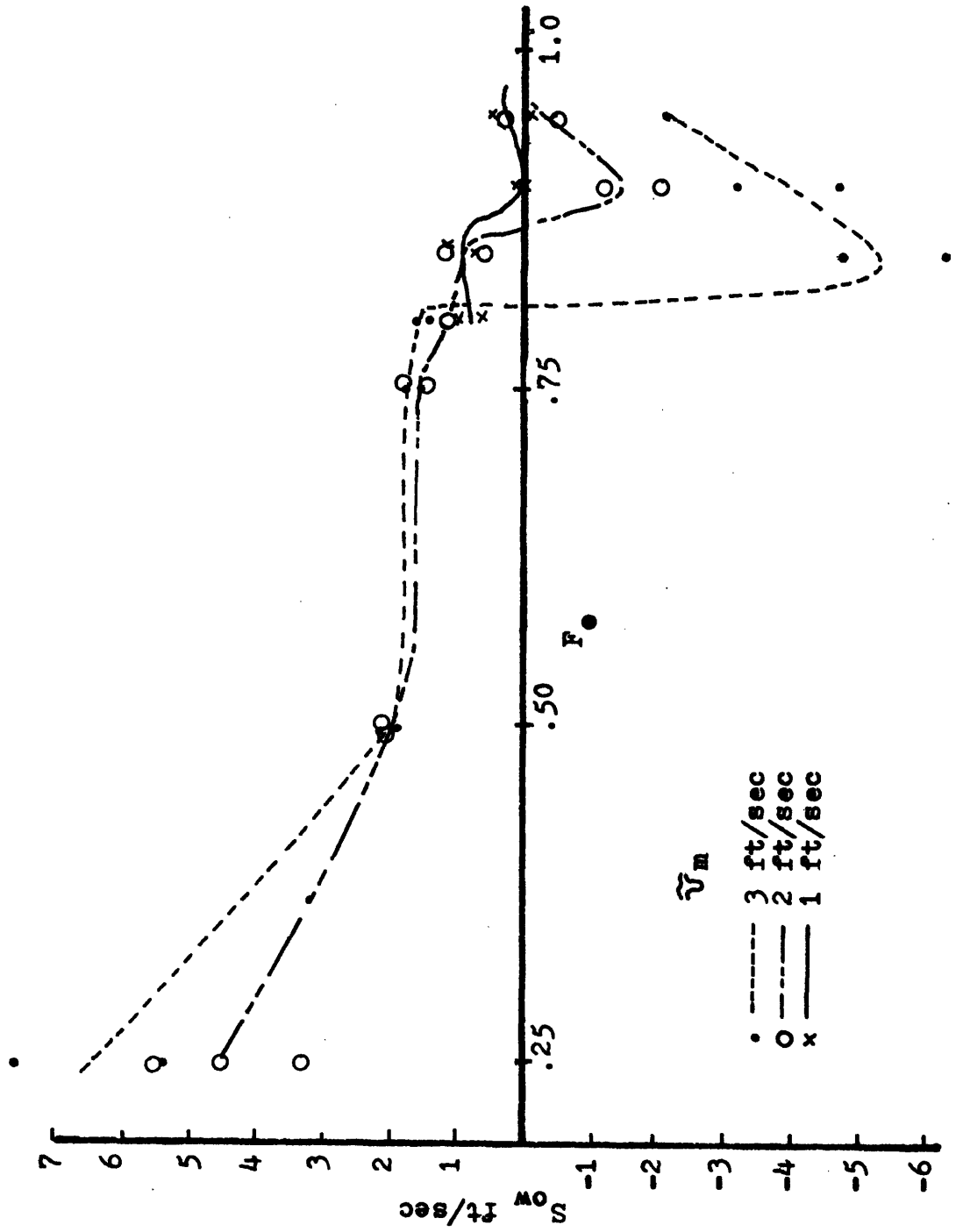

In both bases the switching appeared dependent upon the oil in liquid volume fraction. In Figure 10 the curves approach the straight homogeneous line (βo) with increasing mixture velocity. The two ft/sec curve appeared to be the limit from which α_o approached β_o. Also the void defect from that of the homogeneousline is in the fluid away from the wall, i.e. in oil when water is on the wall. This fact further reinforces our assumed velocity and concentration profile of Figure 5.

The examination of the pressure drop curves (figures 12 and 13) shows further consequences of the oil-water position switching. In both cases a very sharp jump in pressure occurs at an Fo corresponding to that where the fluids exchange places at the wall. Before and after the switching, the friction pressure curves are relatively constant at values close to that of the individual fluids flowing alone in the tube. The coupling of the levels and the identity of the fluid next to the wall suggests that the effective viscosity of the fluid mixture is that of the fluid flowing next to the wall. This is not unreasonable since most friction losses in a viscous fluid flow occur near the wall where the fluid is slowed down to match the no slip condition. Again the picture in Fig. 5b seems more plausible. Another observation from Figure 12 and 13 is that the total pressure loss curve has the same shape as the friction pressure curve alone. The only difference being the level. This indicates that the friction pressure loss causes the major deviation in the total pressure loss.

In order to clarify the dependence of the friction pressure loss on

Figure 12. Total Pressure Loss: Two Phase Flow.

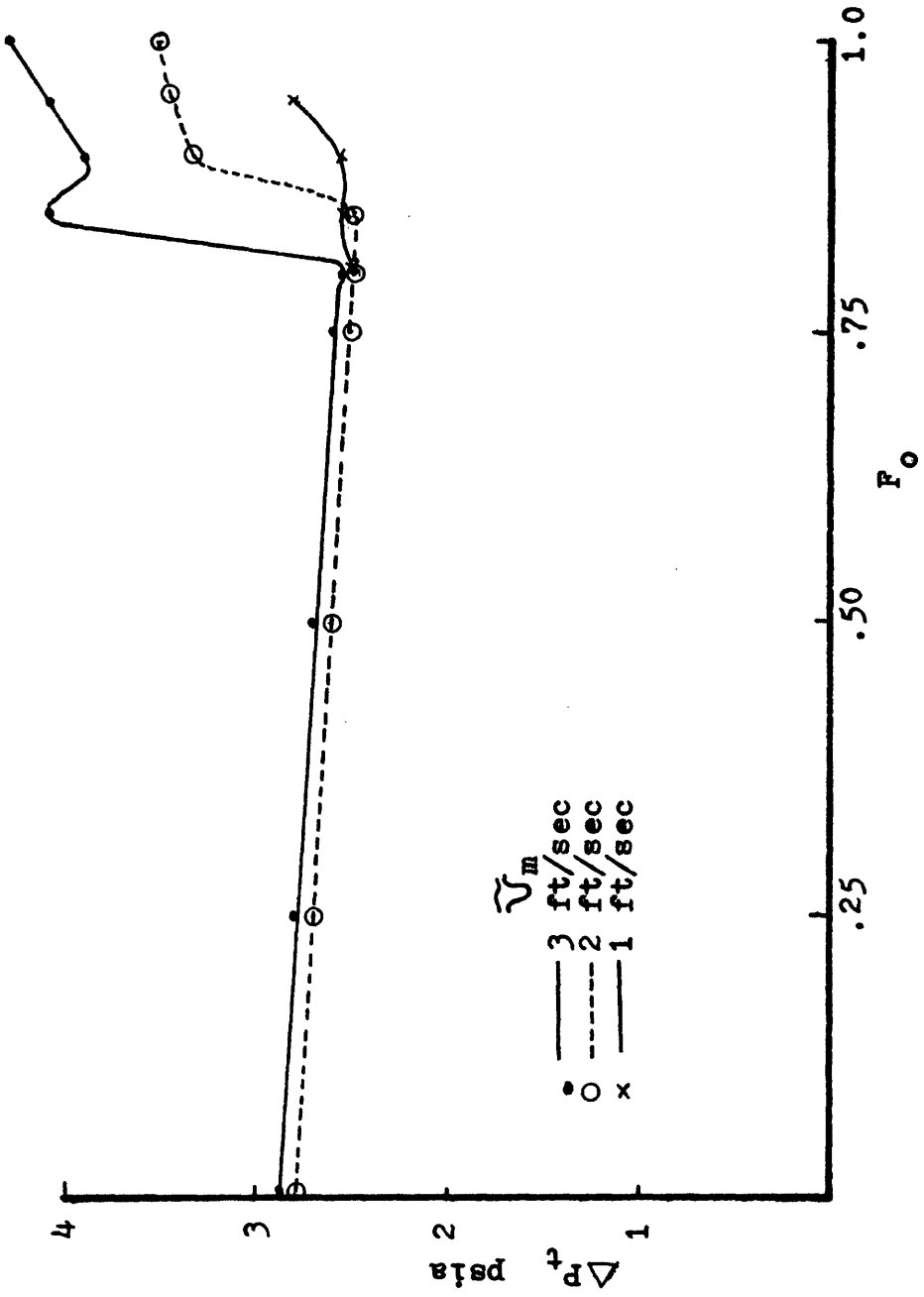

Figure 13. Friction Pressure Loss: Two Phase Flow.

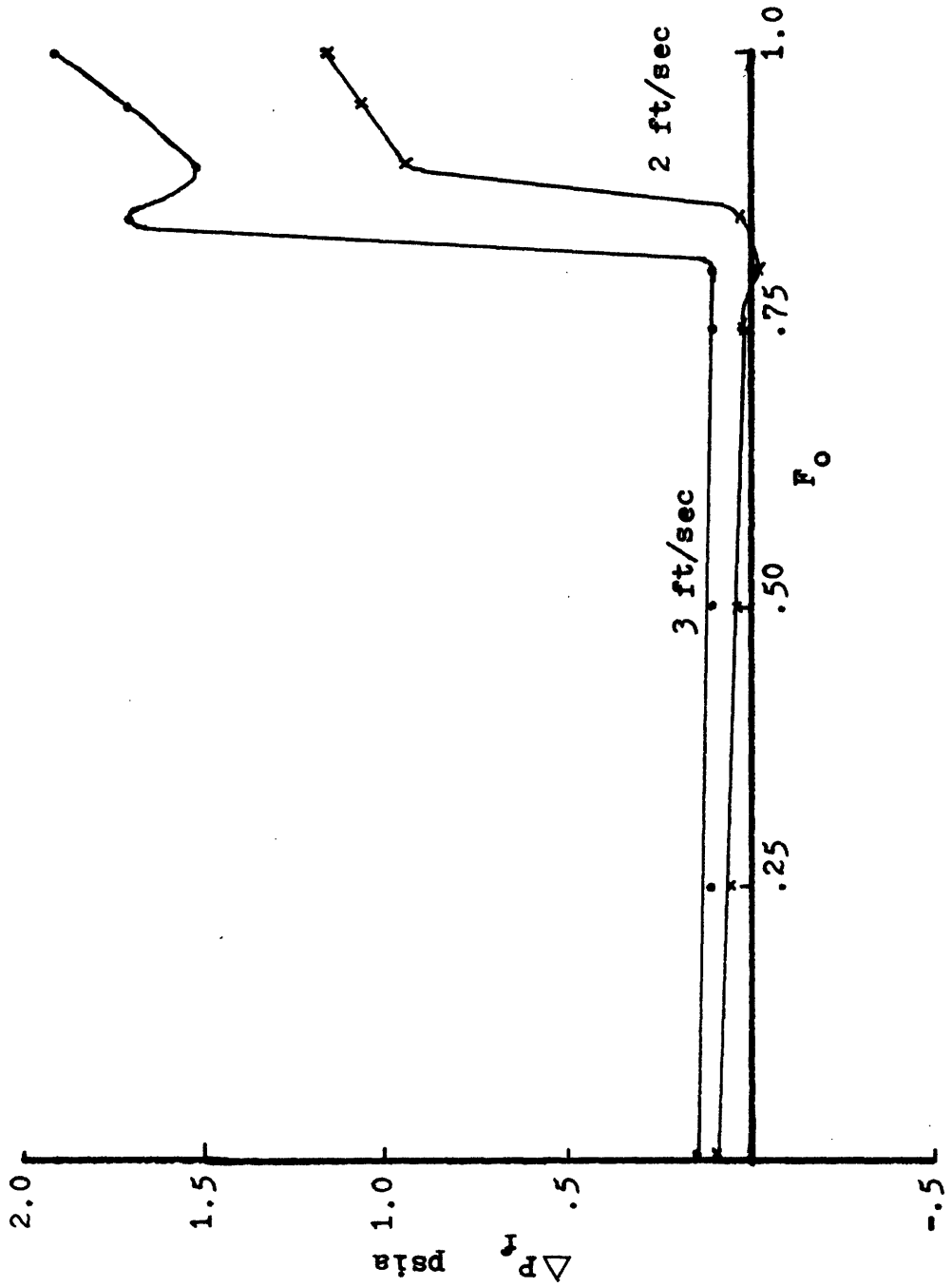

Figure 14. Govier's Flow Regime Map.

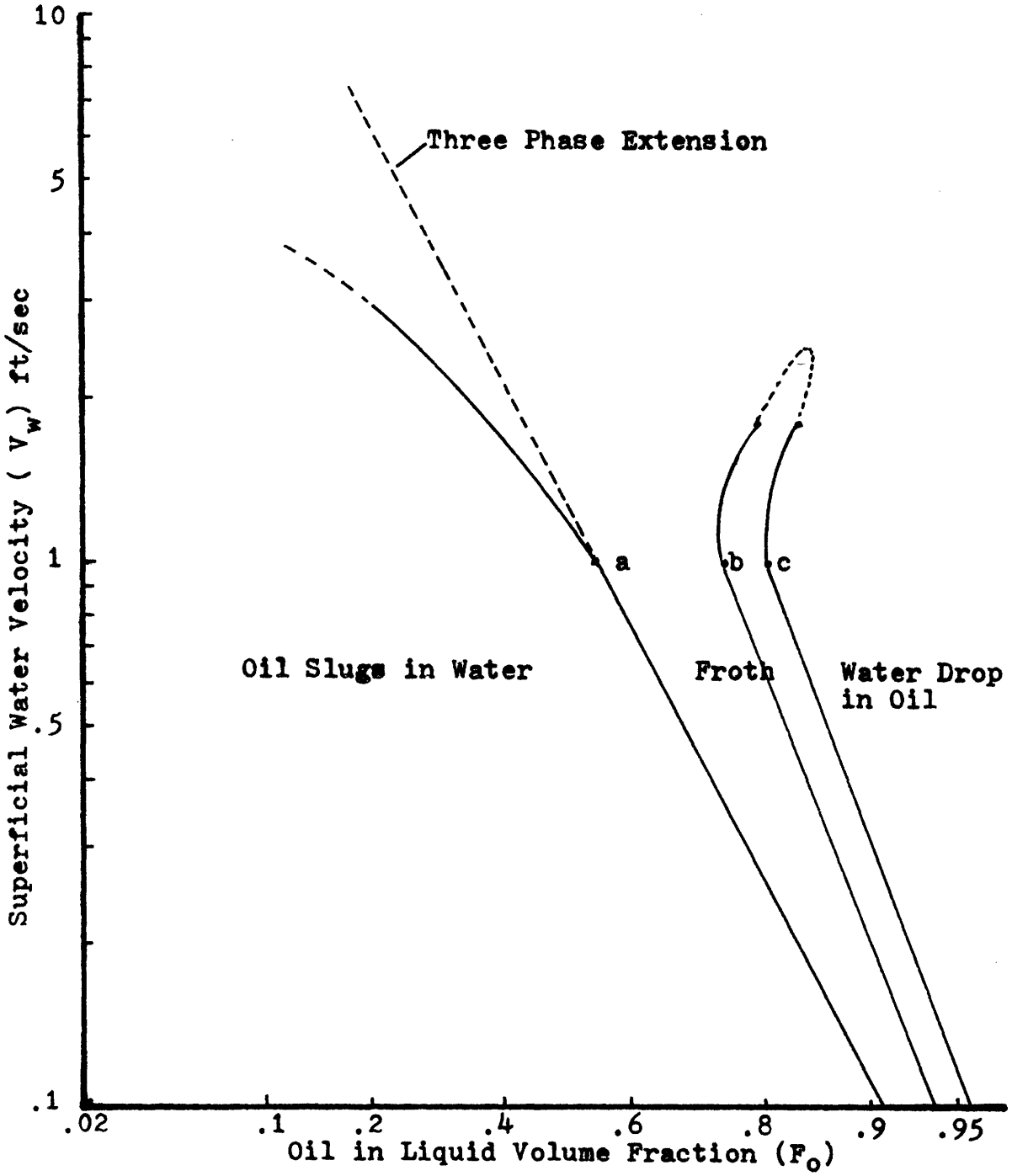

Figure 15. Govier's 20.1 cp Oil Total Pressure Drop: Two Phase Flow.

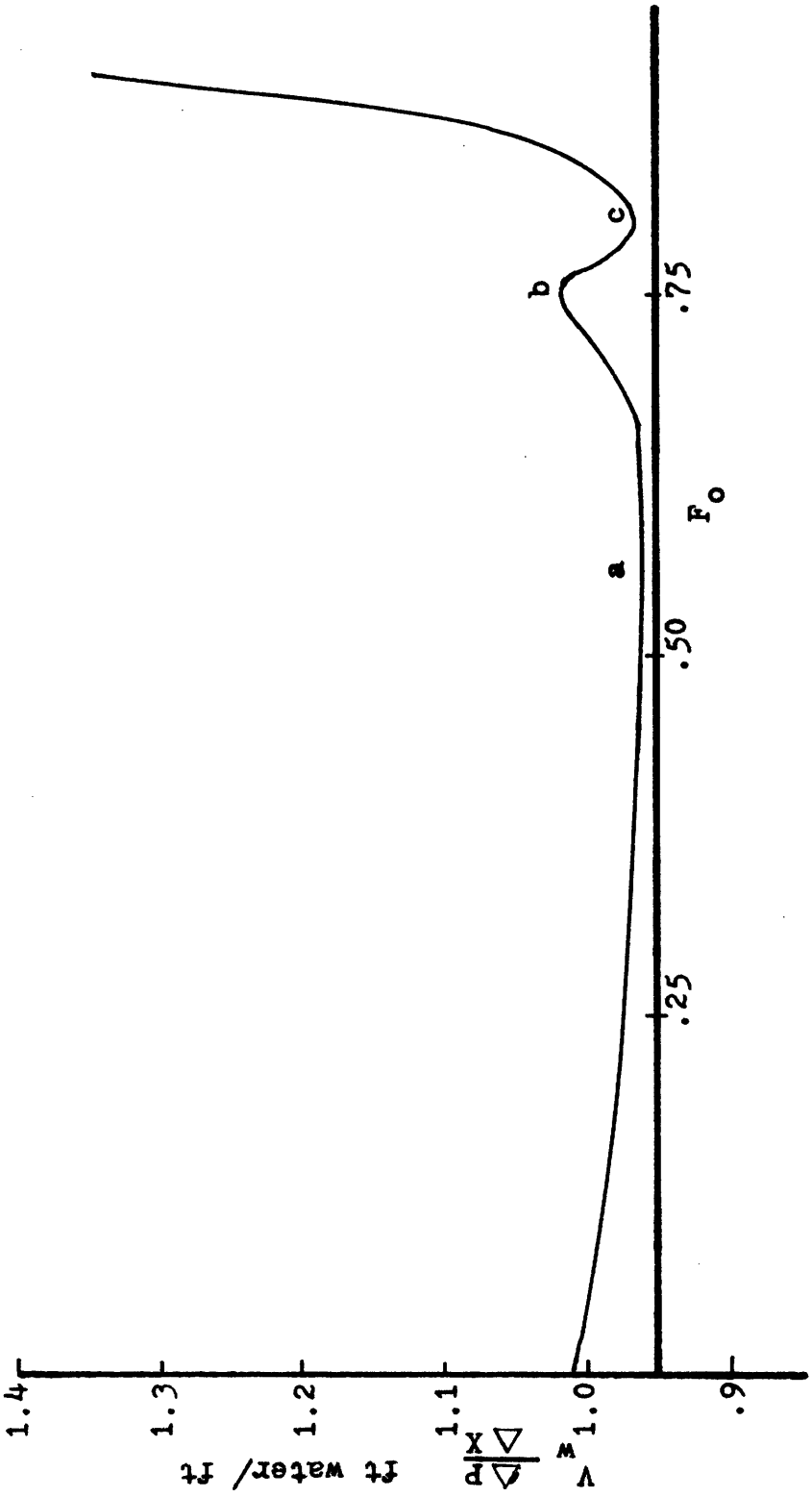

TABLE 1.

Predicted F_o Versus Actual F_o: Two Phase Flow

Fo	Vw(ft/sec)	Qpred	Qact	Qp ≷ Qc	Fo crit(pred)	Fo crit (act)
			$\tilde{v}_m$ = 3 ft/sec			
.8	.64	.002	.0018	>	*	*
.85	.35	.0011	.0014	<		
.90	.21	.0006	.0009	<		
			$\tilde{v}_m$ = 2 ft/sec			
.8	..64	.002	.012	>	*	*
.85	.35	.0011	.0009	>		
.90	.21	.0006	.0006	=		

Predictions made using curve b Fig. 14.

* Predicted value of Fo or actual value of Fo.

various flow parameters, the above data was plotted with that of Govier[6] in Appendix B. The parameters were diameter, mixture velocity and viscosity. The results were as follows:

1. The location of the switching was independent of the diameter while the effect on the level decreased with higher mixture velocities.

2. The velocity had a marked effect on the level, but relatively little effect on the switching location.

3. The viscosity of the oil affected the level only after the shift but did not affect the switch location.

From the above investigation it has become apparent that the single most important item in dividing the oil from the water is determining the location of the shift from water to oil on the wall also that this location appears to be based on a critical oil in liquid volume fraction. Govier in his work with Sullivan and Wood[6] addressed the problem by creating a regime map (Figure 14) based upon Regime observations and the fluctuations of the total pressure curves (Figure 15). Govier stated that this map was relatively insensitive to a change in the oil viscosity except that the froth lines (points a, b and c, Figure 15) merge in the data for high viscosities (150 cp). In this investigation a similar absence of separate points is observed. The map became valuable because it successfully located the critical oil in liquid volume fraction for the current test to within the accuracy of this data (±.05, see Table 1). The implications of this are that for two phase flow one can predict when the α_o will be above or below β_o and the viscosity of

which fluid can be used as the effective fluid viscosity. The most important point, however, is that these results will be extended to three phase flow in the next section.

C. Three Phase Flow Void Fraction and Pressure Drop Test

The results of this final test draw together all the information of the previous two tests and provide acceptable prediction methods for gas void, liquid phase Volume Fraction, critical oil in liquid volume fraction (Fo), and effective viscosity in a three phase flow. These results will be presented in three parts. 1. Void fraction results and prediction method. 2. Pressure drop results and 3. Pressure drop prediction methods and comparison.

1. Void Fraction: In part A, the results indicated that the plotting method of Zuber and Findley successfully correlated the air void data. Likewise in this test the same method was successful. Figure 16 shows the individual air void curves for each of the oil in liquid volume fractions (Fo) tested. The distribution of these lines except for .95 and 1.0 show no systematic arrangement. This fact indicates that the distribution is independent of Fo. Because of this, a single averaged curve may likewise be independent of Fo. In fact, the two consolidated curves are shown in Fig. 17. From these curves the following equations may be derived:

$$o \leq Fo \leq .9 \qquad \tilde{v}_a = 1.28\, \tilde{v}_m + .4 \text{ ft/sec} \tag{5.6}$$

Figure 16. Zuber-Findley Plots Varying F_o: Three Phase Flow.

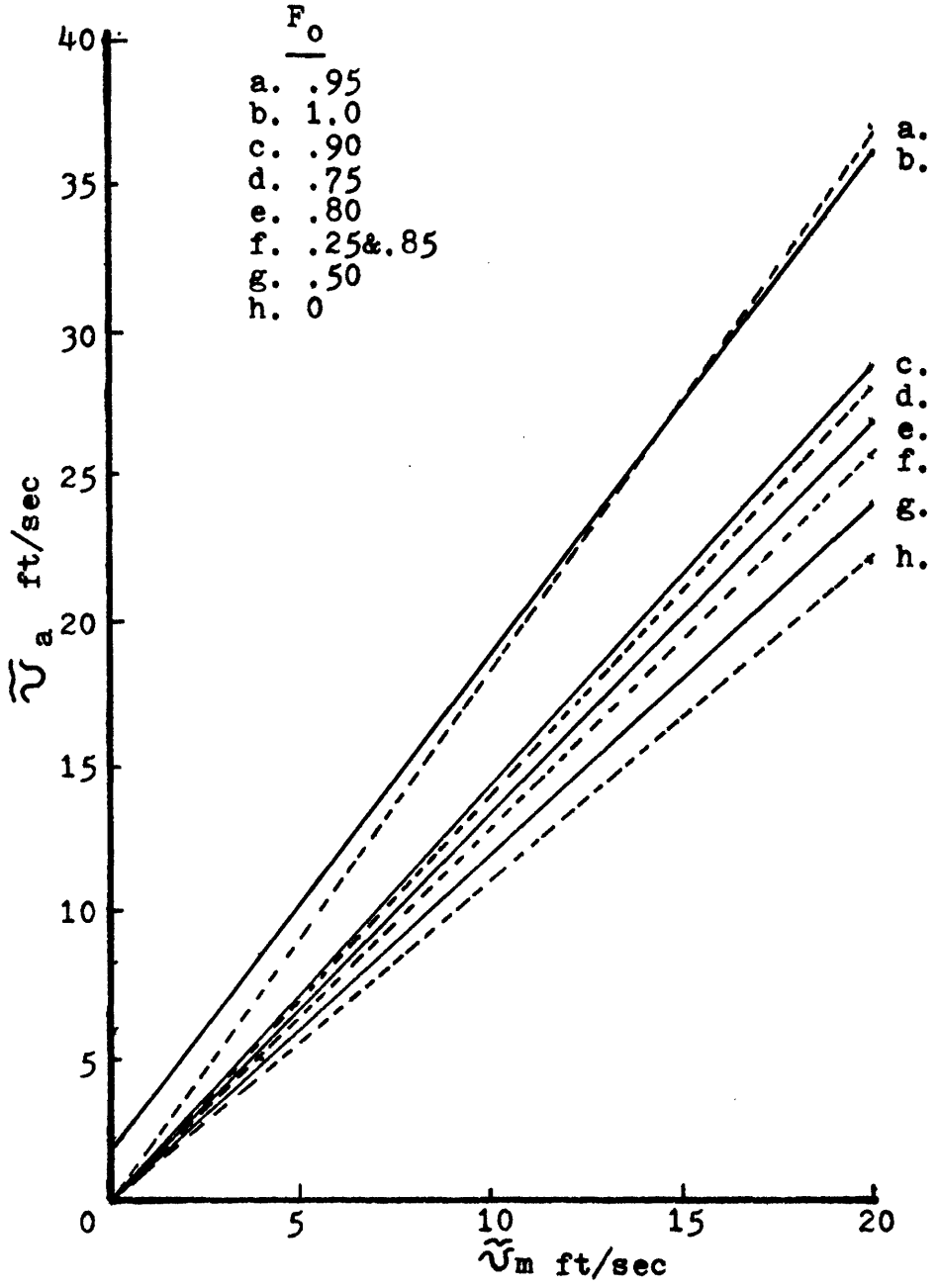

Figure 17. Consolidated Zuber-Findley Plots: Three Phase Flow.

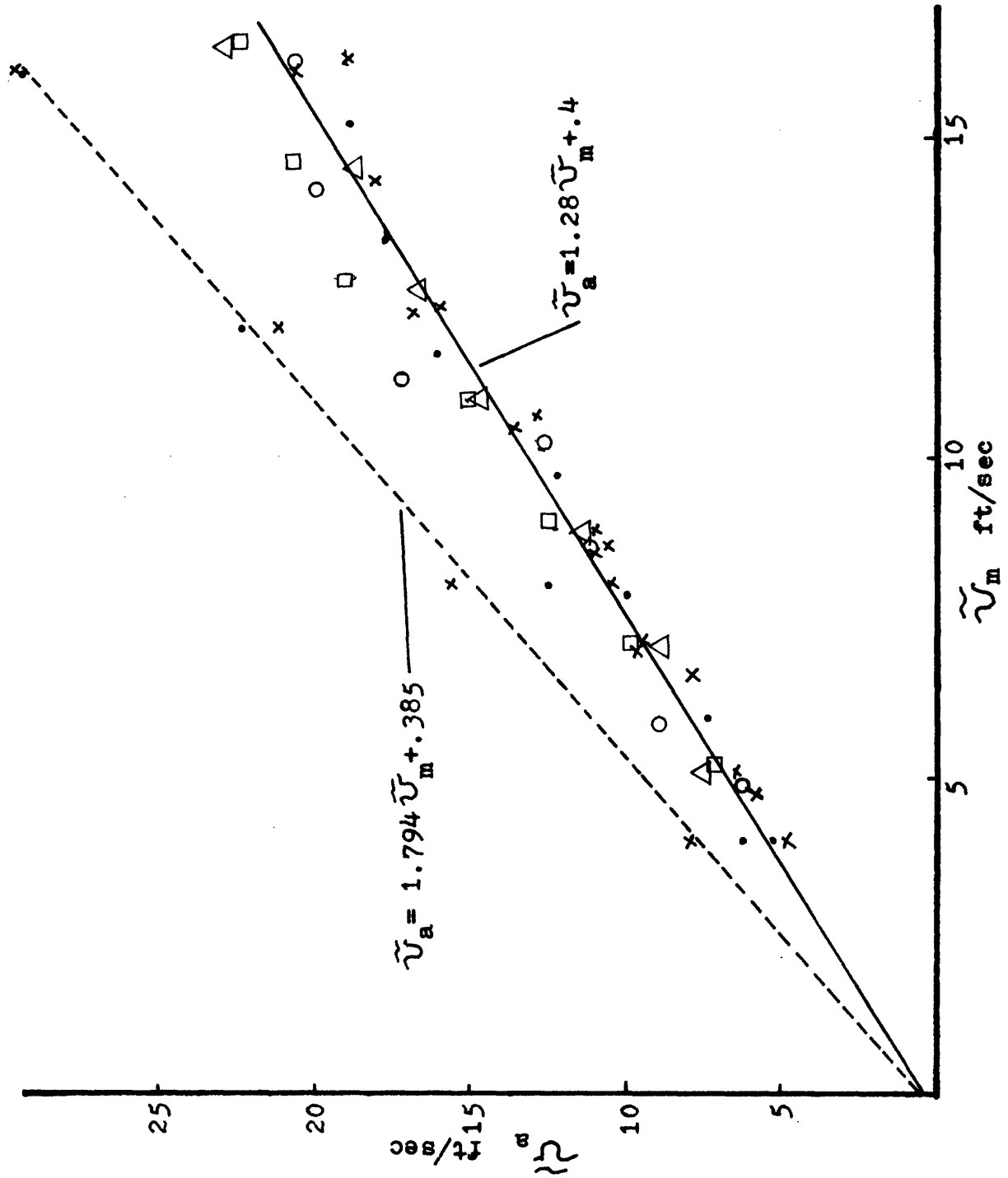

$$.9 \leq F_o \leq 1.0 \qquad \tilde{v}_a = 1.794\ \tilde{v}_m + .384 \text{ ft/sec} \tag{5.7}$$

The fact that two equations are achieved is reassuring because for Fo >.9 the oil dominates the flow and as was mentioned earlier, the oil was in laminar flow throughout these experiments. For laminar flow several authors [8,12] suggest that the Zuber-Findley constant may range up to 1.7 for two phase laminar flows. Hence when the oil is on the wall of the tube a value of 1.794 as in Eq. 5.7 is reasonable. Likewise, 1.28 for turbulent slug flow is akin to the values suggested by Govier and Aziz and Griffith for similar two phase flows. The above equations may be rearranged to obtain the following prediction method for the air void fraction.

$$0 \leq Fo \leq .9 \qquad \alpha_a = \frac{Va}{1.28\ \tilde{v}_m + .4} \tag{5.8}$$

$$.9 < F_o \leq 1.0 \qquad \alpha_a = \frac{Va}{1.794\ \tilde{v}_m + 3.85} \tag{5.9}$$

In all three phase cases examined in this experiment, the bubble rise velocity was small with respect to the mixture velocity and may be neglected without loss of accuracy. When the bubble rise velocity is neglected, the following equations for air void are obtained:

$$0 \leq F_o \leq .9 \qquad \alpha_a = \frac{Qa}{1.28\ Q_T} \tag{5.10}$$

$$,9 < Fo \leq 1.0 \qquad \alpha_a = \frac{Qa}{1.794\ Q_T} \tag{5.11}$$

As a result of this simplification the only information necessary for field calculation of the air void is the oil, water and air volume flow rates. It should be noted that equations 5.7, 5.9 and 5.11 are valid only when the Reynolds number based on the mixture velocity and the oil viscosity indicate the flow is laminar. These equations are compared against the data obtained in Part A and that of Foreman and Woods (Fig. 18 and 19). In both cases these equations give excellent results. The comparison with Foreman and Woods is especially interesting because their data is based on kerosene which has a significantly lower viscosity than Nujol. In an effort to separate the two fluid Volume Fractions, the method of plotting the Insitu oil phase volume fraction versus the oil in liquid volume fraction of Part B may be employed. However, this method must be modified to isolate the fluids from the gas. The Insitu oil phase volume fraction must be divided by the liquid phase Volume Fraction and the oil in liquid volume fraction (Fo) is defined as $\beta o/\beta f$. In this way Figure 20 may be obtained. This curve has a striking resemblance to Figure 10 for oil and water alone. In fact, both ordinates reduce to those of Figure 10 when the air flow is zero. The most important point of both curve is that they both cross the homogeneous line as the fluids exchange places near the wall. In Figure 10 the curves show dependence on the mixture velocity while Figure 20 does not. The difference is that the mixture velocity in the two phase is obtained by varying the fluid mass flow rate while in the three phase flows the fluid mass flow rate was constant. The air flow was varied instead.

Figure 18. Air Void, Predicted Versus Actual: Foreman and Woods.

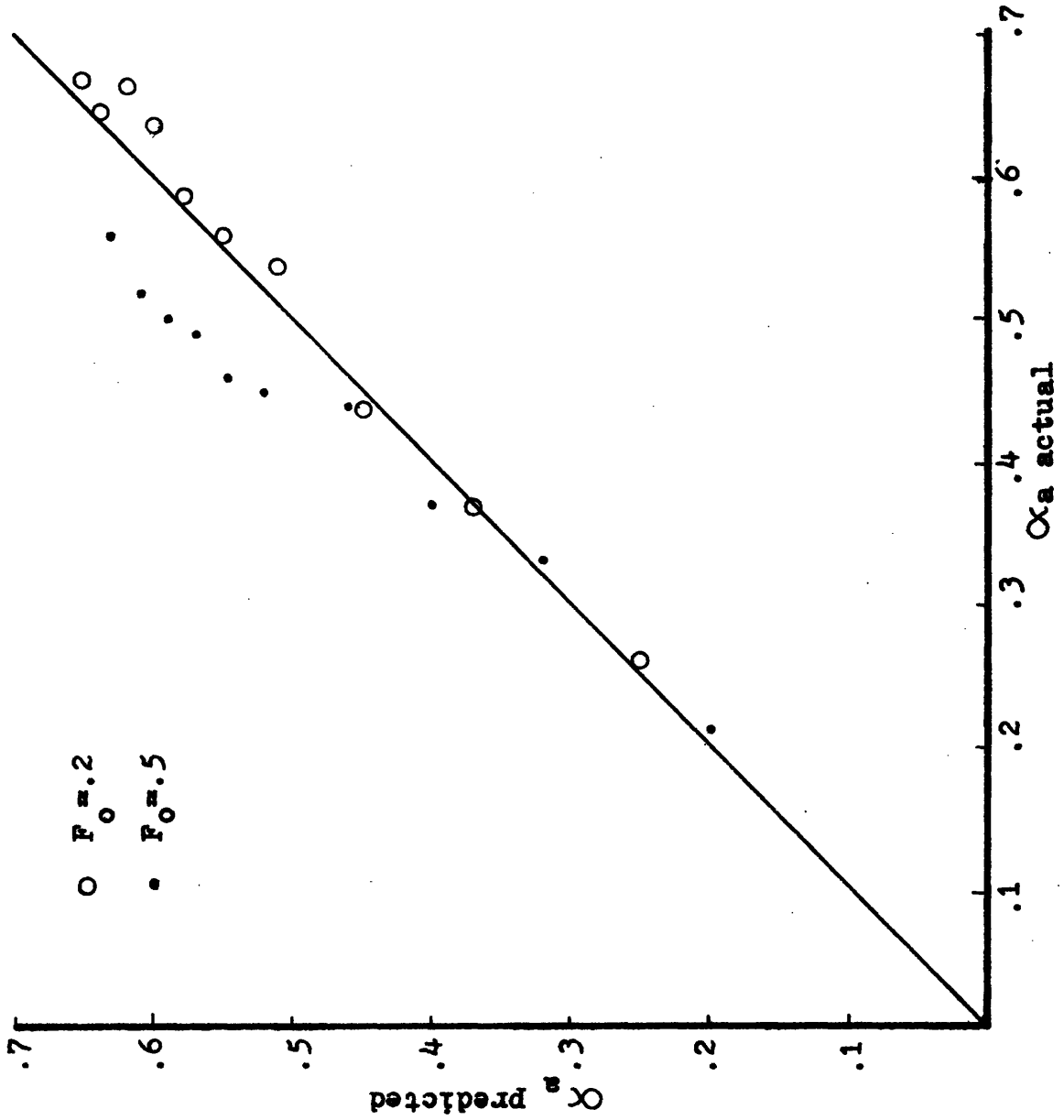

Figure 19. Air Void, Predicted Versus Actual: Three Phase Void Data.

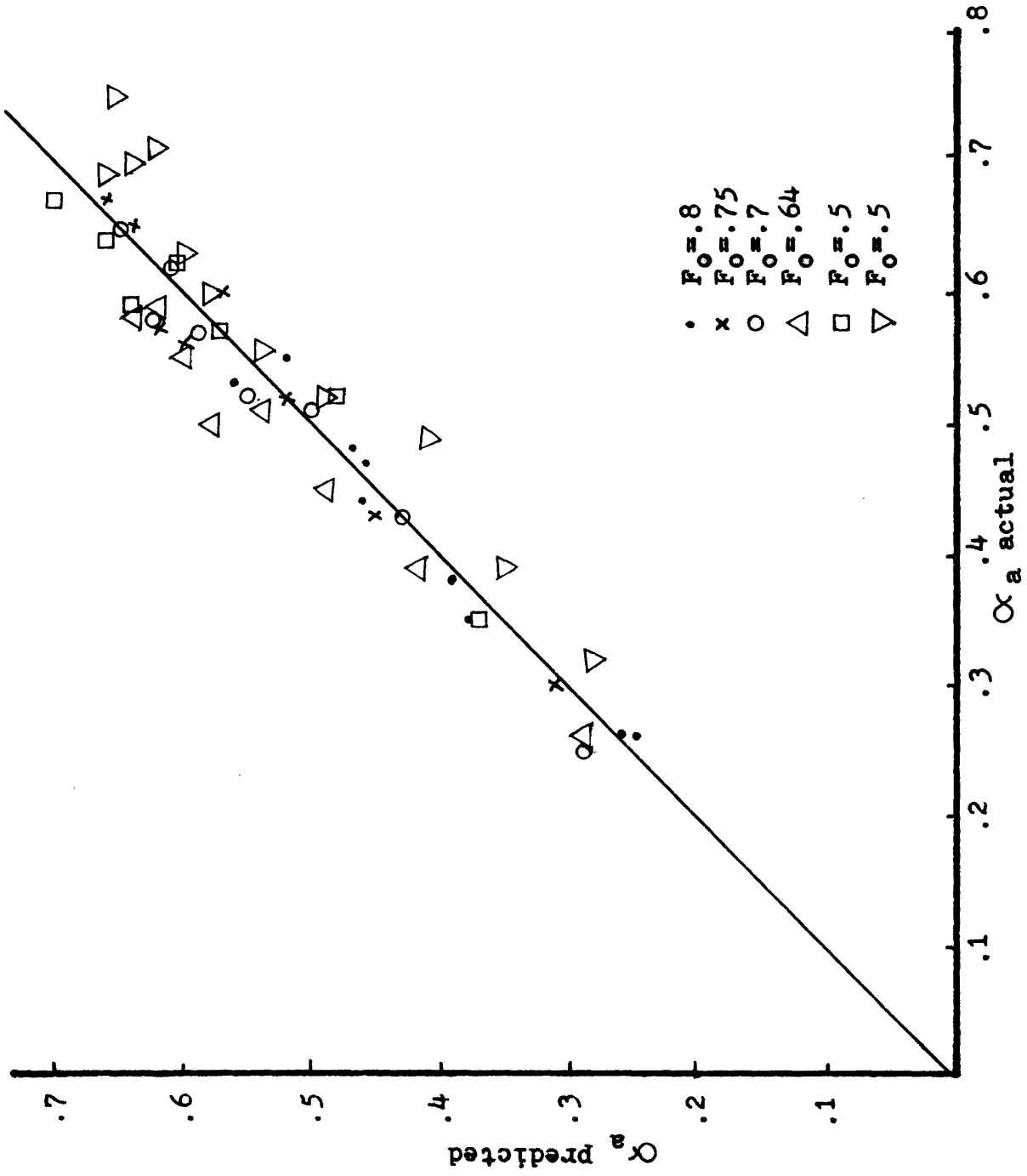

Figure 20. In Situ Oil Phase Volume Fraction/ In Situ Fluid Phase Volume Fraction Versus F_o.

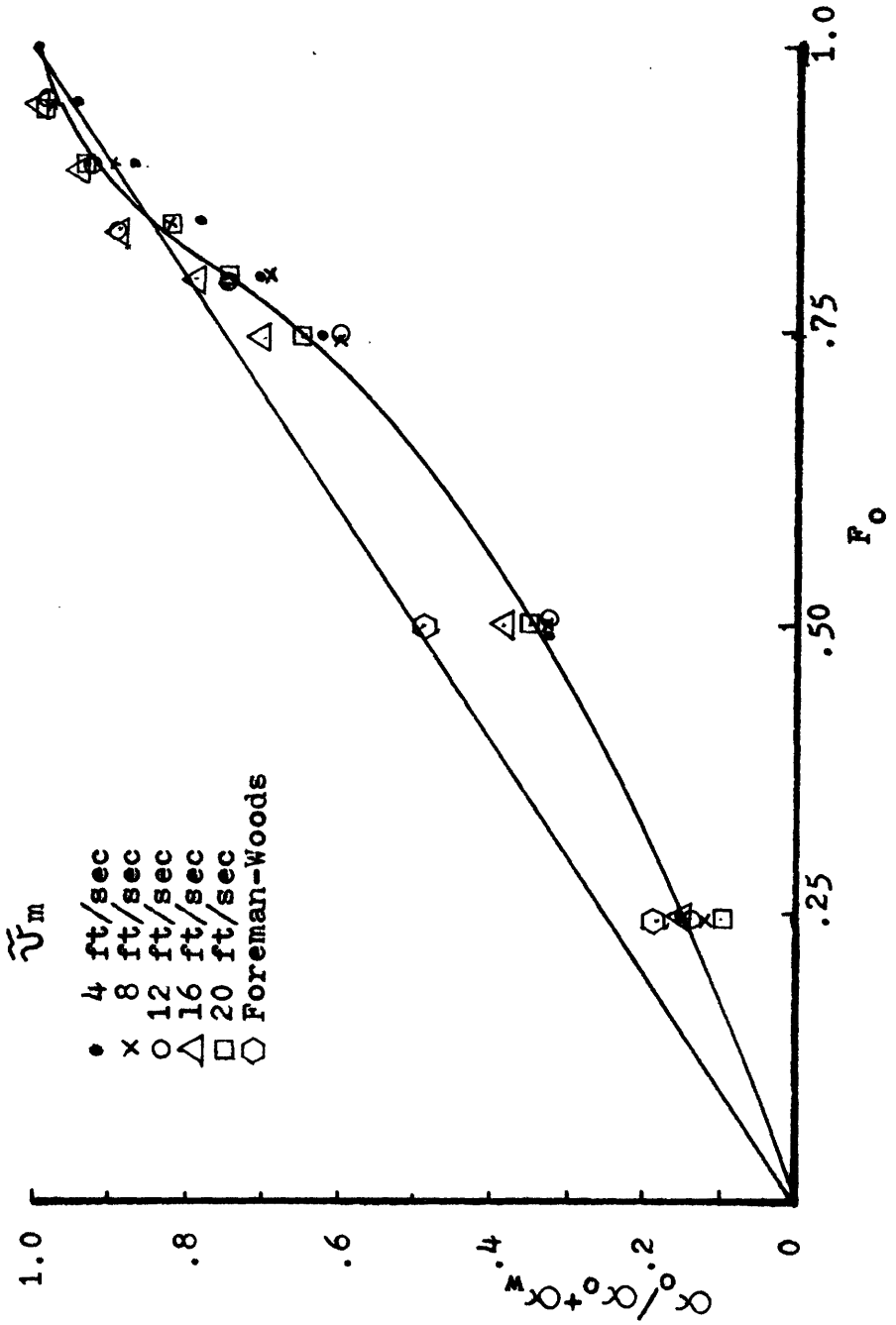

Therefore, the results appear to be dependent on the fluid mass flow rate and oil in liquid volume fraction (Fo) only. In this test then, because the mass flow rate is constant, a single equation for the curve may be obtained. This equation is:

$$\alpha_o = 1.037\ \alpha_f(Fo)^{1.536} \tag{5.12}$$

where $$\alpha_f = 1-\alpha_a \tag{5.13}$$

As a consequence of this equation, and that for the air void, we can now estimate the Insitu water phase Volume fraction as follows:

$$\alpha_w = 1-(\alpha_a+\alpha_o) \tag{5.14}$$

or for $0 \leq F_o \leq .9$

$$\alpha_w = .964-\alpha_f(Fo)^{1.536} \tag{5.15}$$

Again the data of Part A and Foreman and Woods are compared with the new correlation (Figures 21 and 22). The Part A data show good results while that of Foreman and Woods show a systematic deviation. When the latter data is plotted in Figure 20, it plots closer to the homogeneous line. From Figure 10 this indicates that the Foreman-Woods data has a higher fluid mass flow rate and, in fact, it is 50% higher. Also, the kerosene has a much lower viscosity than that of Nujol. This difference allows for more turbulent flow with greater mixing of the two fluids. The mixing flattens the concentration curves of Figure 5b, and reduces the fluid velocity difference. Finally, the reduced velocity difference

Figure 21. In Situ Oil Phase Volume Fraction, Predicted Versus Actual: Three Phase Void Data.

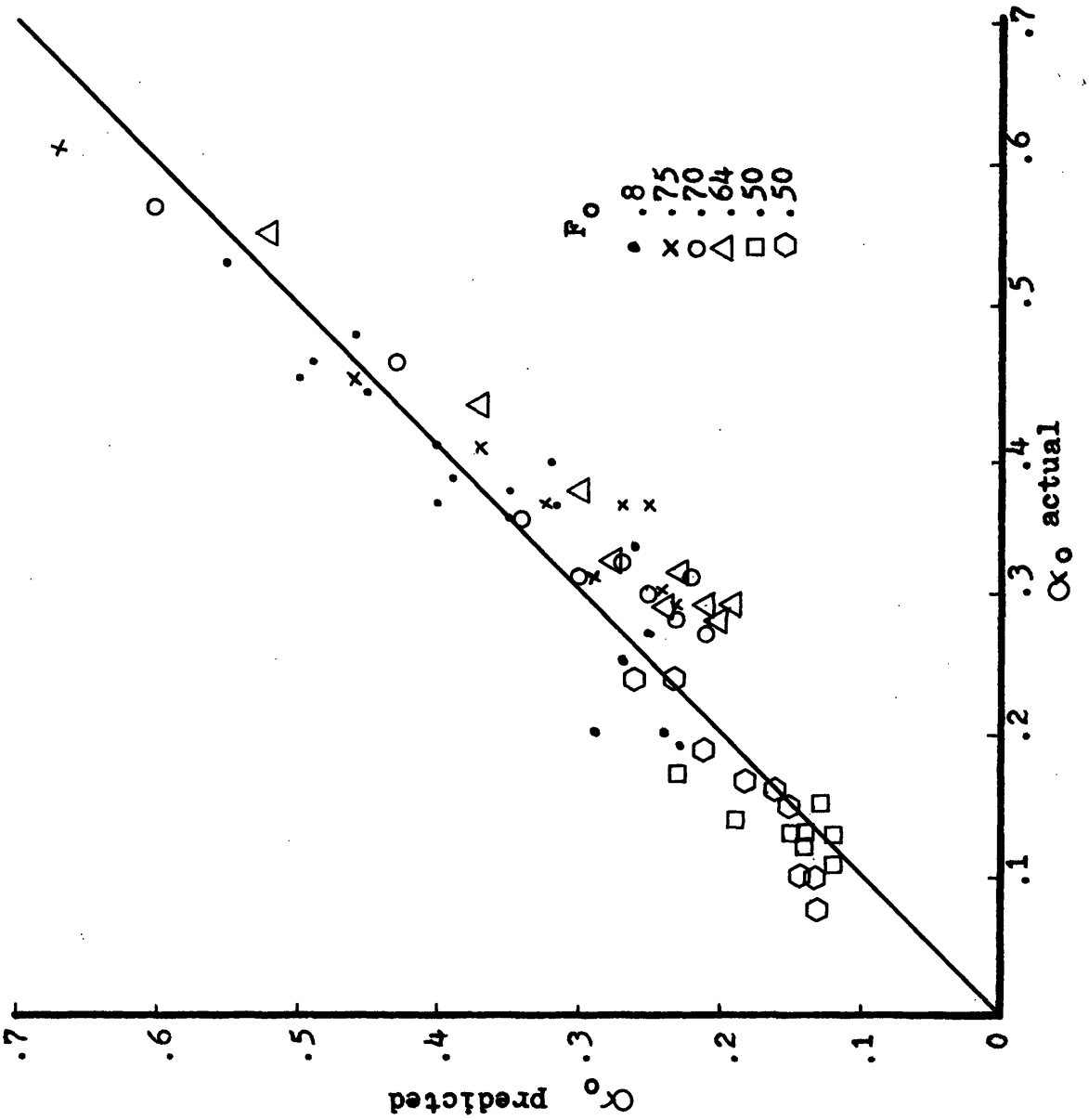

Figure 22. In Situ Oil Phase Volume Fraction, Predicted Versus Actual: Foreman and Woods.

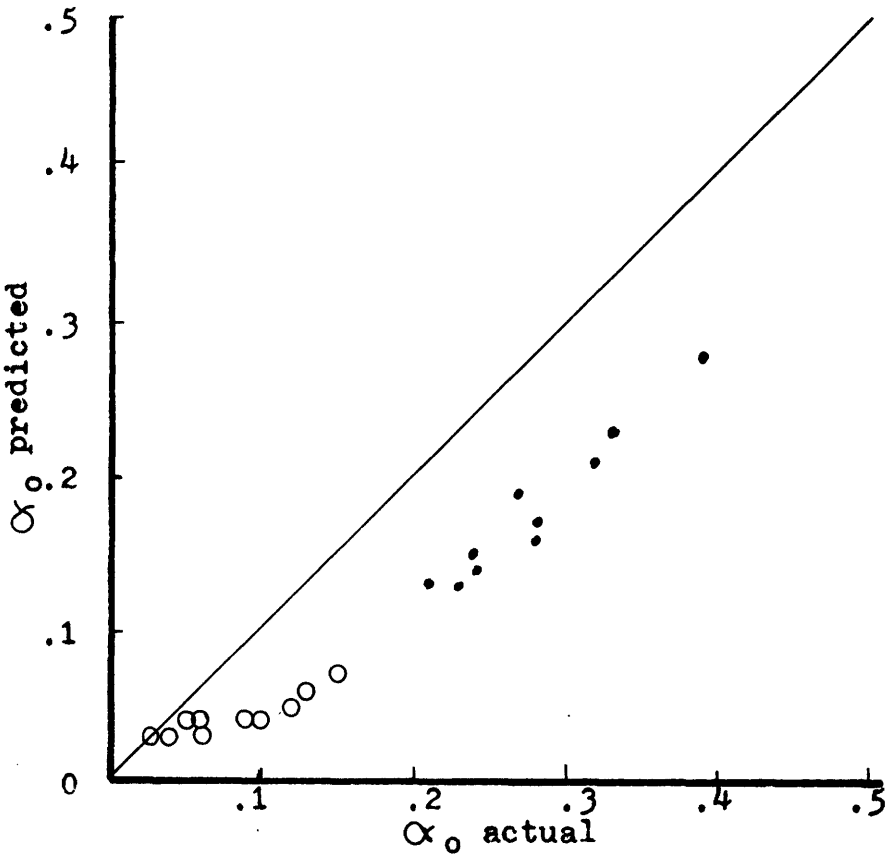

implies a slower oil velocity and a larger in situ oil phase volume fraction. As a result, the predicted values of Eq. 5.12 are less, and the values should fall below the diagonal in Fig. 22 as they do. Some of the fluid mass flow rates of Part A also differ from those of Part C. The step near α_o actual of .3 is a junction between several runs with different fluid mass flow rates. Again, those below the diagonal generally had higher flow rates than did Part C. It should be noted that these correlations for void fractions are only estimates and adjustments may be necessary to insure the total of all three Volume Fractions is one. This is especially true at the higher values of the oil in liquid volume fraction (Fo).

To complete the void fraction results the oil water velocity difference is shown plotted versus Fo and mixture velocity in Figures 23 and 24. From these curves we may observe the switch point is again strongly dependent upon Fo while the mixture velocity weakly influences the location of the crossing. Later it will be shown that the superficial water velocity, is the actual cause of this weak dependence. Finally, Figure 24 is very similar to Figure 6 for two phase flow. Therefore, the characteristic shape of the velocity difference curves appear relatively independent of the gas volume flow rate.

2. Pressure Drop

Figures 25 and 26 summarize the pressure drop data obtained from this test. In Figure 25 the friction pressure loss curves show a marked dependence on the mixture velocity for their level while the shape of

Figure 24. Oil-Water Velocity Difference Versus Mixture Velocity.

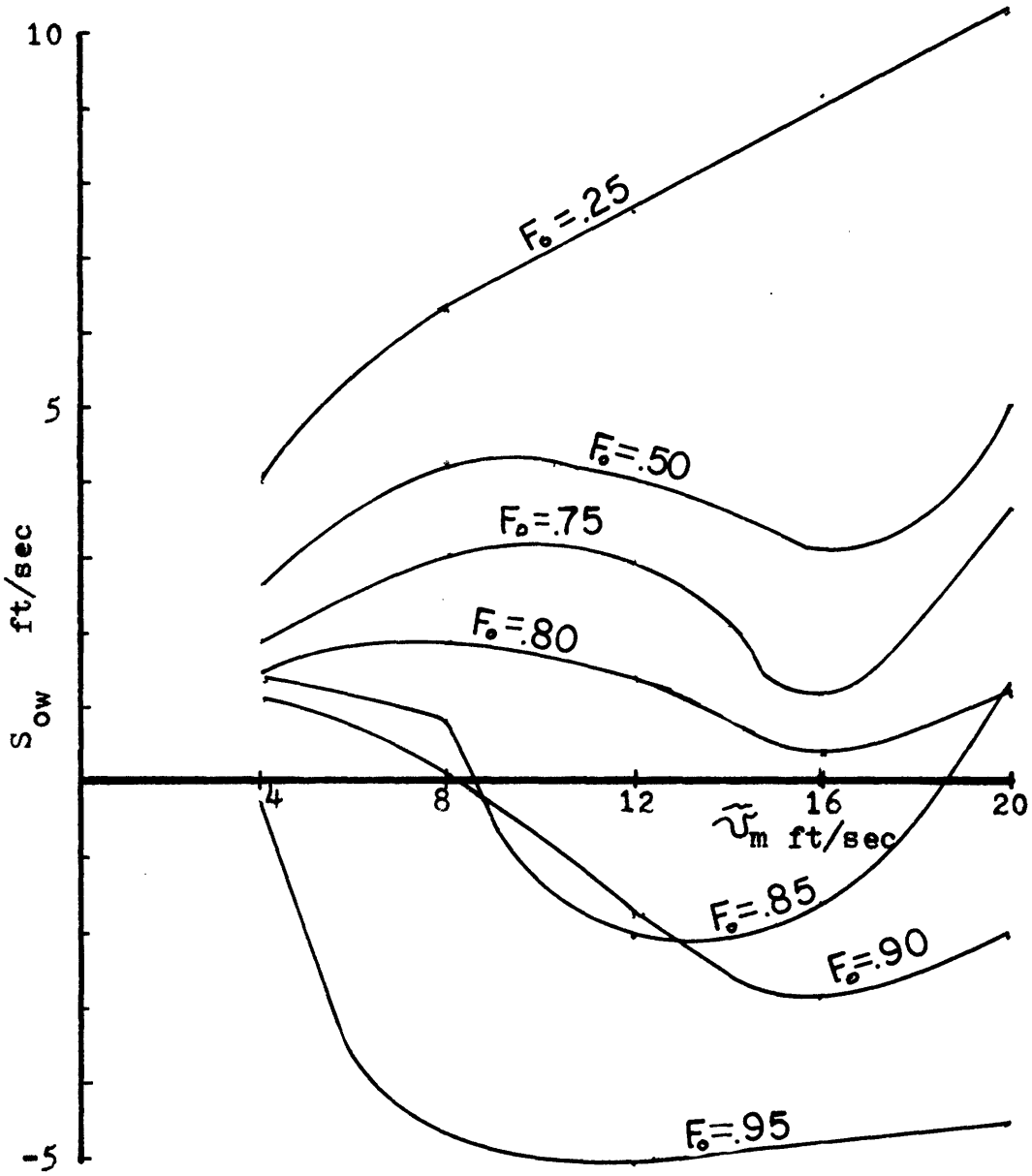

Figure 23. Oil-Water Velocity Difference Versus F_o.

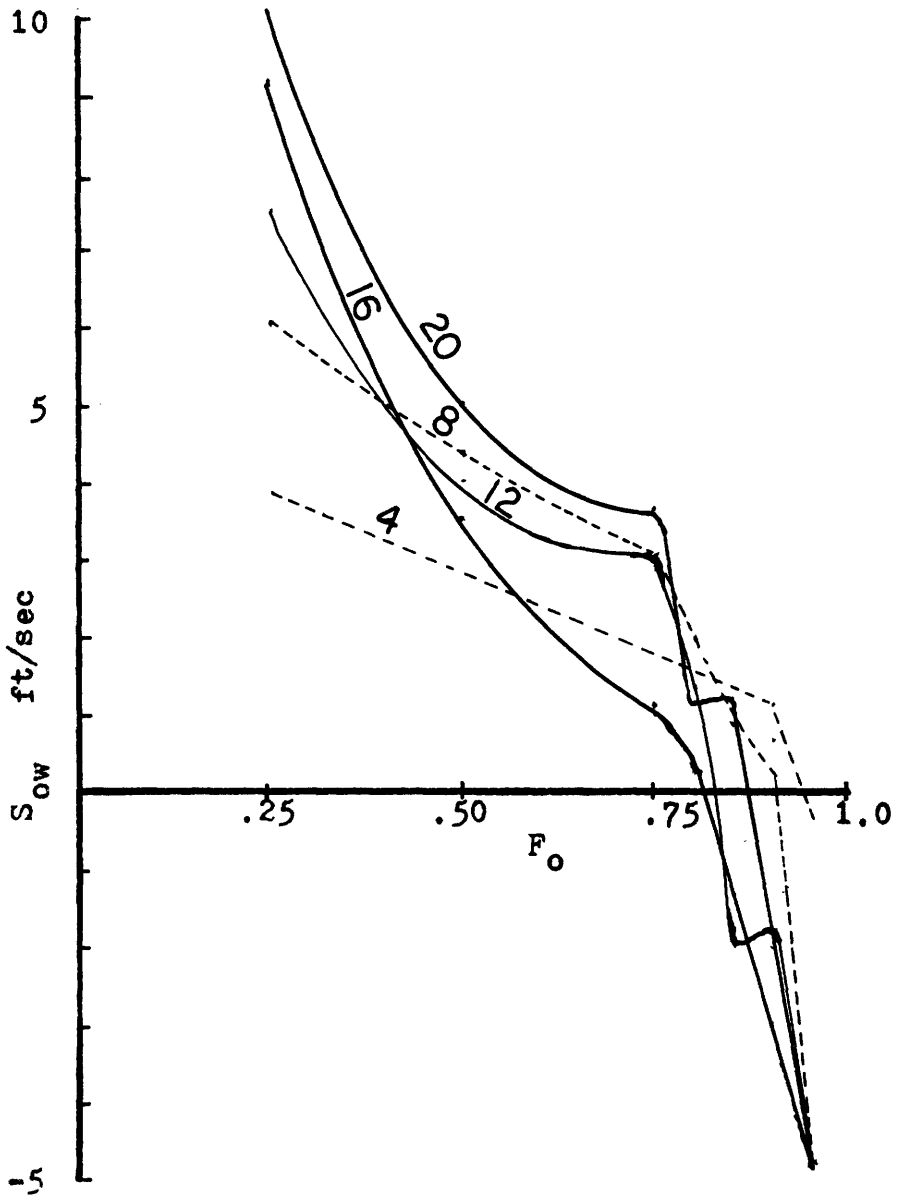

Figure 25. Friction Pressure Loss Versus F_o: Three Phase Flow.

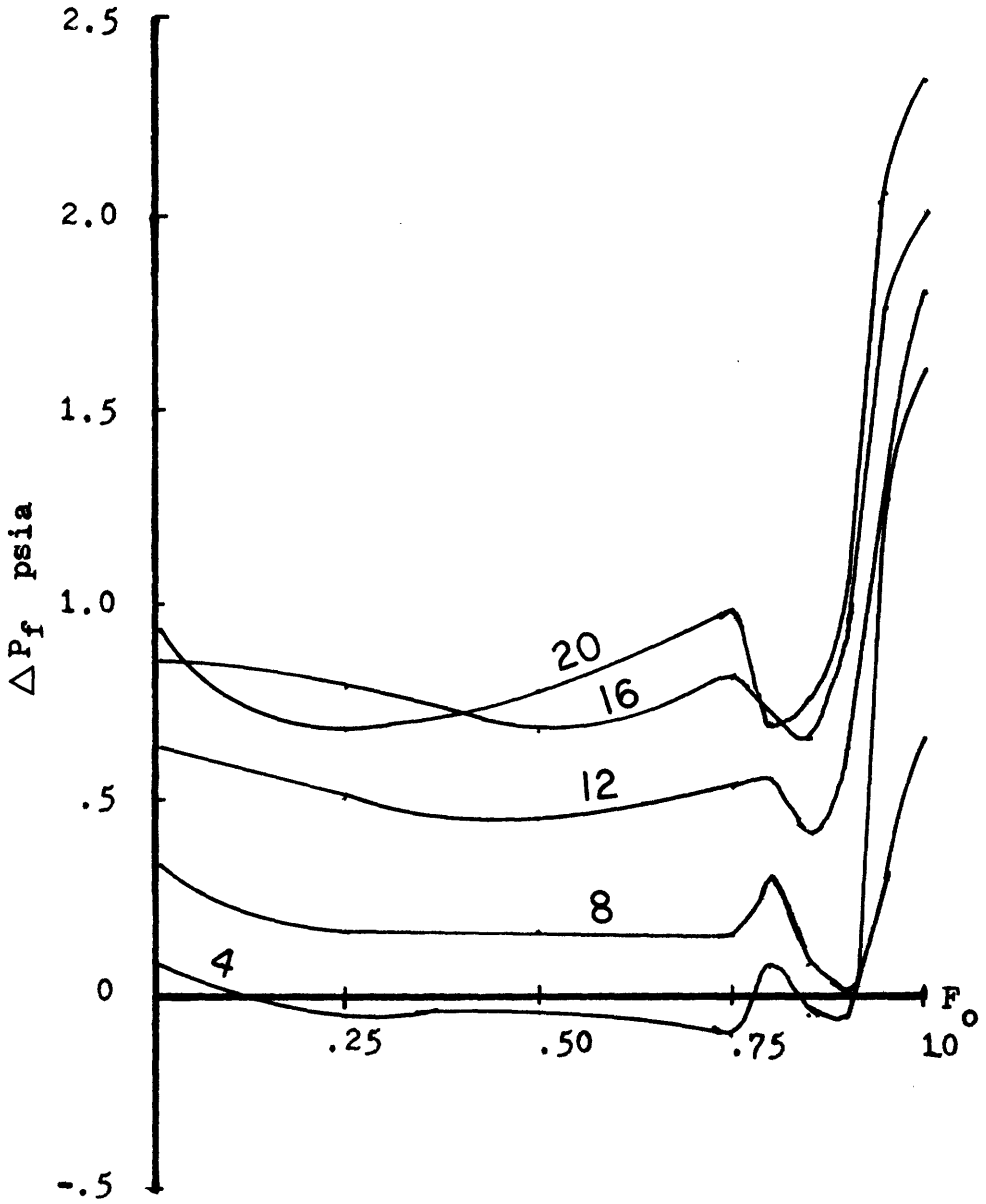

Figure 26. Total Pressure Loss Versus F_o: Three Phase Flow

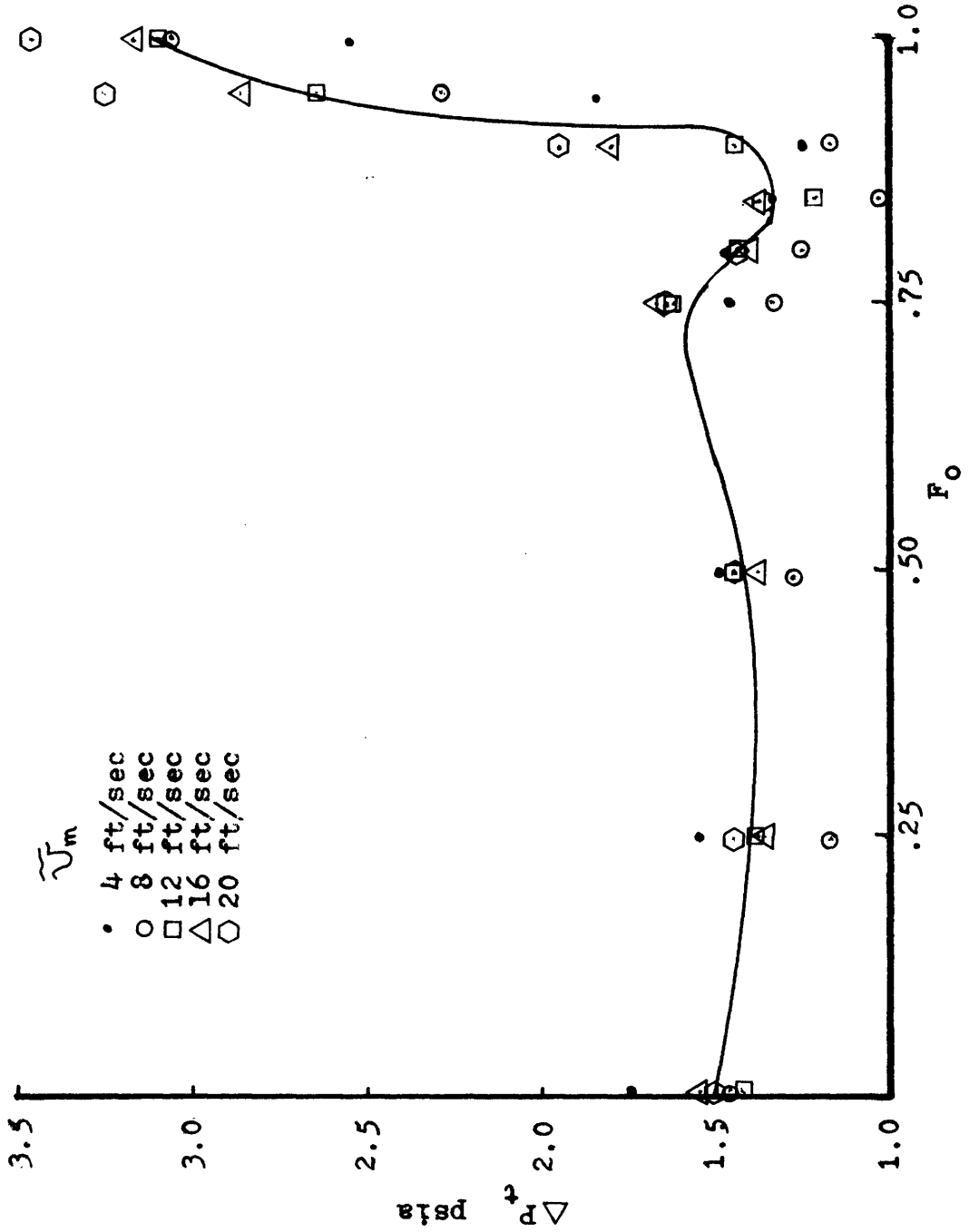

the curves appears to be independent. Also, the shape appears to be very similar to Govier's oil water curves in Appendix B. Because of this similarity, and the fact the variance in mixture velocity is a function of air flow only, the shape can be assumed to be a characteristic of the fluid flow only. As with Figure 13, the friction pressure drop is relatively uniform up to the critical Fo for transition to water bubble flow. As a result, for estimate purposes, the viscosity of the water may be used as the mixture viscosity up to the critical Fo. The negative pressure losses shown in Figure 25 may be attributed to the counter-flow experienced as a slug of air passes through the tube. Collier [11] comments on this effect in his book. Figure 27 gives an idealized view of such a flow over a slug. As can be seen, the shear over the bubble can balance the loss over the fluid slug and give a positive time averaged shear stress and a negative friction pressure loss.

The total pressure drop is unaffected by the mixture velocity. As the air flow increases, the gravity pressure loss decreases, but the resulting increase in mixture velocity increases the friction pressure loss. Figure 26 indicates that these two effects balance one another under the test flow conditions. The shape of this curve resembles that of Govier's 20.1 cp oil-water curve, Figure 15, especially the critical points a,b and c. This indicates that the air flow apparently lowered the effective viscosity of the oil as experienced by the water. This similarity of the total pressure curves suggests that we may use Govier's map to predict the critical oil in liquid volume fraction. With some

Figure 27. Idealized Slug Flow

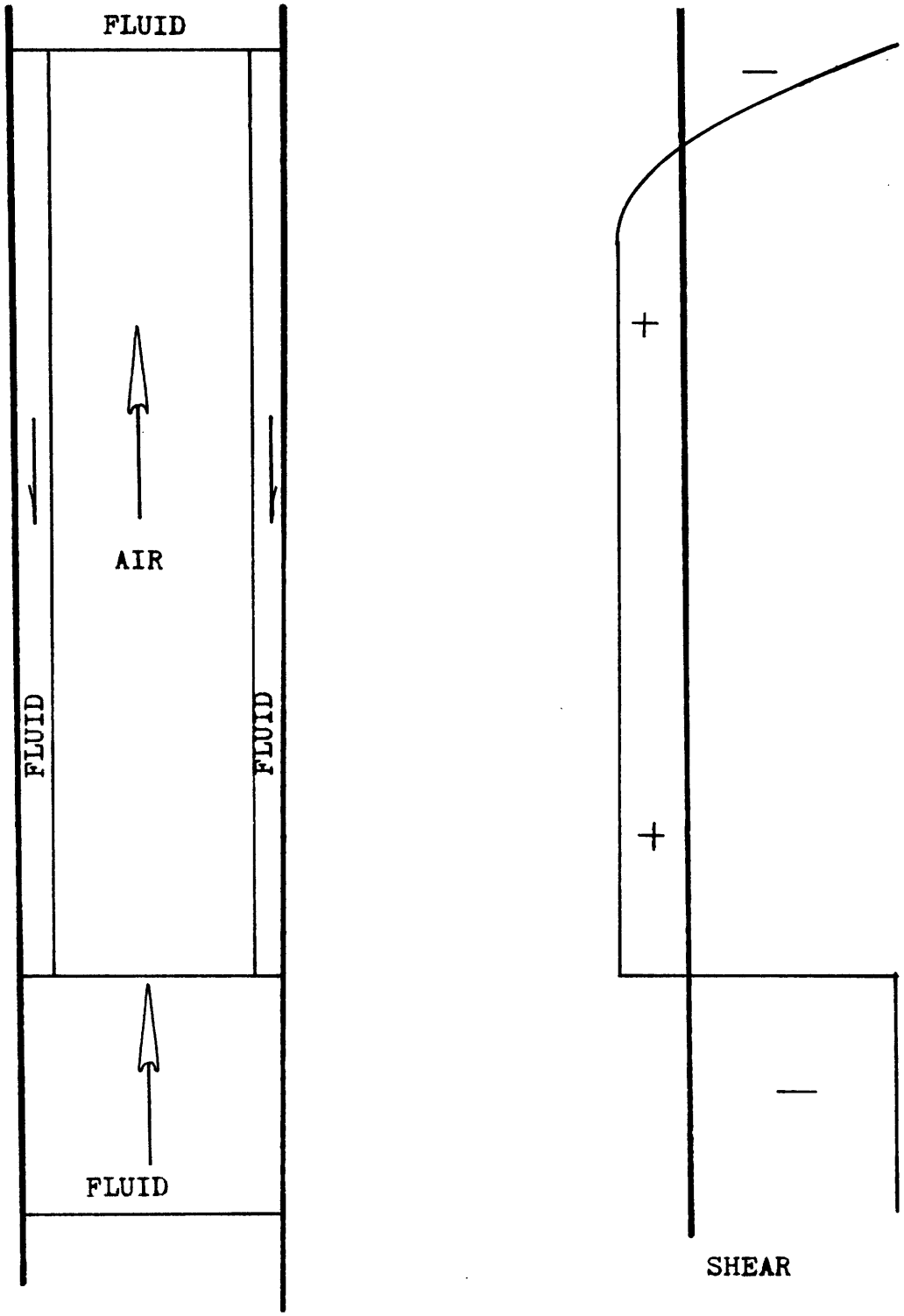

modification this appears to be true. These modifications are: The boundary between the oil slugs and froth must be extended as in Figure 14, and the superficial water velocity is redefined as flowing through the liquid Phase Volume Fraction as follows:

$$V_w = \frac{Q_w}{\alpha_f A} \tag{5.16}$$

Because all three critical points appear in the three phase total pressure curve, all three will be predicted. Table 2 shows a summary of the modified Govier map applied to the current data. The results are very good considering the accuracy of the data.

3. Pressure Loss Prediction Methods, Comparison and Discussion

Based on the foregoing information and data, several known methods for predicting two phase friction pressure loss may be applied to the three phase flow. These are the Singh-Griffith[10] method, McAdams - Homogeneous[11] method and Lochart-Martinelli[11] correlation. The first two are based on assumptions of the flow regime while the latter is basically imperical. In addition, an annular flow method suggested by Griffith is applied at the higher oil-in-liquid volume fractions. A derivation is shown in Appendix D. The method used by Singh-Griffith to estimate the gravity pressure loss is also used herein. In applying these methods several modifications are necessary. As was discussed earlier, the viscosity of the mixture is assumed to be that of water up to an Fo of .9 and that of Nujol from there to 1.0. In the Singh-

Table 2. Predicted Fo Versus Actual Fo:

Three Phase Flow

v_m ft/sec	a_p	a_a	b_p	b_a	c_p	c_a
4	.25-.50	.75	.75-.80	.80	.85	.90
8	.25	.25	.75-.80	.80	.85-.90	.85
12	.25	.25	.75-.80	.75	.80	.85
16	0-.25	.25	.75-.80	.75	.80-.85	.85
20	.25	.25	.75-.80	.75	.85-.90	.85

p predicted

a actual

a,b,and c keyed from figure 15.

Griffith method, the in situ water phase volume fraction alone must be used up to an Fo of .5. Then the total in situ fluid volume fraction is used for the remainder. The reason being that the oil bubbles do not interfere with the water counter-flow until that point. Finally, in order to truly test these methods and not the void prediction technique, the actual measured in situ Volume fractions were used where necessary. Table 3 summarizes the results obtained from these methods, while Figures 28 and 29 show a comparison between the actual values of the gravity and friction pressure losses against estimated values. As can be seen, the gravity pressure loss estimates are very good, however the friction pressure loss estimates vary in success.

The inconsistency of the various friction pressure loss prediction methods is the result of the variety of flow regimes encountered as Fo is varied. Appendix C, outlines these regimes in detail. As a result, the Singh-Griffith method fails in the slug and quasi annular areas and the Annular method fails in slug and froth flow. The Lockhart-Martinelli method applies only where its data base applies. Consequently, no method alone adequately predicts the friction pressure loss. Instead, a combination of methods must be employed.

The above data suggests the following assortment of methods be used to achieve acceptible pressure loss predictions. For gravity pressure loss the Singh-Griffith methods are recommended:

a. $0<F_o \leq$ oil slug-froth boundary and Fo=.9. The Singh-Griffith

TABLE 3.

PRESSURE LOSS COMPARISON

$\tilde{U}_m$	F_o	ΔP_{f1}	ΔP_{f2}	ΔP_{f3}	ΔP_{f4}	ΔP_{f5}	$\Delta P_{\rho 1}$	$\Delta P_{\rho 2}$	ΔP_{t1}	$\Delta P_{t\ est}$
4	0	.08	.17	.16	.13		1.67	1.73	1.75	1.90
	25	-.04	.13	.15			1.57	1.71	1.55	1.84
	50	-.03	.10	.15			1.53	1.66	1.50	1.81
	75	-.10	.06	.14			1.56	1.60	1.47	1.74
	80	.09	.14	.14			1.39	1.59	1.48	1.73
	85	-.03	.14	.14	.13		1.37	1.58	1.34	1.72
	90	-.06	.13	.14		.70	1.32	1.56	1.26	1.69
	95	.31	1.65	1.31		1.03	1.54	1.77	1.86	2.80
	100	.67	1.67	1.31	1.24	1.31	1.88	1.80	2.55	3.11
8	0	.33	.39	.32	.30		1.14	1.18	1.47	1.57
	25	.14	.32	.32			1.05	1.17	1.19	1.49
	50	.14	.25	.31			1.16	1.14	1.30	1.45
	75	.15	.15	.30			1.19	1.10	1.34	1.40
	80	.31	.36	.30			.96	1.09	1.27	1.39

8	85	.08	.34	.30	.28		.94	1.08	1.01	1.38
	90	0	.39	.30		.98	1.20	1.07	1.20	1.46
	95	1.32	2.33	2.19		1.40	1.28	1.43	2.60	2.83
	100	1.60	2.75	2.19	1.62	1.61	1.49	1.42	3.09	3.03
12	0	.62	.58	.47	.42		.80	.99	1.43	1.57
	25	.51	.56	.46			.88	.98	1.39	1.54
	50	.44	.49	.45			1.03	.95	1.47	1.40
	75	.53	.30	.44			1.09	.92	1.62	1.36
	80	.55	.67	.43			.91	.91	1.46	1.34
	85	.41	.58	.43	.40		.81	.90	1.21	1.33
	90	.62	.55	.43		1.42	.83	.80	1.45	1.45
	95	1.32	3.72	2.89		1.40	1.33	1.31	2.65	2.71
	100	1.83	3.53	2.91	1.89	1.89	1.26	1.33	3.10	3.22
16	0	.87	.80	.60	.54		.67	.89	1.54	1.69
	25	.79	.65	.60			.60	.88	1.39	1.53
	50	.68	.57	.58			.72	.86	1.39	1.44

16	75	.81	1.12	.57			.87	.83	1.68	1.40
	80	.68	.98	.57			.75	.82	1.43	1.39
	85	.65	.98	.56	.51		.75	.81	1.40	1.37
	90	1.02	1.13	.56		1.41	.78	.81	1.80	1.94
	95	1.74	4.66	3.58		1.57	1.15	1.25	2.89	2.82
	100	2.01	4.72	3.57	2.14	1.92	1.17	1.27	3.18	3.19
20	0	.91	1.04	.72	.65		.59	.83	1.50	1.87
	25	.66	1.25	.69			.79	.82	1.45	2.07
	50	.76	.81	.70			.70	.80	1.47	1.50
	75	.98	1.18	.68			.67	.77	1.64	1.45
	80	.64	1.50	.66			.83	.77	1.48	1.43
	85	.75	1.15	.66	.61		.64	.76	1.39	1.42
	90	1.05	1.65	.69		1.59	.91	.75	1.96	2.40
	95	2.07	5.62	4.26		1.71	1.20	1.21	3.27	2.92
	100	2.27	5.72	4.26	2.34	2.02	1.21	1.23	3.48	3.25

Notation: 1. Actual

2. Singh-Griffith Method

3. Homogeneous Method

4. Lockhart-Martinelli Method

5. Quasi-Annular Method

Figure 28. Gravity Pressure Loss, Predicted and Actual: 12 ft/sec.

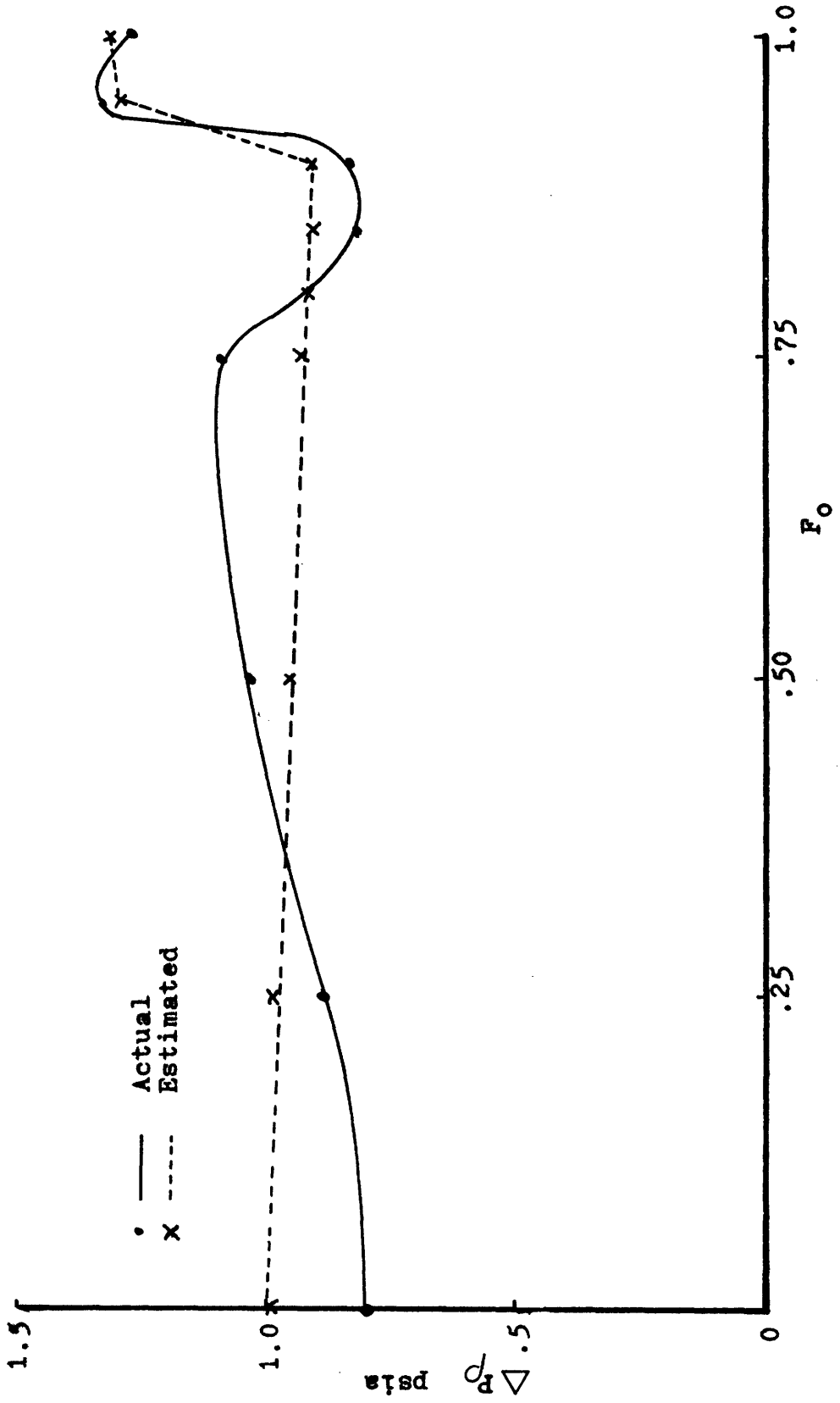

Figure 29. Friction Pressure Loss, Predicted and Actual: 12 ft/sec

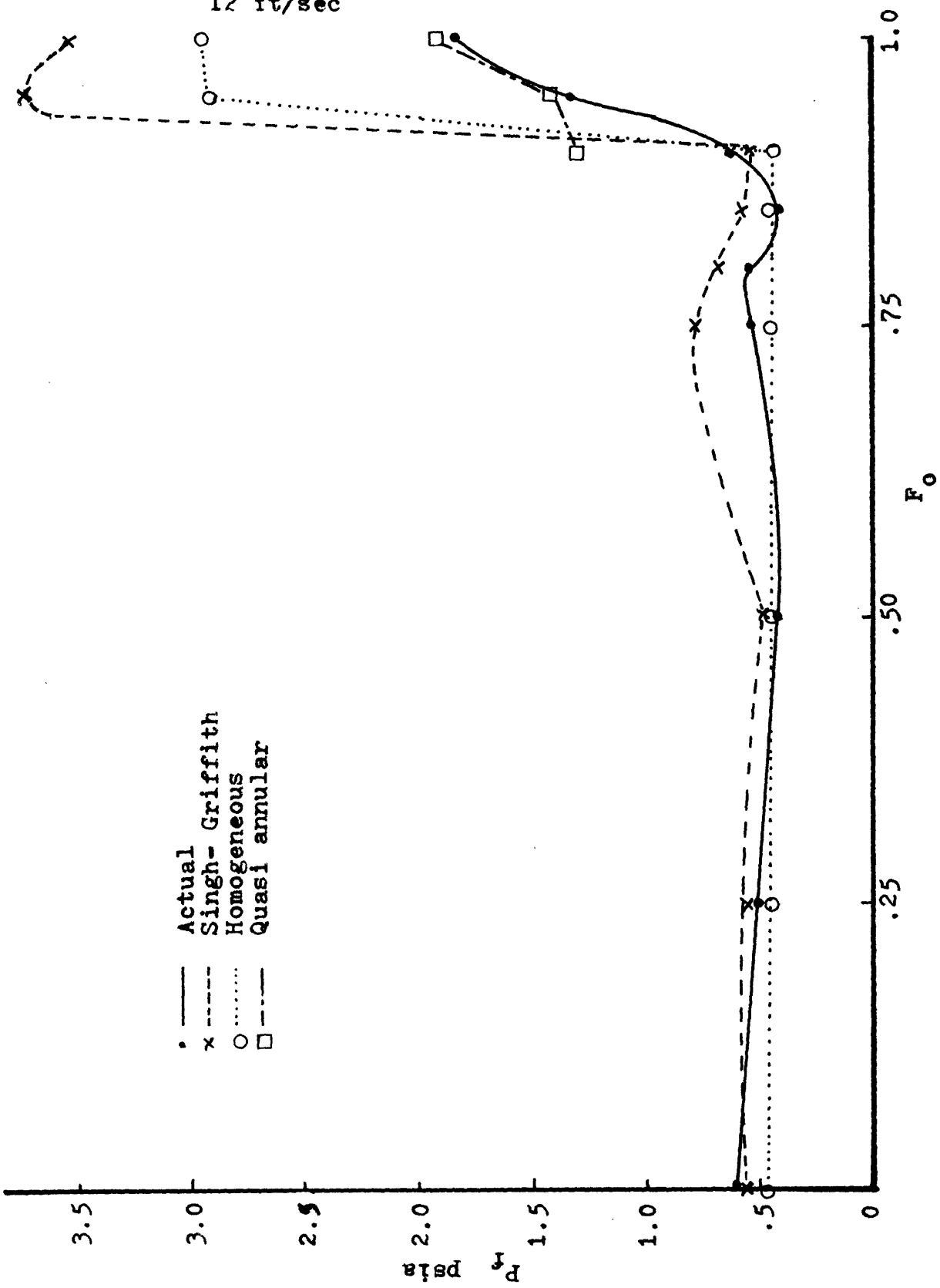

method. In this region the flow is predominately slug flow which this method is based upon.

b. Water froth boundary $<Fo\leq$ oil froth-water bubble boundary: The McAdams-Homogeneous method. In this region the fluid is in a froth state and the oil and water are mixed fairly uniformly. Also, the form of the air slugs is somewhat broken up. This method does not follow the actual values well, however, the average values match.

c. $F_o > .9$: The Quasi Annular Flow method. In this region the slugs of air become exceedingly long while the velocity of the oil on the wall reverses to an upward velocity, characteristic of annular flow. However, oil slugs are still present. The resulting values follow the actual pressure losses rather well.

When the estimates for the gravity and friction pressure losses are combined, acceptible estimates of the total pressure are obtained. Table 3 for all test values and Figure 31 for a mixture velocity of 12 ft./sec. show the comparison of actual to estimated values of total pressure loss. Although the individual pressures vary, the average deviation for the 12 ft//sec. case is .016 psi. Finally it should be noted that at low velocities the negative friction pressure loss discussed earlier causes the estimated values of total pressure to be consistently high.

D. Contact Angle Data

The results of the contact angle test are shown in Table 4. All materials except glass were preferentially wetted by the oil. This indicates that the oil would be expected next to the tube where the contact

TABLE 4.

Nujol and Water Contact Angles

Material	Contact Angle
Plexiglass	15.5°
Glass	154°
Copper	17.5°
Aluminum	13°
Cold rolled steel	28.5°
Galvanized sheet metal	34°

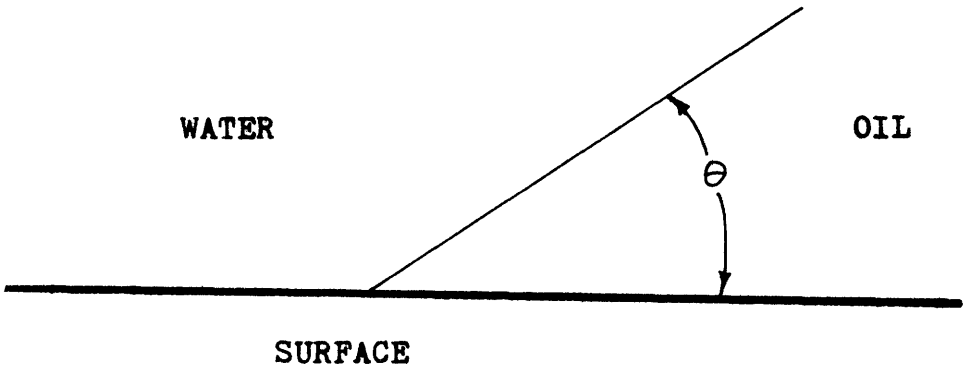

Figure 30. Contact Angle Definition.

Figure 31. Total Pressure Loss, Predicted and Actual: 12 ft/sec.

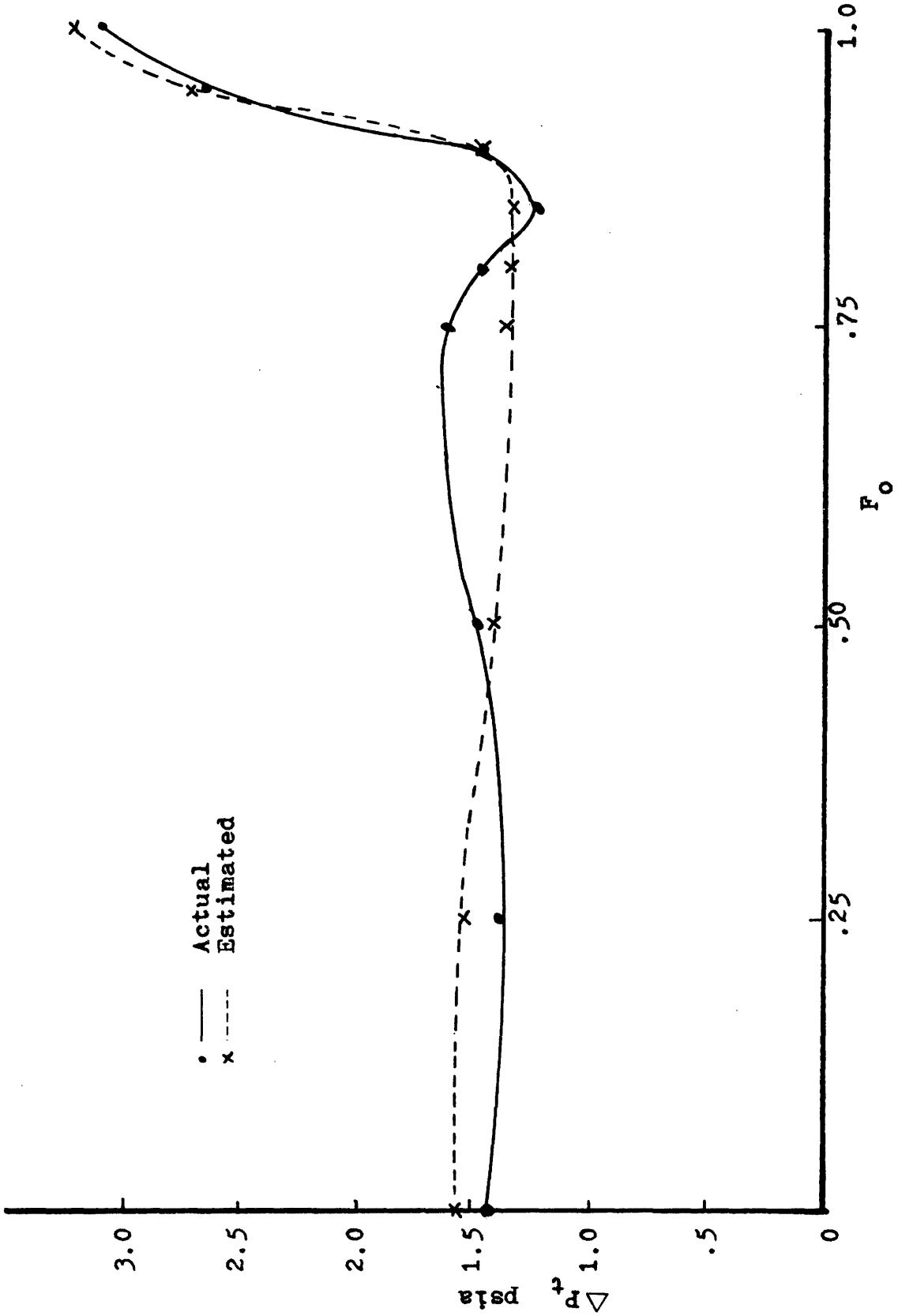

angle influence predominates. This, however, as indicated earlier is in opposition to the effects of density. In the case of glass, however, we can expect the water to remain next to the wall totally. This is because the contact angle and density effect are reinforcing.

The metals tested are those normally used in commercial piping. The contact angles of these metals are similar to those of plexiglass. Therefore, the trends and data obtained herein may be transferred, while those of tests in glass tubes should be employed only after the effect of contact angle has been proven negligible. Finally, these contact angle measurements are static tests and the dynamic contact angles may vary.

CHAPTER VI

CONCLUSIONS

A. GENERAL

1. The gas void fraction for a three phase slug flow may be determined by treating the two liquid phases as a single phase and using the Zuber Findley Plot.

2. The individual In Situ Liquid Phase Volume fractions can be correlated through knowledge of the gas void fraction, oil-in-liquid volume fraction and the liquid mass flow rates. See equation 5.12.

3. The relative velocities of the two liquids and the friction pressure loss depend on which fluid dominates the flow next to the wall.

4. The transition from water on the wall to oil on the wall depends on the relative liquid flows only.

5. Two phase oil-water flow is the limiting case of a three phase air-oil-water flow with negligible air flow.

6. A combination of pressure drop prediction methods based on flow regime is necessary to adequately predict the pressure losses of a three phase flow.

B. SPECIFIC

1. The transition from water on the wall to oil on the wall is independent of the gas flow rate and may be predicted using a flow regime map based on pressure deviations with the superficial water velocity as

a parameter.

2. In preparing engineering estimates of the friction pressure loss the viscosity of water may be used as the effective fluid viscosity up to the transition from liquid froth flow to oil dominated liquid flow. After which the viscosity of the oil may be used.

3. A flow regime map based on two phase oil-water flow may be used successfully to predict three phase flow liquid regime transitions.

4. The contact angles observed in these flow experiments are similar to those expected in actual applications.

CHAPTER VII

SUGGESTIONS FOR FURTHER WORK

The following further work is suggested:

A. The current work was performed at near atmospheric conditions. Hence, further testing should be performed at elevated pressures.

B. The mass flow rates for these tests did not vary substantially. Therefore, work with larger flow rates should be examined in order to determine the influence on the In Situ Oil phase Volume Fraction prediction correlation.

C. At the transition from water froth to oil froth at an F_o of about .85, the friction pressure loss abruptly rose then fell. The hypothysis that this pressure jump is caused by the shearing of oil bubbles between the wall and the air slugs should be verified or dismissed.

D. Further work should be done to verify and refine the Govier flow regime map for three phase flow.

E. Finally a method of dealing with the negative friction pressure loss effect should be investigated.

REFERENCES

1. Rasin Tek, M., "Multiphase Flow of Water, Oil and Natural Gas Through Vertical Flow Strings", Journal of Petroleum Technology, pp. 1029-1036, October, 1961.

2. Galyamov, M. N. and Karpushin, N. L., "Change in the Viscosity of the Liquid Phase During The Movement of Gas-Water-Oil Mixtures in Pipelines", Transport i khranenie nefti i nefteproduktov, no. 2, pp.14-16, 1971.

3. Bocharov, A. N., Andriasov, R. S. and Sakharov, V. A., "Investigation of the Motion of Gas-Water-Oil Mixtures in Horizontal Pipes", Neftepromyslovoe delo, no. 6, pp. 27-30, 1972.

4. Foreman, F. J. and Woods, P. H., "Void Fraction Calculations for Three Phase Flow in a Vertical Pipe", Project Report Course 2.673, M.I.T., 1975.

5. Govier, G. W., Radford, B. A. and Dunn J.S.C., "The Upwards Flow of Air-Water Mixtures", The Canadian Journal of Chemical Engineering, pp. 58-70, August, 1957.

6. Govier, G. W., Sullivan, G. A. and Wood, R. K. "The Upward Flow of Oil-Water Mixtures", The Canadian Journal of Chemical Engineering, pp. 67-75, April, 1961.

7. Zuber, N. and Findlay, J. A., "Average Volumetric Concentration in Two-Phase Flow Systems", Journal of Heat Transfer, pp. 453-468, November, 1965.

8. Griffith, P. and Wallis, G. B., "Two Phase Slug Flow", Journal of Heat Transfer, Trans. ASME, p. 307, August, 1961.

9. Orkiszewski, J., "Predicting Two-Phase Pressure Drops in Vertical Pipe", Journal of Petroleum Technology, pp. 829-838, June, 1967.

10. Singh, G. and Griffith, P., "Determination of the Pressure Drop Optimum Pipe Size for a Two-Phase Slug Flow in an Inclined Pipe", ASME Paper No. 70-Pet-15.

11. Collier, J. G., "Convective Boiling and Condensation", McGraw-Hill, 1972.

12. Govier, G. W. and Aziz, K., "The Flow of Complex Mixtures in Pipes", Van Nostrand Reinhold Company, 1972.

13. Rohsenow, W. M. and Choi, H. Y., "Heat, Mass, and Momentum Transfer", Prentice-Hall, 1961.

APPENDIX A: Foreman and Woods Data:

TABLE A-1

Void Fraction Data

Q_o (GPM)	Q_w (GPM)	Q_a (GPM)	h_o (in.)	h_w (in.)	h_a (in.)	p_{1a} (psi)	p_{2a} (psi)
3.5	3.5	2.07	31.75	32.5	16.75	20.0	13.5
3.5	3.5	4.14	27.25	27.25	26.75	20.8	13.8
3.5	3.5	6.21	26.0	25.0	30.0	21.75	14.75
3.5	3.5	8.28	22.25	23.25	35.5	23.0	16.0
3.5	3.5	10.35	22.75	22.0	36.25	27.0	20.0
3.5	3.5	12.42	22.75	21.5	37.0	27.0	20.0
3.5	3.5	14.49	19.0	21.75	40.0	27.5	20.5
3.5	3.5	16.56	19.0	20.75	41.0	28.0	21.0
3.5	3.5	18.63	19.0	20.25	42.0	29.0	22.0
3.5	3.5	20.70	17.25	18.5	45.75	30.0	23.0
1.0	4.0	2.07	12.5	47.25	21.0	18.0	11.0
1.0	4.0	4.14	10.25	40.75	30.0	17.0	10.0
1.0	4.0	6.21	9.5	35.5	36.25	17.5	10.5
1.0	4.0	8.28	8.0	29.5	43.75	18.0	11.0
1.0	4.0	10.35	7.0	28.0	45.0	19.0	12.0
1.0	4.0	12.42	5.0	28.0	47.0	19.0	12.0
1.0	4.0	14.49	4.0	24.0	49.0	20.0	13.0
1.0	4.0	16.56	3.0	22.0	51.0	21.0	14.0
1.0	4.0	18.63	4.5	23.0	52.5	21.0	14.0
1.0	4.0	20.70	2.5	25.0	56.5	22.0	15.0

TABLE A-2

Three-Phase Flow Data Reduction

Q_o (ft^3/sec)	Q_w (ft^3/sec)	Q_a (ft^3/sec)	α_a (in/in)	$Q_a/A\alpha_a$ (ft/sec)	Q/A (ft/sec)
.0022	.0089	.00443	.26	5.554	5.062
.0022	.0089	.00886	.37	7.805	6.506
.0022	.0089	.0133	.4475	9.687	7.953
.0022	.0089	.0177	.54	10.684	9.387
.0022	.0089	.0221	.55	13.097	10.82
.0022	.0089	.0266	.58	14.95	12.3
.0022	.0089	.031	.605	16.7	13.72
.0022	.0089	.0354	.629	18.34	15.156
.0022	.0089	.0399	.648	20.07	16.62
.0022	.0089	.0443	.6975	20.7	18.06
.0078	.0078	.00443	.2068	6.98	6.53
.0078	.0078	.00886	.33	8.75	7.973
.0078	.0078	.0133	.37	11.72	9.42
.0078	.0078	.0177	.438	13.2	10.85
.0078	.0078	.0221	.4475	16.1	12.3
.0078	.0078	.0226	.4568	18.98	13.76
.0078	.0078	.031	.494	20.45	15.2
.0078	.0078	.0354	.506	22.8	16.62
.0078	.0078	.0399	.52	25.0	18.09
.0078	.0078	.0443	.565	25.56	19.52

APPENDIX B: Analysis of Parametric Effects on Two Phase Friction Pressure Loss.

The data obtained in the two phase portion of this experimentation can be combined with the constant velocity data obtained from Govier, Sullivan and Wood (Table B-1) to ascertain the influences on the friction pressure loss of the diameter, viscosity of the fluid, and the mixture velocity. The results of this comparison are shown in Figures B1 to B7. From these figures we may conclude the following:

1. A variation in the diameter of the tube shows no definite influence on the pressure loss, however the location of the transition from water on the wall to oil is not influenced. Figs. B1 and B2.

2. The viscosity of the oil influenced the level of pressure loss after the transition. As a result we see clearly where the viscosity of the water is important and where the oil predominates. Also, the oil viscosity did not influence the location of the transition F_o. Figs. B3 and B4.

3. Finally the mixture velocity influences the level of the pressure loss, but again the transition F_o is relatively independent. Figs. B5 to B7.

TABLE B 1.

Govier, Sullivan and Wood Data

Test #	$\tilde{\upsilon}_m$	T	Q_w	Q_o	Q_o/Q_w	ΔP_t	ΔP_ρ	ΔP_f	Q_t	F_o
μ_o= .936 cp										
425	1	78	.000573	.00596	4.35	.822	.797	.025	.0065	.92
327	1	80	.00183	.00358	1.27	.879	.854	.025	.0054	.66
277	1	80	.00573	.00056	.079	.993	.982	.011	.0063	.09
429	2	77	.000573	.0108	12.0	.807	.789	.018	.0114	.95
332	2	79	.00183	.00955	3.06	.842	.818	.024	.0114	.84
271	2	76	.00573	.00591	.800	.918	.886	.032	.0116	.51
368	2	73	.0103	.00146	.103	.996	.974	.022	.0117	.12
434	3	79	.000573	.01675	17.0	.817	.787	.030	.0173	.97
337	3	79	.00183	.0156	6.78	.834	.800	.034	.0174	.90
266	3	74	.00573	.0119	1.75	.893	.850	.043	.0176	.67
372	3	75	.0103	.00716	.362	.959	.905	.054	.0175	.41
487	3	82	.0149	.00252	.133	1.007	.965	.042	.0174	.14
439	4	79	.000573	.0225	-	.840	.782	.058	.0231	.98
342	4	79	.00183	.0215	9.20	.851	.795	.056	.0233	.92
258	4	73	.00573	.0189	3.41	.887	.834	.053	.0246	.77

375	4	75	.0103	.0144	1.15	.956	.871	.085	.0247	.58
490	4	82	.0149	.00955	.530	.989	.915	.074	.0245	.39
300	4	78	.0183	.00474	.241	1.016	.935	.063	.0230	.21
440	5	79	.000573	.0264	-	.853	.782	.071	.0270	.98
344	5	76	.00183	.0264	10.0	.869	.792	.077	.0282	.94
274	5	71	.00573	.0225	3.84	.890	.825	.065	.0282	.80
377	5	75	.0103	.0191	1.83	.958	.857	.101	.0294	.65
492	5	82	.0149	.0144	.839	.996	.893	.103	.0293	.49
303	5	77	.0183	.0120	.530	1.012	.910	.102	.0303	.40
μ_o= 20.1 cp										
217AA	1	78	.000588	.00568	6.13	.897	.855	.042	.0063	.91
132AB	1	72	.00188	.00396	1.09	.927	.679	.248	.0058	.68
39AA	2	66	.000589	.0110	21.6	.926	.854	.072	.0116	.95
67AB	2	73	.00188	.00945	7.05	.943	.607	.336	.0113	.73
89AC	2	75	.00586	.00663	.784	.953	.931	.022	.0125	.53
103AD	2	73	.0106	.00157	-	1.006	.980	.026	.0122	.13
198AA	3	75	.000589	.01815	39.05	.945	.847	.098	.0187	.97
133AB	3	71	.00188	.01618	11.94	.957	.608	.349	.0181	.90

176AC	3	70	.00586	.01216	1.62	.972	.902	.070	.0180	.68
237AD	3	73	.01060	.00753	.619	.997	.945	.052	.0181	.41
70AA	4	75	.000589	.0238	62.0	.966	.845	.121	.0244	.98
76AB	4	74	.00188	.01995	17.3	.971	.568	.403	.0218	.91
179AC	4	78	.00586	.01819	2.36	.966	.885	.081	.02405	.76
228AD	4	75	.0106	.01457	1.21	1.028	.915	.113	.0252	.58
122AE	4	66	.01885	.00565	.225	1.039	.965	.074	.0245	.23
205AA	5	67	.000589	.02795	52.0	.994	.842	.152	.0285	.98
134AB	5	72	.00188	.02719	23.2	1.003	.557	.446	.0291	.94
96AC	5	78	.00586	.02385	3.16	.961	.881	.080	.0292	.80
109AD	5	74	.0106	.01813	-	1.045	.906	.139	.0287	.63
124AE	5	70	.01885	.01340	.476	1.052	.937	.115	.0323	.42
μ_o = 150 cp										
50BA	1	82	.000589	.00529		.902		.017	.00588	.90
40BB	1	83	.00188	.00356		.945		.243	.00544	.65
62BA	2	84	.000589	.01132		1.046		.171	.0119	.95
32BB	2	82	.00188	.00995		1.224		.607	.0118	.84
12BC	2	81	.00586	.00613		.966		.027	.0120	.51
81BD	2	74	.01060	.001823		1.007		.025	.0124	.15

54BA	3	78	.000589	.01653	1.384	.509	.0171	.97
135BB	3	77	.00188	.01562	1.418	.826	.0175	.89
13BC	3	82	.00589	.01131	.964	.042	.0172	.66
71BD	3	78	.0106	.00785	.989	.041	.0185	.43
55BA	4	78	.000589	.02118	1.576	.700	.02177	.97
34BB	4	82	.00188	.0239	1.681	1.102	.02578	.93
16BC	4	84	.00586	.0188	.979	.072	.0247	.76
73BD	4	78	.0106	.0148	1.006	.075	.0254	.58
122BE	4	75	.01885	.00616	1.043	.07	.0251	.25
57BA	5	76	.000589	.03045	1.943	1.068	.0310	.98
138BB	5	76	.00188	.0281	1.894	1.320	.02998	.94
128BC	5	77	.00586	.02355	1.002	.124	.0294	.80
77BD	5	78	.0106	.02120	1.059	.139	.0318	.67
90BE	5	74	.01885	.01131	1.052	.097	.0302	.38

Figure B1. Friction Pressure Loss, Diameter Varied, 2 ft/sec: Two Phase Flow.

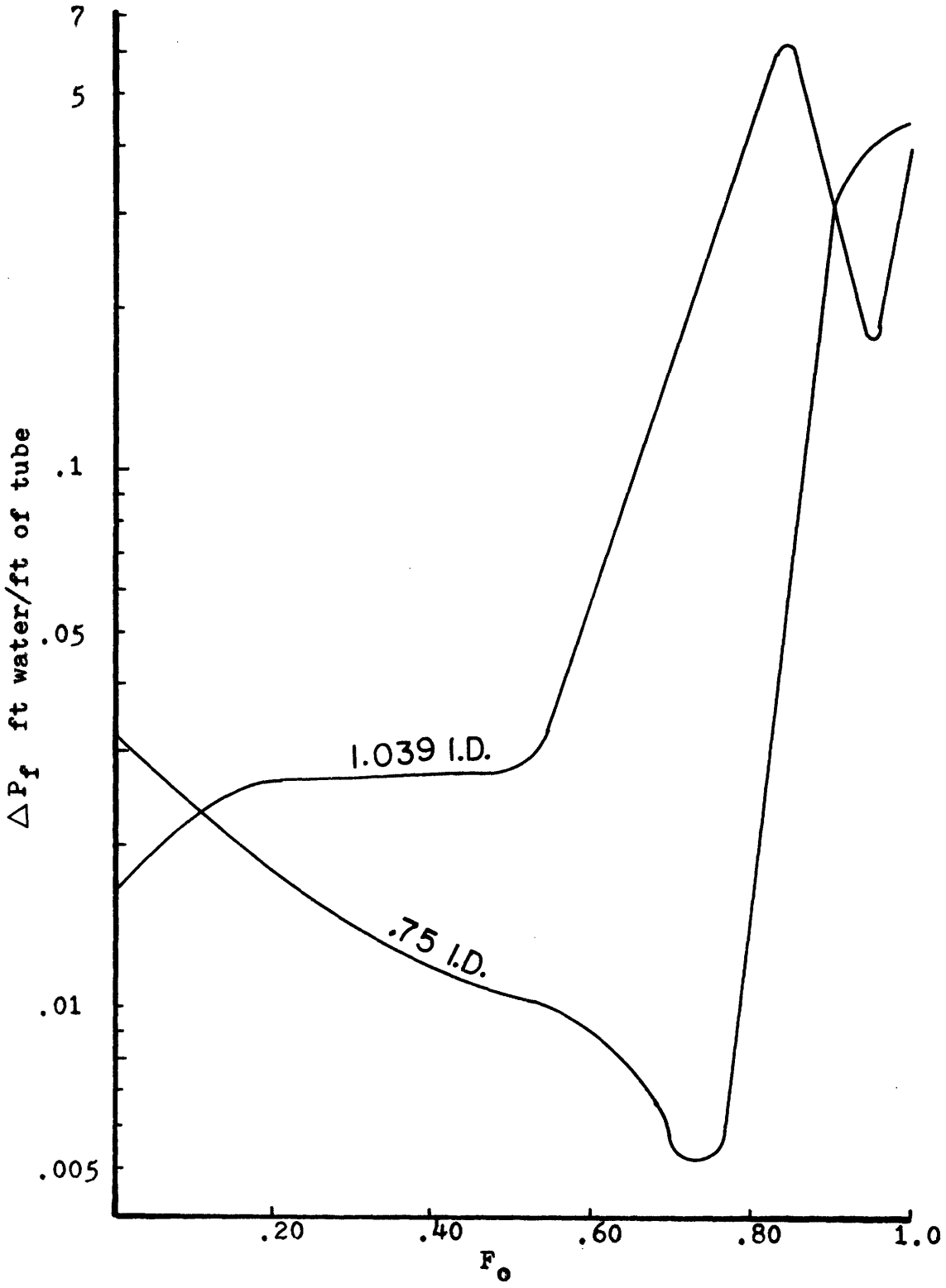

Figure B2. Friction Pressure Loss, Diameter Varied, 3 ft/sec: Two Phase Flow.

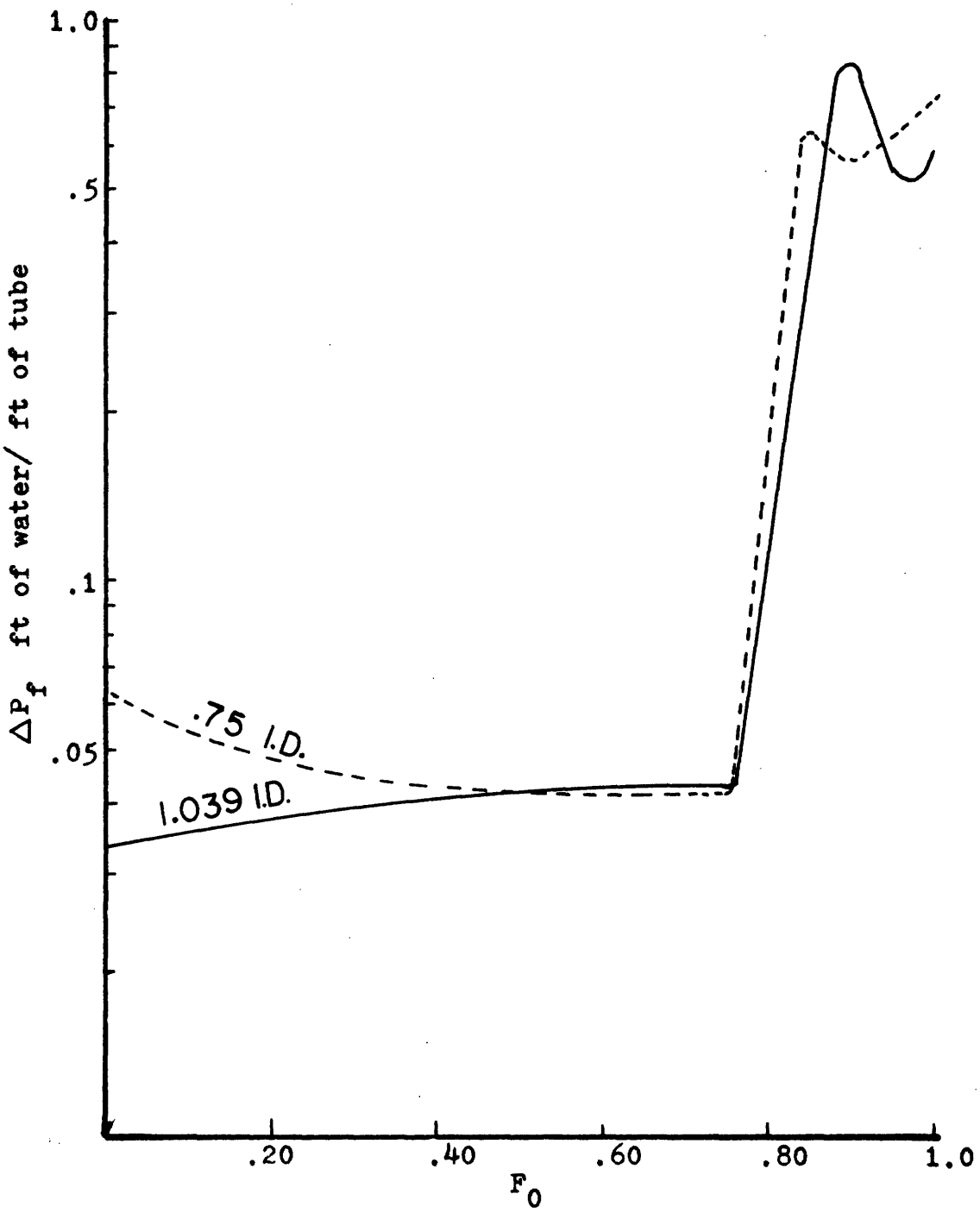

Figure B3. Friction Pressure Loss, Viscosity Varied, 2 ft/sec: Two Phase Flow.

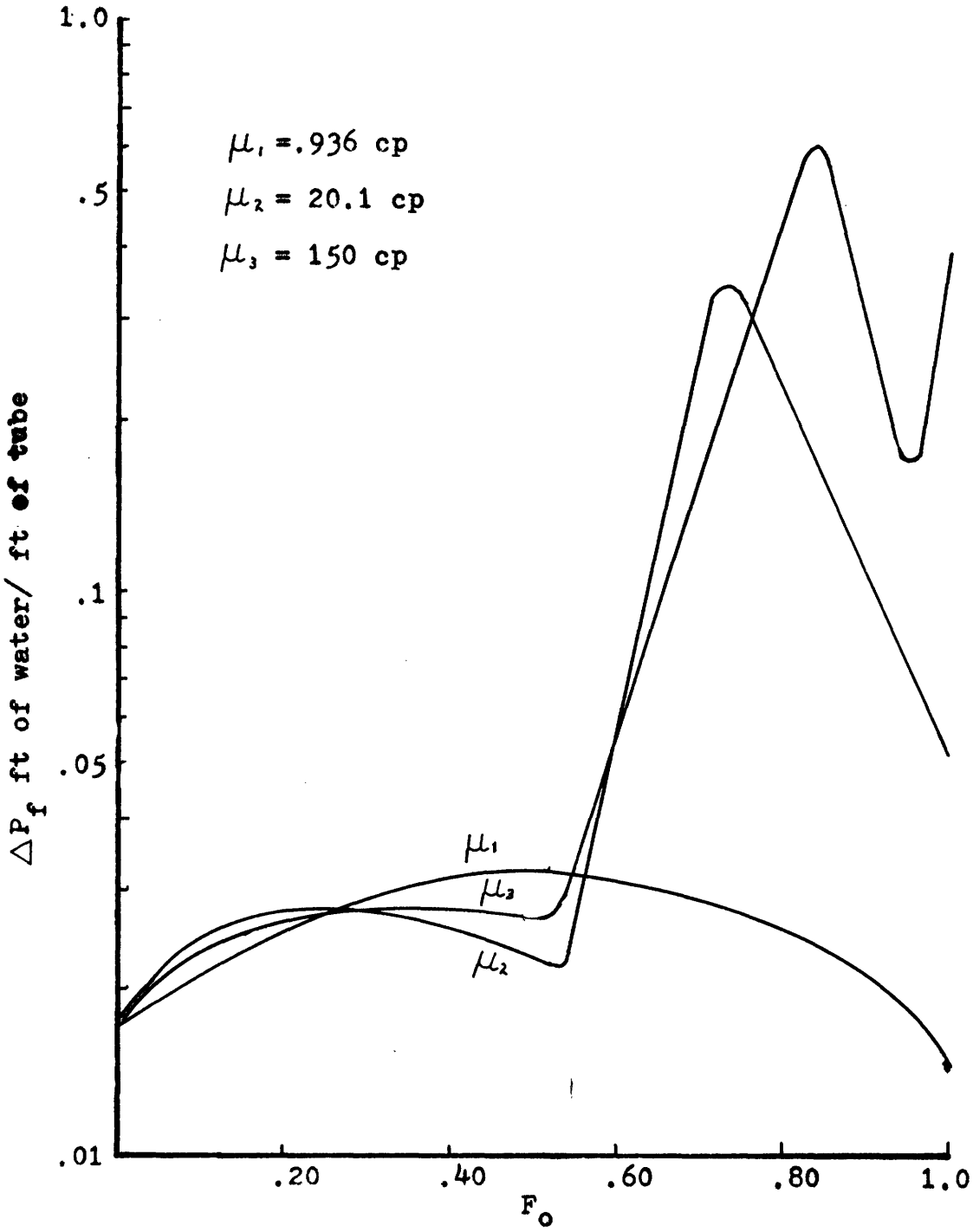

Figure B4. Friction Pressure Loss, Viscosity Varied, 3 ft/sec: Two Phase Flow.

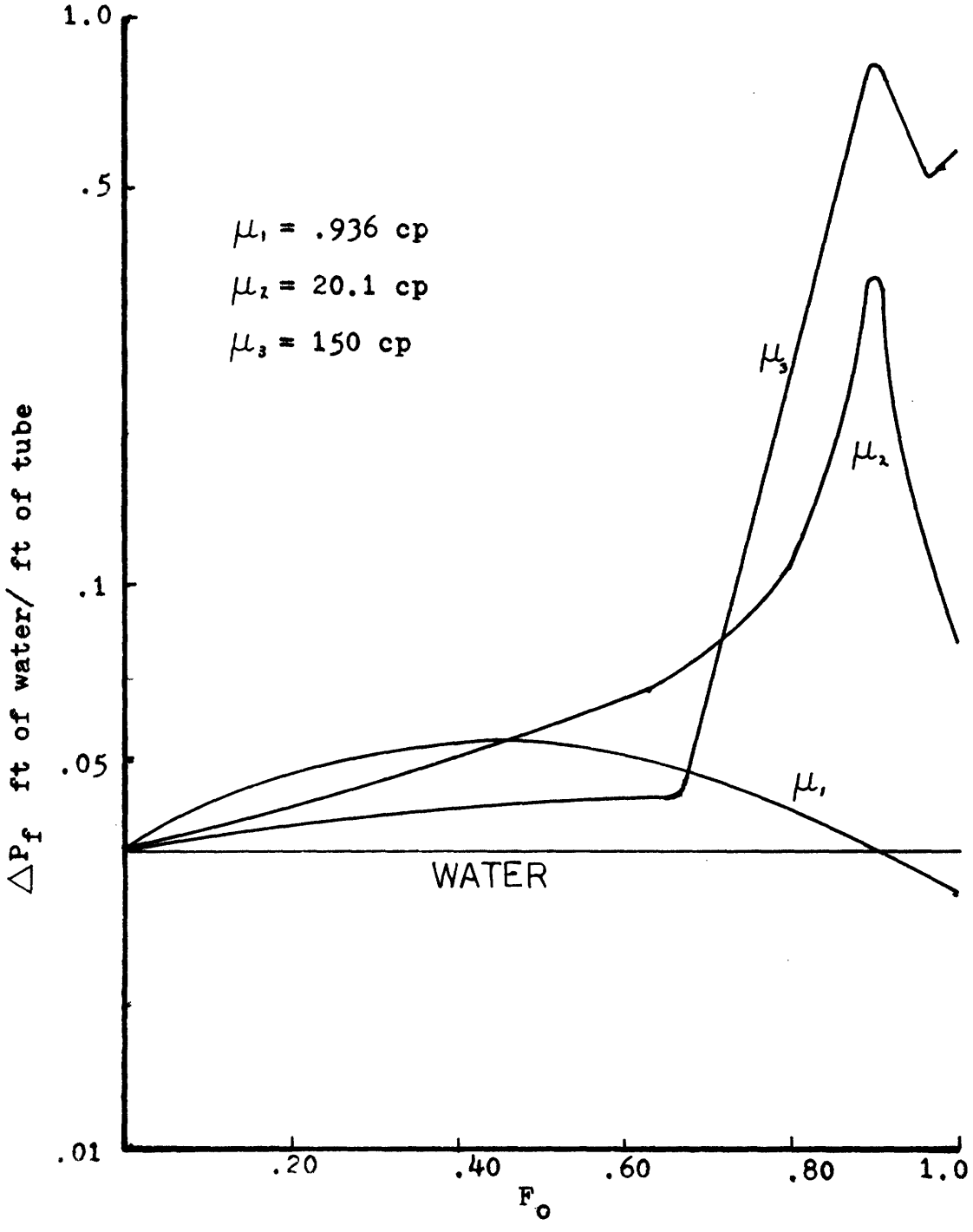

Figure B5. Friction Pressure Loss, Mixture Velocity Varied, 150 cp: Two Phase Flow.

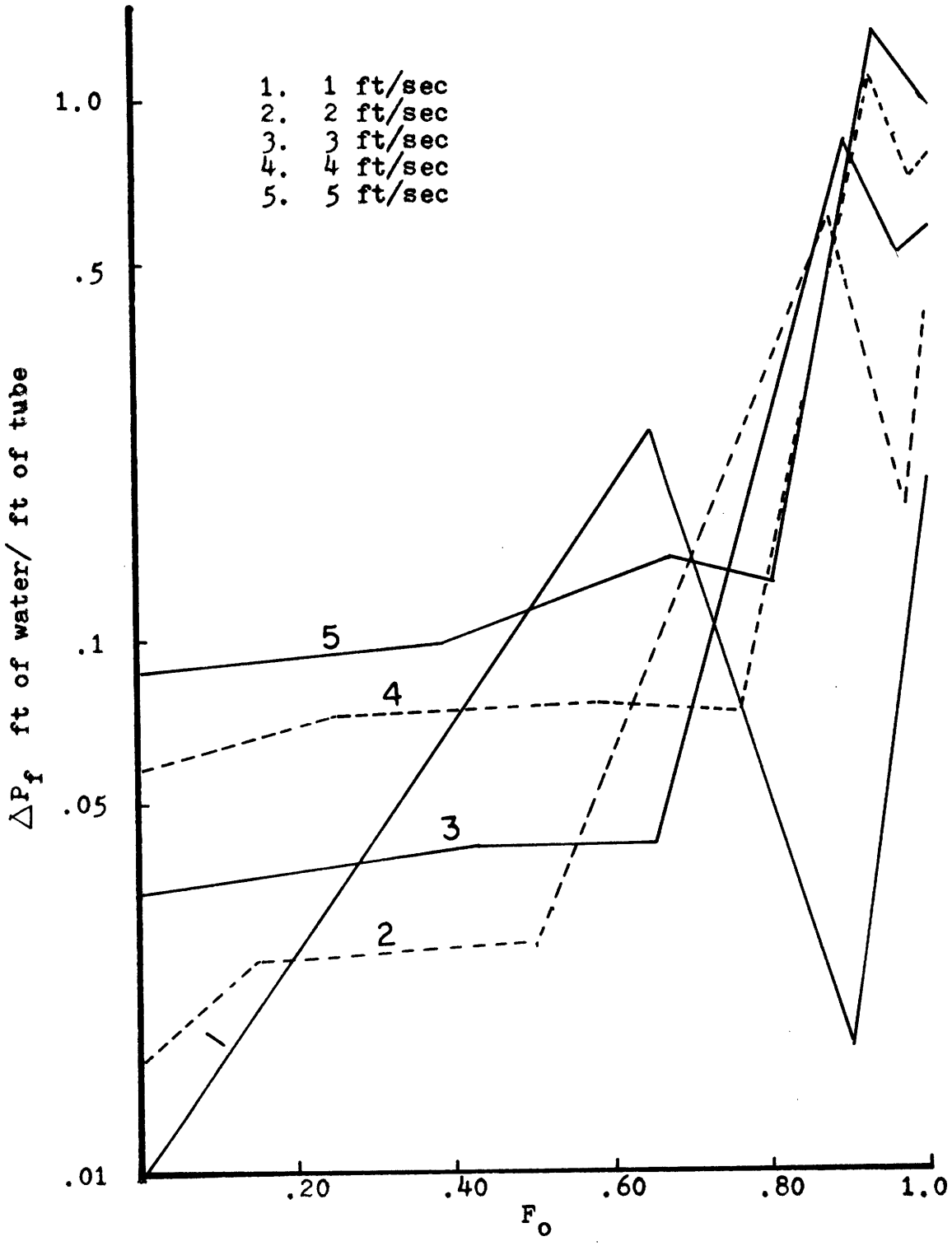

Figure B6. Friction Pressure Loss, Mixture Velocity Varied, 20.1 cp: Two Phase Flow.

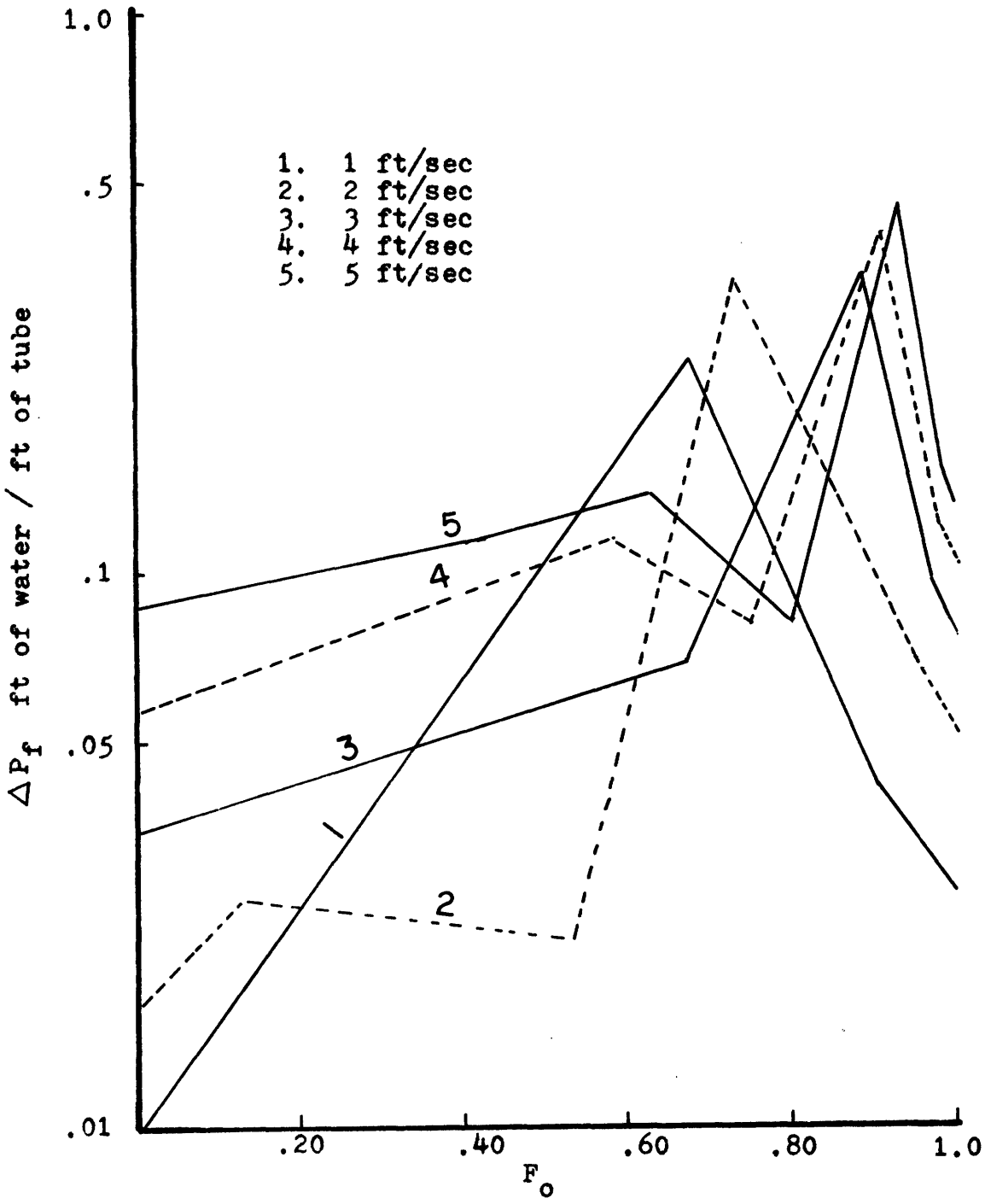

Figure B7. Friction Pressure Loss, Mixture Velocity Varied, .936 cp: Two Phase Flow.

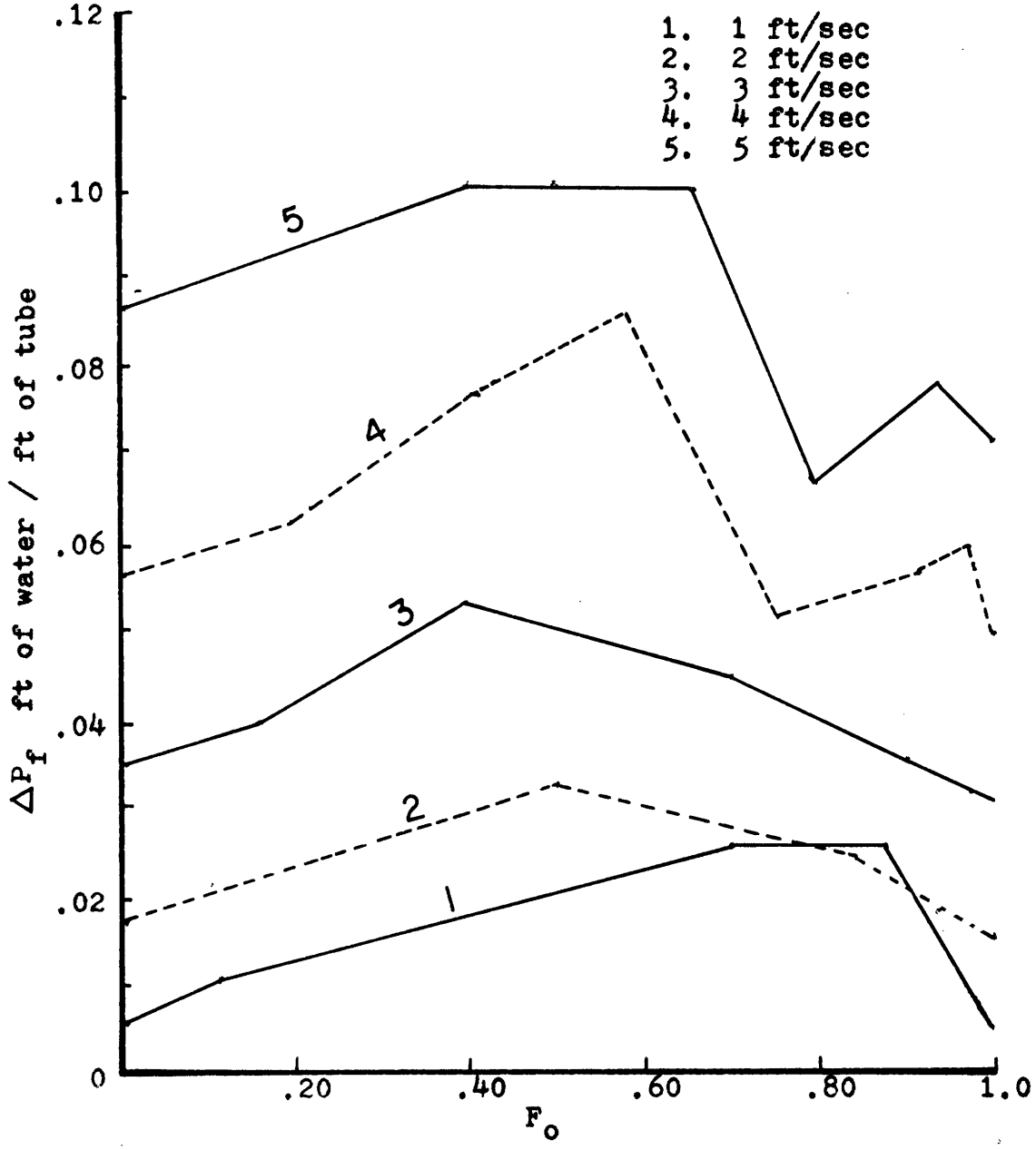

APPENDIX C: Flow Regime Visual Observations.

Figure C1 shows a typical friction pressure loss curve disected into four main flow regime areas. The variation of this curve is keyed to Govier's flow regime map (Fig. 14) and can be explained as follows:

A. $0<F_o \leq a$: In this region the water predominates the fluid flow and can be characterized as a typical slug flow. Figure C2 shows a typical view of the tube. In region A the fluid is in counter flow around the air slugs while in region B the fluid flows at a rate commensurate with that of the air slugs. The oil is distributed throughout the water in small bubbles. At higher velocities the negative shear around the air slugs is small compared to that in the liquid slugs. As does Singh and Griffith the negative shear can be assumed to be neglected in most cases. When the oil in liquid volume fraction is increased from 0, the size of the liquid slugs decreases and the counterflow area thickens. This causes a decrease in the friction pressure loss. This decrease continues until the regime change at a.

B. $a<F_o<b$: At the transition a, the liquid flow changes to a froth. The water still predominates the flow (Fig. C3) next to the wall, but the oil bubbles in the water slug area begin to coalesce into oil slugs. The area A is still in counterflow, however in area B the water flow around the oil slugs in cocurrent. Hence the effective length of the water slugs begins to increase and the friction loss increases. As the water in the fluid slug is completely replaced by oil, the layer of

Figure C1. Typical Friction Pressure Loss Curve.

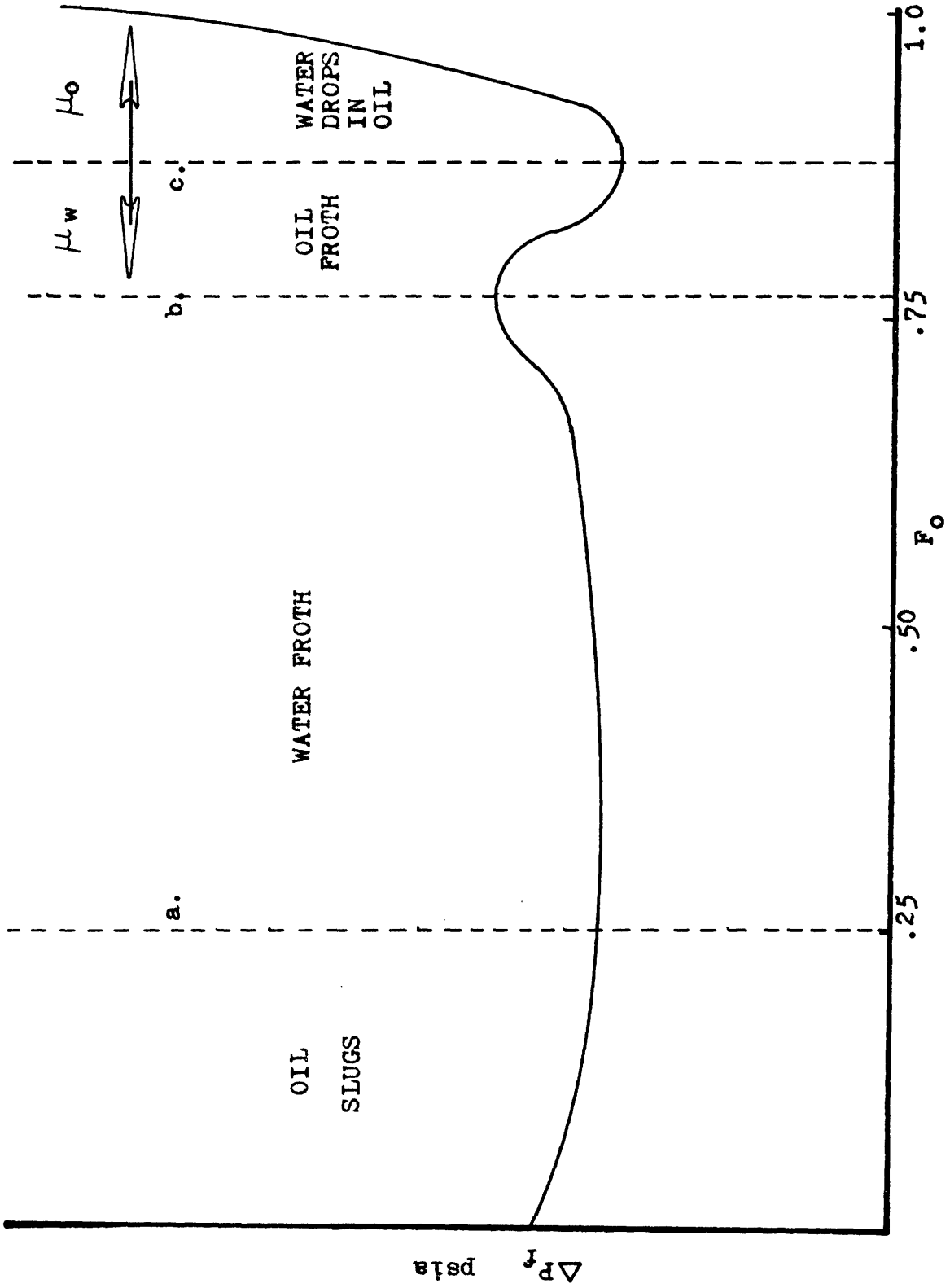

Figure C2 & C3. Flow Regime Diagram.

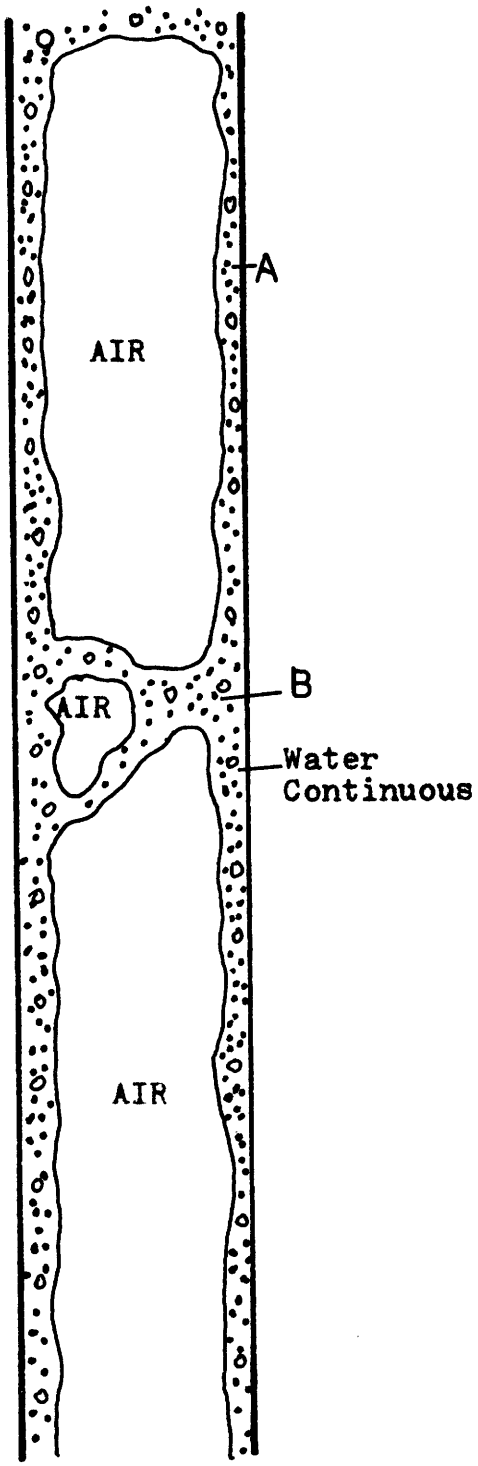

Fig. C2.

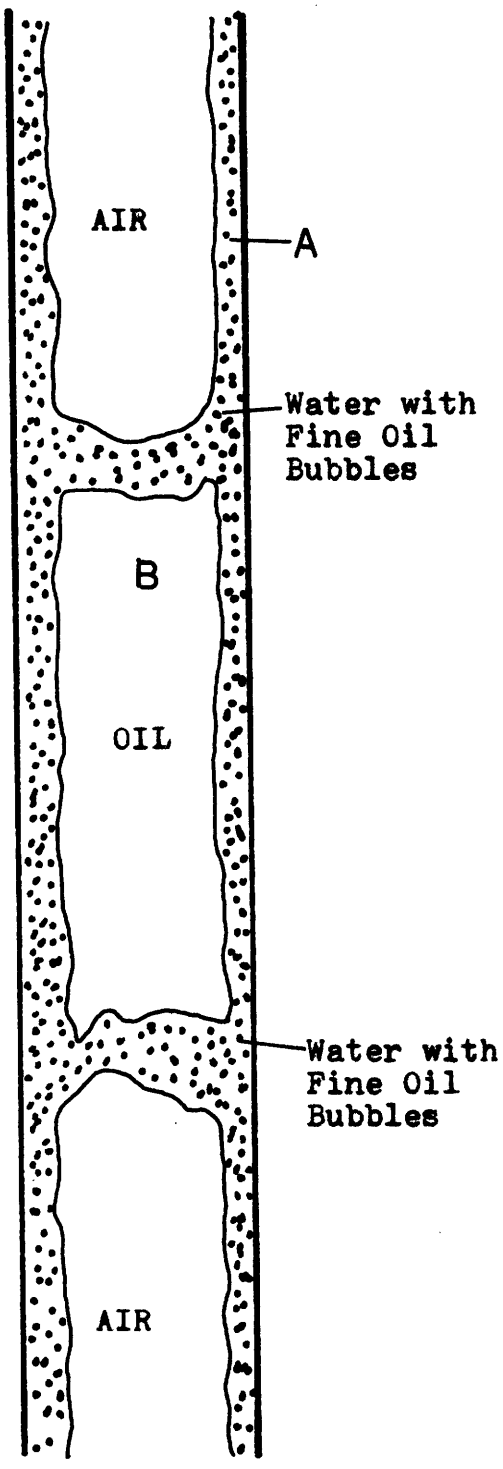

Fig. C3.

water on the tube wall becomes thinner and thinner until at the transition b the layer is too thin to contain any oil bubbles, and the bubbles are sheared between the wall and the air slugs. When this occurs the friction loss makes a sharp upward jump until the oil bubbles are forced out of the water layer. The pressure jump is point b on Figure C1.

C. $b<Fo<c$: At b the flow changes from water dominated froth to oil froth and the water is considered to be bubbles of water in oil. The exception is that a thin layer of water still persists on the wall of the tube. However, this layer is too thin to contain any oil bubbles. The laminar nature of the oil flow dampens the turbulence of the water and air and transition to pure slug flow is quickly achieved. At point c, full slug flow is achieved and the water is finally replaced by oil on the wall. When this occurs the counterflow friction loss dominated now by the viscosity of the oil, decreases. This dip can be seen at point c in Figure C1.

D. $c<Fo\leq 1.0$: In this region the flow transitions from pure slug flow to a quasi annular flow. As Fo increases, the counterflow velocity region (A in Fig. C5) reverses to co-current and increases in thickness while that of the slug region (B) decreases in size. After this reversal the combination of the oil viscosity and the increased upward velocity cause a sharp rise in the pressure losses. Again, this is apparent in Figure C1.

Figure C4 & C5. Flow Regime Diagram.

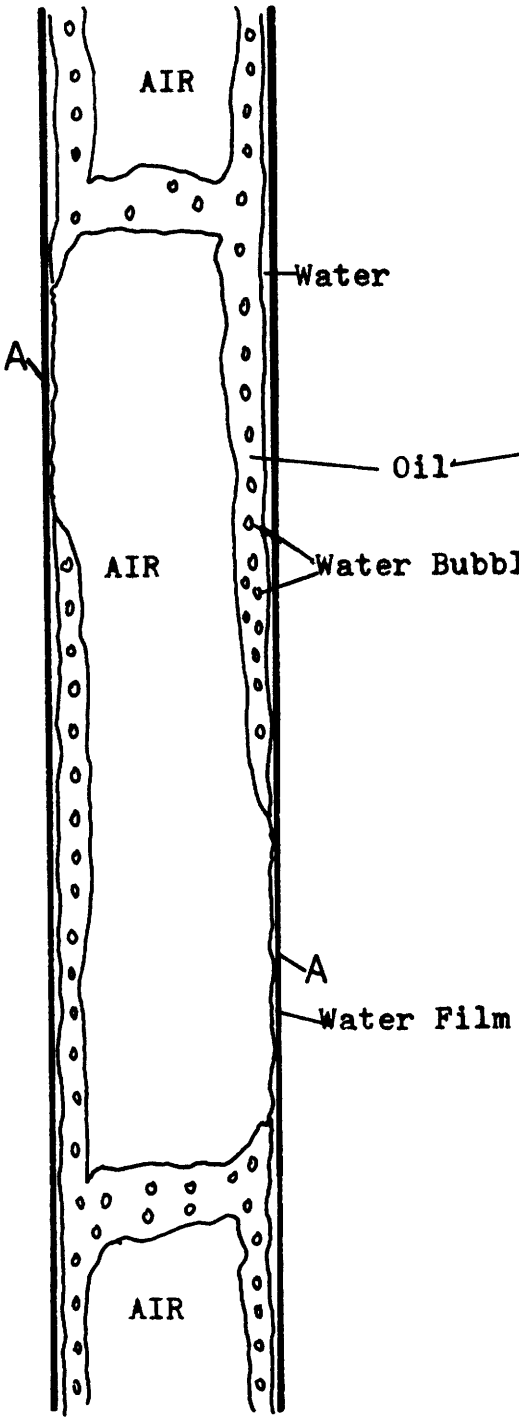

Fig. C4.

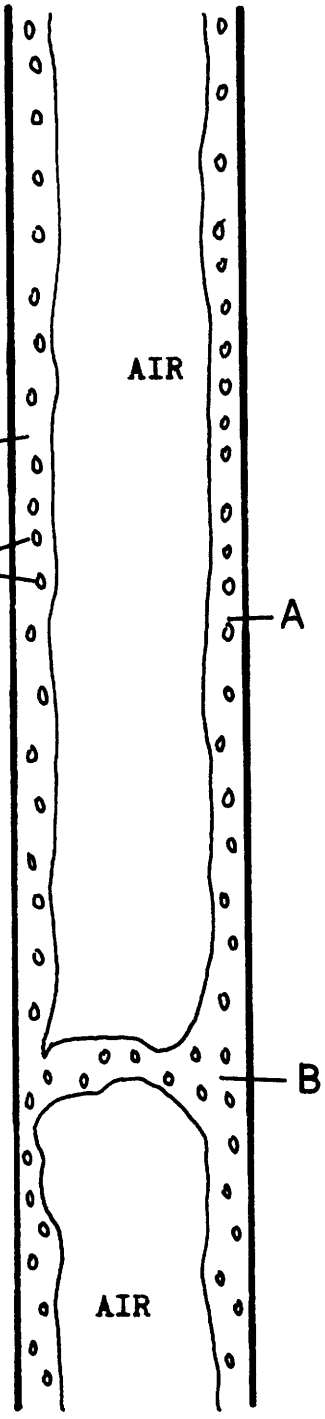

Fig. C5.

APPENDIX D: Derivation of Annular Flow Pressure Drop Method.

Annular flow is characterized by a continuous column of gas and a continuous annulus of fluid in co-current flow (A in Fig. D1) while slug flow is characterized by counter fluid flow over the gas slugs and co-current flow in the fluid slugs (B in Fig. D1). However, in the transition both co-current annulus and slug fluid flows occur simultaneously. Therefore the basis of this method is the assumption that transition flow can be modeled as a basic annular flow with a decreased annular fluid velocity. The decrease accounts for the remaining fluid slugs. In addition, in calculating the friction pressure loss the modified annular velocity of the fluid in the annulus is assumed to be the velocity of the fluid flowing alone in the entire tube.

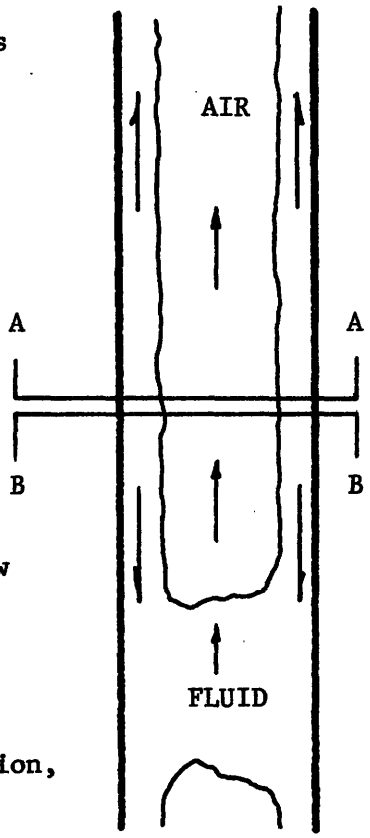

FIG. D1

From annular flow the fluid velocity is as follows:

$$\tilde{v}_f = \frac{Q_f}{A\alpha_f} \qquad (D\ 1)$$

This can then be modified for the Quasi-annular flow by a constant K, which is less than one.

$$\tilde{v}_f = \frac{KQ_f}{A\alpha_f} \qquad (D\ 2)$$

Based on this the following pressure loss analysis is derived:

$$Re_f = \frac{KQ_f D\rho_f}{A\alpha_f \mu_f g_o} \qquad (D\ 3)$$

Due to the high viscosity of the Nujol, the oil flow was laminar throughout the experiment. Hence the laminar friction factor equation is used.

$$f = \frac{16}{Re_f} = \frac{16A\alpha_f \mu_f g_o}{KQ_f D\rho_f} \qquad (D\ 4)$$

The shear stress is then:

$$\tau = \frac{f\rho v_f^2}{2g_o} = \frac{8\mu_f KQ_f}{A\alpha_f D} \qquad (D\ 5)$$

and the friction pressure loss is:

$$\Delta p_f = \frac{4\tau}{D} = \frac{32K\ \mu_f Q_f}{AD^2\alpha_f} \qquad (D\ 6)$$

which is a constant (K) times the loss associated with a complete annular flow.

In calculating the total friction pressure loss of the flow, we must recognize the transitional nature of the flow. That is, both annular and slug flows contribute to the loss. Therefore, we can assume that the total loss due to friction will be a portion of a full annular flow superimposed over the slug losses. We may then say that the total friction pressure loss is as follows:

$$\Delta p_f = K \Delta p_{f_{annular}} + (1-K)\Delta p_{f_{slug}} \qquad (D\ 7)$$

The annular flow portion is calculated as in equation D 6 while the slug flow portion can be assumed to be that at Fo equal to zero where slug flow predominates.

Finally, the weighting factor K must be determined. In the flow investigated the quasi annular flow appeared only above the froth critical oil in liquid volume fraction. In this case approximately .85. Also, the flow was nearly annular at Fo equal to one. If, based on this, we assign a value of .9 to K at Fo equal to one, we may linearly interpolate the values of K as shown in Fig. D 2.

The values for the total friction pressure loss derived from the above analysis are shown in Table 3 of the main text and show very close results.

Figure D 2. Linear Interpolation of the Factor K.

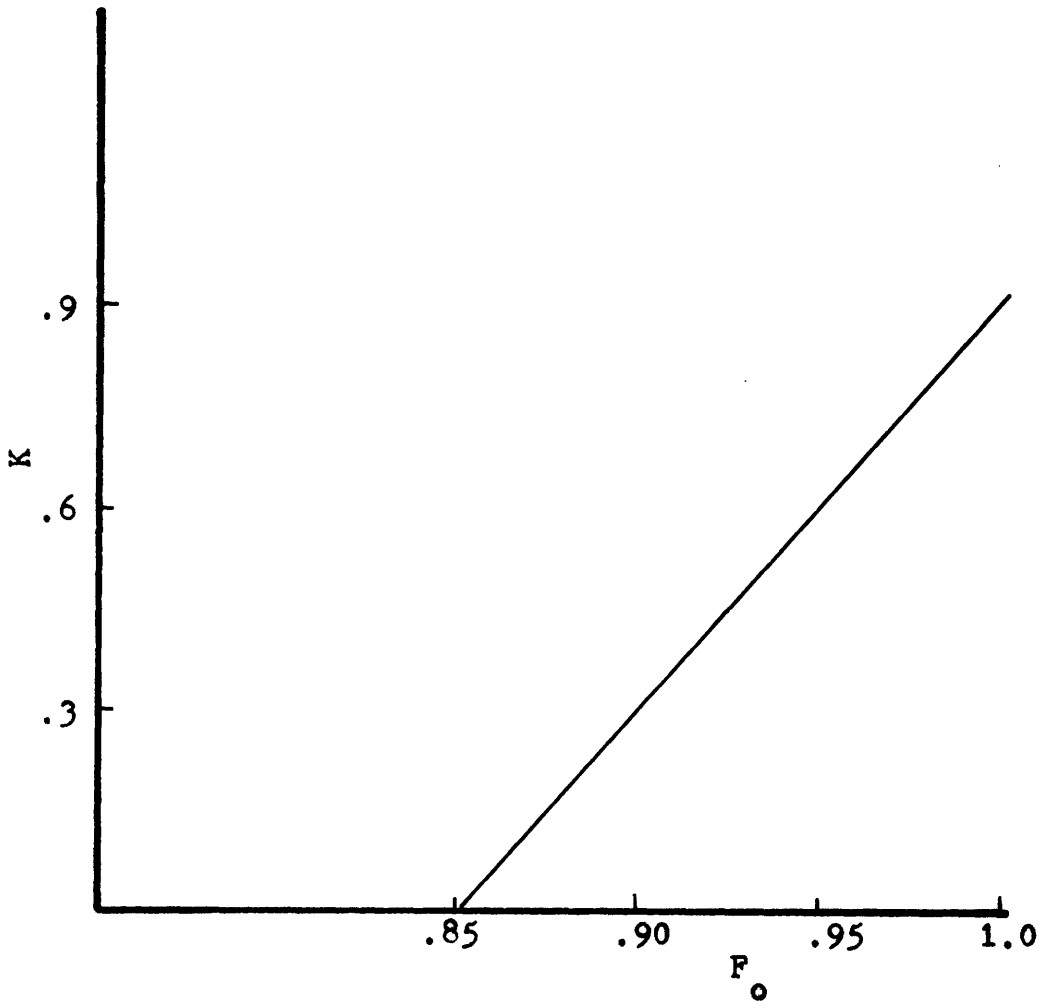

APPENDIX E. Physical Data.

OIL(NUJOL)

μ = .0015 lb sec/ ft^2 at 100°F

ρ = 55.5 lbm/ ft^3

WATER

μ = .000015 lb sec/ft^2 at 100°F

ρ = 62.4 lbm/ ft^3

AIR

μ = 3.9×10^{-7} lb sec/ ft^2 at 100°F

ρ = .075 lbm/ ft^3

APPENDIX F. Sample Calculations.

A. Example of Slug Flow:

1. Data: Q_w= .282 CFM, Q_o=.094 CFM, Q_a= 1.82 CFM,
D= .75 inches,& L=74.25 inches.

2. Void Fraction:

$$F_o = \frac{Q_o}{Q_w + Q_o} = \frac{.094}{.282+.094} = .25$$

Eq. 5.10 $$\alpha_a = \frac{Q_a}{1.28\, Q_t} = \frac{1.82}{1.28(1.82+.282+.094)} = .65$$

Eq. 5.12 $$\alpha_o = 1.037\,\alpha_f\, F_o^{1.536} = 1.037(1-.65)(.25)^{1.536}$$
$$= .04$$

Eq. 5.14 $$\alpha_w = 1-(\alpha_a+\alpha_o) = 1-(.65+.04) = .31$$

3. Pressure Loss:

$$\Delta P_\rho = \frac{gL}{g_o}(\rho_w \alpha_w + \rho_o \alpha_o + \rho_a \alpha_a)$$
$$= \frac{32.2 \times 74.25}{32.2 \times 12 \times 144}\,(55.5(.04)+62.4(.31)+.65(.075))$$
$$= .93 \text{ psi/ length}$$

From Fig.14 for F_o=.25 and $V_w = \frac{Q_w}{\alpha_f A}$ = 4.38 ft/sec

the flow regime is slug. Therefore we use the Singh-Griffith method for the friction loss.

$$Re = \frac{\bar{v}_m \rho_f D}{\mu_f} = 58,544.$$

f= .0051

$$\Delta P_f = \frac{2\, L\, f\, \rho_f \bar{v}_m \alpha_w}{g_o D} = .58 \text{ psi/ length}$$

Total Pressure Loss = 1.51 psi/length

B. Example of Froth Flow:

1. Data: Q_w= .076 CFM, Q_o= .30 CFM,& Q_a= 1.82 CFM.

2. Void Fraction:

Same as method in A-2.

$$\alpha_a = .63$$

$$\alpha_w = .10$$

$$\alpha_o = .27$$

3. Pressure Loss:

Same as method in A-3.

$$\Delta P_\rho = .91 \text{ psi/ length}$$

$$F_o = \frac{Q_o}{Q_o + Q_w} = .80$$

$$V_w = \frac{Q_w}{\alpha_f A} = 1.11 \text{ ft/sec}$$

From fig. 14 the flow regime is froth. Therefore we use the homogeneous method.

Velocity of the fluid flowing in the tube alone:

$$f_o = \frac{Q_f}{A} = 2.04 \text{ ft/sec}$$

$$Re = 9387$$

$$f = .008$$

Quality(X):

$$X = \frac{\rho_a Q_a}{\rho_a Q_a + \rho_f Q_f} = .006$$

$$\Delta P_f = \frac{2f \rho_f \tilde{v}_{fo}}{D g_o} \left[1+X \quad \frac{\rho_{fa}}{\rho_a}\right]\left[1+X \quad \frac{\mu_{fa}}{\mu_a}\right]^{-1/4}$$

ΔP_f = .41 psi/ length

C. Example of Quasi-Annular Flow:

1. Data: Q_w = .019, Q_o = .36 CFM, & Q_a = 1.82 CFM.

2. Void: Same Method as A2 except eq. 5.11 was used instead of eq. 5.10.

α_a = .46

α_w = .02

α_o = .52

3. Pressure Loss:

Same method as A-3.

ΔP_ρ = 1.30 psi/lemgth

F_o = .95

V_w = 5.16 ft/sec

From fig.14 the flow regime is the water drop in oil regime. Therefore the quasi-annular flow method is used.

From eq. D 6: ΔP_f annular $= \frac{32 L \mu_f Q_f}{A D^2 \alpha_f}$ = 2.0 psi/ L

From the Singh-Griffith Method ΔP_f = .712 psi/L

From fig. D 2 K= .6

From eq. D 7:

$$\Delta P_{f\ tot} = K\Delta P_{f\ ann} + (1-K)\Delta P_{f\ slug}$$

$$\Delta P_{f\ tot} = .6(2.0) + .4(.712) = 1.48 \text{ psi/length}$$

The total pressure loss is:

$$\Delta P_t = 1.30 + 1.48 = 2.78 \text{ psi/ length}$$

APPENDIX G: Data Listing

The following code was used to designate the various runs:

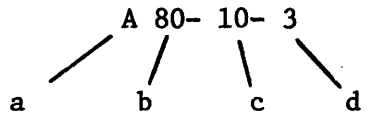

a. Test Disignation.

A. Three Phase Void Fraction Test

B. Two Phase Oil-Water Pressure Void Test

C. Three Phase Pressure and Void Test

D. Contact Angle Test

b. Introduced oil in liquid volume fraction (Fo)

c. Percent of maximum input air flow for test A and the mixture velocity for test B and C.

d. Identification number of individual run.

A. THREE PHASE VOID FRACTION DATA.

Run	Flow(CFM) Q_w	Q_o	Q_a	T	α_w	α_o	α_a	Velocity(ft/sec) $\tilde{v}_w$	$\tilde{v}_o$	$\tilde{v}_a$	$\tilde{v}_m$
A80-10-1	.134	.519	.333	92	.23	.50	.27	3.23	5.62	6.56	5.34
2	.134	.519	.333	94	.23	.52	.25	3.16	5.41	7.22	5.34
3	.134	.519	.333	94	.23	.51	.26	3.23	5.51	6.81	5.34
4	.134	.519	.309	98	.22	.52	.26	3.3	5.41	6.44	5.21
5	.134	.519	.309	98	.20	.55	.25	3.63	5.11	6.7	5.21
6	.134	.519	.309	98	.21	.53	.26	3.54	5.31	6.32	5.21
7	.1	.389	.348	87	.21	.45	.34	2.7	4.7	5.45	4.54
A80-20-1	.134	.519	.654	95	.18	.45	.38	4.15	6.39	9.28	7.11
2	.134	.519	.654	96	.18	.45	.37	4.03	6.25	9.65	7.11
3	.134	.519	.654	96	.18	.45	.37	4.03	6.25	9.65	7.11
4	.134	.519	.62	99	.16	.44	.40	4.54	6.39	8.4	6.9
5	.134	.519	.62	99	.18	.50	.32	4.13	5.62	10.34	6.9
6	.134	.589	.62	99	.18	.48	.34	4.03	5.86	9.88	6.9
7	.1	.389	.699	86	.14	.36	.50	3.8	5.9	7.5	6.44
A80-30-1	.134	.519	.983	97	.14	.45	.50	5.01	6.25	13.15	8.87
2	.134	.519	.983	98	.13	.38	.49	5.59	7.40	10.87	8.87
3	.134	.519	.983	98	.13	.32	.55	5.59	8.79	9.67	8.87
4	.134	.519	.929	100	.12	.48	.48	6.05	7.03	10.49	8.51
5	.134	.519	.929	101	.12	.38	.50	6.05	7.40	10.07	8.57
6	.134	.519	.929	101	.12	.43	.45	6.05	6.54	11.19	8.57
7	.1	.389	1.049	86	.13	.37	.50	4.3	5.7	11.3	8.33

A. THREE PHASE VOID FRACTION DATA. (Continued)

Run	Q_w	Q_o	Q_a	T	α_w	α_o	α_a	$\tilde{v}_w$	$\tilde{v}_o$	$\tilde{v}_a$	$\tilde{v}_m$
A80-40-1	.134	.519	1.312	99	.09	.35	.56	8.07	8.04	12.7	10.65
2	.134	.519	1.312	99	.10	.34	.56	7.26	8.27	12.7	10.65
3	.134	.519	1.312	99	.09	.37	.54	8.07	7.60	13.17	10.65
4	.1	.389	1.399	86	.10	.36	.54	5.5	5.8	14.1	10.23
A80-50-1	.134	.519	1.64	100	.10	.41	.49	6.92	6.94	18.14	12.43
2	.134	.519	1.64	100	.07	.34	.59	10.37	8.27	15.06	12.43
3	.134	.519	1.64	100	.07	.41	.52	10.37	6.86	17.09	12.43
4	.1	.389	1.748	85	.07	.20	.73	8.0	10.8	12.9	12.12
A80-60-1	.1	.389	2.098	84	.07	.25	.68	8.0	8.4	16.7	14.02
A80-70-1	.1	.389	2.448	84	.07	.33	.60	8.0	6.4	21.9	15.92
A80-80-1	.1	.389	2.797	83	.07	.27	.66	8.0	7.8	22.9	17.81
A80-90-1	.1	.389	3.147	82	.05	.20	.75	11.7	10.4	22.7	19.7
A80-100-1	.1	.389	3.497	81	.06	.19	.75	9.8	11.1	25.10	21.6

Run	Q_w	Q_o	Q_a	T	α_w	α_o	α_a	$\tilde{v}_w$	$\tilde{v}_o$	$\tilde{v}_a$	$\tilde{v}_m$
A75-0-1	.134	.40	0	91	.38	.62	0	1.91	3.50	0	2.89
2			0	91	.39	.61	0	1.86	3.55	0	2.89
3			0	91	.39	.61	0	1.86	3.55	0	2.89
A75-10-1			.353	93	.24	.45	.31	3.03	4.82	.617	4.81
2			.353	94	.25	.44	.31	2.90	4.93	.617	4.81
3			.353	96	.23	.46	.31	3.16	4.71	.617	4.81
A75-20-1			.707	97	.17	.37	.46	4.27	5.86	8.33	6.72
2			.707	97	.17	.45	.38	4.27	4.82	10.08	6.72
3			.707	98	.16	.38	.46	4.54	5.70	8.33	6.72
A75-30-1			1.060	100	.13	.39	.48	5.59	5.56	11.97	8.64
2			1.060	100	.15	.39	.46	4.84	5.56	12.49	8.64
3			1.049	101	.10	.35	.55	7.26	6.19	10.34	8.64
4			1.049	101	.10	.31	.59	7.26	6.99	9.63	8.64
A75-40-1			1.399	102	.09	.34	.56	8.07	6.38	13.54	10.47
2			1.399	102	.08	.29	.63	9.08	7.47	12.03	10.47
3			1.399	103	.09	.29	.62	8.07	7.47	12.23	10.47
A75-50-1			1.749	104	.08	.38	.54	9.08	5.70	17.55	12.37
2			1.749	103	.09	.33	.58	8.07	6.57	16.34	12.37
3			1.749	102	.08	.38	.54	9.08	5.70	17.55	12.37

Continued

Run	Q_w	Q_o	Q_a	T	α_w	α_o	α_a	$\tilde{v}_w$	$\tilde{v}_o$	$\tilde{v}_a$	$\tilde{v}_m$
A75-60-1			2.099	103	.08	.38	.54	9.08	5.70	21.06	14.27
2			2.099	103	.07	.36	.57	10.37	6.02	19.96	14.27
3			2.099	103	.06	.34	.60	12.10	6.38	18.96	14.27
A75-70-1			2.449	104	.05	.29	.66	14.52	7.47	20.11	16.16
2			2.449	104	.06	.31	.63	12.10	6.99	21.07	16.16
3			2.449	104	.05	.31	.64	14.52	6.99	20.74	16.16
A75-80-1			2.798	104	.05	.32	.63	14.52	6.77	24.07	18.06
2			2.798	104	.04	.25	.71	18.15	8.67	21.36	18.06
3	.134	.40	2.798	105	.04	.30	.66	18.15	7.23	22.97	18.06

Run	Q_w	Q_o	Q_a	T	α_w	α_o	α_a	$\tilde{v}_\omega$	$\tilde{v}_o$	$\tilde{v}_a$	$\tilde{v}_m$
A70-0-1	.179	.405	0	90	.43	.57	0	2.26	3.85	-	3.16
2			0	91	.43	.57	0	2.26	3.85	-	3.16
3			0	91	.43	.57	0	2.26	3.85	-	3.16
A70-10-1			.353	91	.29	.46	.25	3.34	4.77	7.65	5.08
2			.353	92	.28	.44	.28	3.46	4.99	6.83	5.08
3			.353	93	.31	.46	.23	3.13	4.77	8.32	5.08
A70-20-1			.698	94	.21	.34	.45	4.62	6.45	8.41	6.95
2			.703	94	.22	.39	.39	4.41	5.63	9.77	6.97
3			.703	94	.22	.33	.45	4.41	6.65	8.47	6.97
A70-30-1			1.055	95	.22	.33	.45	4.41	6.65	8.47	6.97
2			1.049	95	.15	.27	.58	6.47	8.13	9.79	8.84
3			1.048	96	.19	.30	.51	5.11	7.32	11.14	9.84
A70-40-1			1.406	96	.16	.30	.55	6.06	7.32	13.85	10.78
2			1.406	96	.18	.34	.48	5.39	6.45	15.87	10.78
3			1.397	96	.15	.32	.53	6.47	6.86	14.28	10.78
A70-50-1			1.746	96	.13	.27	.60	7.46	8.13	15.77	12.63
2			1.746	97	.14	.31	.55	6.93	7.08	17.20	12.63
3			1.746	97	.13	.32	.55	7.46	6.86	17.20	12.63
A70-60-1			2.095	97	.11	.29	.60	8.82	7.57	18.92	14.52
2			2.095	97	.12	.32	.56	8.08	6.86	20.27	14.52
3			2.095	97	.09	.23	.68	10.78	9.54	16.70	14.52
A70-70-1			2.444	98	.13	.27	.60	7.46	8.13	22.07	16.41
2			2.444	98	.11	.35	.55	8.82	6.27	24.08	16.41
3			2.444	98	.10	.31	.59	9.70	7.08	22.45	16.41
A70-80-1	.179	.405	2.794	98	.08	.23	.69	12.3	9.54	21.94	18.31
2			2.794	98	.08	.21	.70	12.3	10.45	21.63	18.31
3	.179	.405	2.794	99	.09	.38	.53	10.78	5.78	28.57	18.31

Run	Q_w	Q_o	Q_a	T	α_w	α_o	α_α	$\tilde{v}_w$	$\tilde{v}_o$	$\tilde{v}_a$	$\tilde{v}_m$
A64-0-1	.224	.389	0	95	.43	.57	-	2.82	3.70	-	3.32
2			0	95	.45	.55	-	2.70	3.83	-	3.32
3			0	95	.47	.53	-	2.58	3.98	-	3.32
A64-10-1			.353	97	.32	.43	.25	3.79	4.90	7.65	5.23
2			.353	97	.30	.43	.27	4.05	4.90	7.08	5.23
3			.349	97	.30	.43	.27	4.05	4.90	7.00	5.21
A64-20-1			.698	98	.26	.38	.36	4.67	5.55	10.51	7.10
2			.698	98	.24	.36	.40	5.06	5.86	9.46	7.10
3			.703	98	.23	.37	.40	5.28	5.70	9.52	7.13
A64-30-1			1.055	98	.23	.33	.44	5.28	6.39	12.99	9.04
2			1.048	98	.23	.31	.46	5.28	6.8	12.35	9.00
3			1.048	99	.23	.31	.46	5.28	6.8	12.35	9.00
A64-40-1			1.397	100	.19	.27	.54	6.39	7.81	14.02	10.89
2			1.406	100	.18	.29	.53	6.74	7.27	14.38	10.94
3			1.397	100	.21	.32	.47	5.78	6.59	16.11	10.89
A64-50-1			1.746	100	.17	.27	.56	7.14	7.81	16.9	12.78
2			1.746	100	.20	.33	.47	6.07	6.39	20.13	12.78
3			1.746	100	.21	.32	.47	5.78	6.59	20.13	12.78
A64-60-1			2.095	100	.14	.26	.60	8.67	8.11	18.92	14.67
2			2.084	101	.18	.36	.46	6.74	5.86	24.55	14.62
3			2.084	101	.14	.26	.60	8.67	8.11	18.82	14.62
A64-70-1			2.432	102	.13	.26	.61	9.34	8.11	21.6	16.5
2			2.432	102	.14	.33	.53	8.67	6.39	24.87	16.5
3			2.432	102	.13	.24	.63	9.34	8.78	20.92	16.5
A64-80-1			2.779	103	.11	.24	.65	11.04	8.78	23.17	18.38
2			2.779	103	.16	.32	.52	7.59	6.59	28.96	18.38
3	.224	.389	2.779	103	.11	.31	.58	11.04	6.80	25.96	18.38

Run	Q_w	Q_o	Q_a	T	α_w	α_o	α_a	$\tilde{v}_w$	$\tilde{v}_o$	$\tilde{v}_a$	$\tilde{v}_m$
A50-10-1	.2	.194	.349	79	.48	.16	.36	2.24	6.49	5.32	4.03
2	.2	.194	.349	79	.46	.19	.35	2.38	5.48	5.37	4.03
3	.2	.194	.349	81	.47	.17	.36	2.29	6.26	5.28	4.03
4	.267	.259	.35	83	.44	.23	.33	.33	6.1	5.8	4.75
5	.267	.259	.35	86	.42	.26	.32	3.4	5.4	5.9	4.75
A50-15-1	.267	.259	.52	86	.37	.24	.39	3.9	5.9	7.2	5.67
A50-20-1	.2	.194	.699	82	.34	.13	.53	3.16	8.21	7.15	5.92
2	.2	.194	.699	83	.36	.15	.49	3.03	7.20	7.65	5.92
3	.2	.194	.699	83	.33	.13	.54	3.31	7.85	7.03	5.92
4	.267	.259	.70	83	.33	.18	.49	4.3	7.6	7.8	6.64
5	.267	.259	.70	86	.31	.20	.49	4.7	6.9	7.7	6.64
A50-30-1	.2	.194	1.049	84	.31	.14	.55	3.52	7.51	10.34	7.82
2	.2	.194	1.044	85	.30	.13	.57	3.61	8.21	9.87	7.82
3	.2	.194	1.044	85	.29	.13	.58	3.78	8.41	9.65	7.82
4	.267	.259	1.05	82	.33	.18	.49	4.4	7.9	11.6	8.54
5	.267	.258	1.05	86	.27	.17	.56	5.3	8.2	10.3	8.54
A50-40-1	.2	.194	1.392	86	.27	.13	.60	4.01	7.85	12.68	9.68
2	.2	.194	1.392	87	.22	.11	.67	4.83	9.39	11.36	9.68
3	.2	.194	1.392	88	.26	.13	.61	4.14	8.41	12.29	9.68
4	.267	.259	1.40	82	.27	.14	.59	5.4	10.2	12.8	10.44
5	.267	.259	1.40	86	.29	.18	.52	5.0	7.8	14.2	10.44
A50-50-1	.2	.194	1.74	88	.26	.14	.60	4.18	7.51	15.69	11.56
2	.2	.194	1.74	89	.29	.16	.55	3.78	6.49	17.17	11.56
3	.2	.194	1.74	90	.26	.14	.60	4.25	7.51	15.61	11.56
4	.267	.259	1.75	81	.22	.12	.66	6.7	11.9	14.2	12.33
5	.267	.259	1.75	85	.28	.18	.54	5.2	7.8	17.6	12.33
A50-60-1	.2	.194	2.077	91	.22	.12	.66	5.04	9.14	16.80	13.39
2	.2	.194	2.077	92	.27	.15	.58	4.09	7.20	19.11	13.39
3	.2	.194	2.077	92	.21	.13	.66	5.26	8.03	16.95	13.39

Run	Q_w	Q_o	Q_a	T	α_w	α_o	α_a	$\tilde{v}_w$	$\tilde{v}_o$	$\tilde{v}_a$	$\tilde{v}_m$
A50-60-4	.267	.259	2.11	80	.24	.14	.62	5.95	10.0	18.5	14.3
5	.267	.259	2.11	85	.28	.13	.64	6.2	11.2	17.7	14.3
A50-20-1	.2	.194	2.423	42	.19	.10	.71	5.62	10.51	18.57	15.27
2	.2	.194	2.423	42	.14	.09	.76	7.74	11.68	17.21	15.27
3	.2	.194	2.423	93	.23	.13	.64	4.71	7.85	20.65	15.27
4	.267	.259	2.46	79	.19	.09	.72	7.5	15.6	18.6	16.2
5	.267	.259	2.46	85	.19	.11	.70	7.6	12.5	19.0	16.2
A50-80-1	.267	.259	2.81	79	.24	.12	.64	6.1	11.6	23.7	18.1
2	.267	.259	2.81	84	.16	.08	.76	9.1	16.7	20.0	18.1
A50-90-1	.267	.259	3.16	78	.19	.09	.72	7.5	5.1	24.0	20.0
2	.267	.259	3.16	84	.15	.08	.77	9.6	18.7	22.0	20.0
A50-100-1	.267	.259	3.51	75	.21	.13	.61	5.5	10.7	31.3	21.9
2	.267	.259	3.51	84	.22	.12	.66	6.7	12.2	28.3	21.9

B. TWO PHASE FLOW DATA

Run	Q_w CFM	Q_o	T	$\tilde{v}_m$ ft/sec	α_w	α_o	v_w ft/sec	v_o ft/sec	ΔP_T Psi	ΔP_f Psi
B0-3-1	.556	0	80	3	1.0	0	3.0	-	2.84	.16
2	.556	0	80	3	1.0	0	3.0	-	2.85	.17
3	.556	0	80	3	1.0	0	3.0	-	2.84	.16
B0-2-1	.368	0	80	2	1.0	0	2.0	-	2.77	.09
2	.368	0	80	2	1.0	0	2.0	-	2.77	.09
3	.368	0	80	2	1.0	0	2.0	-	2.77	.09
B25-3-1	.412	.130	84	3	.91	.09	2.46	7.85	2.78	.12
2	.412	.130	82	3	.93	.07	2.41	10.09	2.75	.09
3	.412	.130	84	3	.93	.07	2.3	10.09	2.77	.10
B25-2-1	.278	.092	88	2	.90	.10	1.68	5.0	2.69	.04
2	.278	.092	80	2	.92	.07	1.62	7.14	2.70	.04
3	.278	.092	80	2	.93	.07	1.62	7.14	2.70	.04
B50-3-1	.278	.276	85	3	.66	.34	2.29	4.41	2.69	.11
2	.278	.276	85	3	.66	.34	2.29	4.41	2.69	.11
3	.278	.276	85	2	.65	.35	2.32	4.28	2.69	.11
B50-2-1	.184	.184	87	2	.71	.29	1.41	3.45	2.62	.03
2	.184	.184	83	2	.72	.28	1.39	2.57	2.62	.03
3	.184	.184	88	2	.72	.28	1.39	3.57	2.64	.03
B75-2-1	.134	.415	85	3	.38	.62	1.92	3.68	2.61	.11
2	.134	.415	82	3	.37	.62	1.97	2.58	2.60	.10
3	.134	.415	86	3	.37	.63	1.97	2.58	2.62	.12
B75-2-1	.092	.276	87	2	.45	.55	1.11	2.73	2.53	.01
2	.092	.276	84	2	.48	.52	1.04	2.88	2.53	.001
3	.092	.276	86	2	.43	.57	1.16	2.63	2.53	.02
B80-3-1	.11	.44	80	3	.32	.68	1.87	3.53	2.55	.06
2	.11	.44	80	3	.31	.69	1.93	3.48	2.63	.15

B. TWO PHASE FLOW DATA (Continued)

Run	Q_w CFM	Q_o	T	v_m	α_w	α_o	v_w ft/sec	v_o ft/sec	ΔP_T Psi	ΔP_f Psi
B80-2-1	.07	.29	84	2	.35	.65	1.14	2.46	2.48	-.07
2	.07	.29	85	2	.35	.64	1.11	2.50	2.49	-.01
B80-1-1	.04	.15	82	1	.34	.66	.59	1.22	2.52	.03
2	.04	.15	85	1	.47	.53	.43	1.52	2.50	-.02
B85-3-1	.08	.47	91	3	.06	.94	7.05	2.71	4.07	1.67
2	.08	.47	90	3	.05	.95	9.0	2.68	4.13	1.72
B85-2-1	.06	.31	88	2	.20	.80	1.51	2.12	2.50	.06
2	.06	.31	90	2	.27	.73	1.21	2.33	2.47	-.001
B85-1-1	.03	.16	87	1	.32	.68	.47	1.25	2.59	.11
2	.03	.16	90	1	.43	.57	.35	1.50	2.48	-.03
B90-3-1	.06	.50	93	3	.05	.95	6.0	2.84	3.91	1.51
2	.06	.50	92	3	.04	.96	7.5	2.81	3.93	1.53
B90-2-1	.04	.33	91	2	.05	.95	3.31	1.91	3.30	.90
2	.04	.33	90	2	.06	.94	3.99	1.89	3.35	.95
B90-1-1	.02	.17	92	1	.11	.89	.90	1.01	2.56	.34
2	.02	.17	90	1	.10	.90	.99	1.0	2.56	.33
B95-3-1	.03	.52	83	3	.03	.97	5.03	2.93	4.18	1.79
2	.03	.52	93	3	.03	.97	5.03	2.93	3.98	1.59
B95-2-1	.02	.35	83	2	.04	.96	2.55	1.98	3.50	1.1
2	.02	.35	93	2	.06	.94	1.70	2.02	3.40	1.0
B95-1-1	.01	.18	82	1	.09	.91	.57	1.04	2.77	.36
2	.01	.18	93	1	.05	.95	1.02	1.00	2.81	.41
B100-3-1	0	.552	80	3	0	1.0	0	3.0	4.34	1.95
2	0	.552	80	3	0	1.0	0	3.0	4.31	1.92

B. TWO PHASE FLOW DATA (Continued)

Run	Q_w	CFM	Q_o	T	$\tilde{v}_m$	α_w	α_o	$\tilde{v}_w$ (ft/sec)	v_o (ft/sec)	AP_T (Psi)	ΔP_f (Psi)
B100-3-3	0		.552	80	3	0	1.0	0	3.0	4.34	1.96
B100-2-1	0		.368	80	2	0	1.0	0	2.0	3.55	1.16
2	0		.368	80	2	0	1.0	0	2.0	3.55	1.16
3	0		.368	80	2	0	1.0	0	2.0	3.57	1.18

C. THREE PHASE PRESSURE LOSS AND VOID TEST

Run	Q_w	Q_o	Q_a	ΔP_T	ΔP_f	T	α_w	α_o	α_a	$\tilde{v}_w$	$\tilde{v}_o$	$\tilde{v}_a$
C0-4-1	.376	0	.364	1.825	-.04	70	.66	0	.34	3.07	-	5.92
2	.376	0		1.678	.008	71	.62	0	.38	3.28	-	5.24
3	.376	0		1.678	.008	71	.62	0	.38	3.28	-	5.24
4	.376	0		1.794	.156	64	.61	0	.39	3.34	-	5.08
C25-4-1	.282	.094		1.57	-.14	69	.51	.08	.36	2.69	6.81	5.57
2	.282	.094		1.57	-	86	.50	.10	.40	3.09	4.96	4.92
3	.282	.094		1.40	-.19	93	.50	.11	.39	3.08	4.82	4.99
4	.282	.099		1.609	.068	64	.53	.05	.42	2.87	10.86	4.71
C50-4-1	.188	.188		1.51	-.05	70	.44	.17	.39	2.34	6.19	4.96
2	.188	.188		1.60	.08	84	.37	.22	.41	2.78	4.56	4.85
3	.188	.188		1.40	-.18	91	.38	.23	.38	2.67	4.36	5.16
4	.188	.188		1.516	.015	66	.41	.17	.42	2.52	5.87	4.70
C75-4-1	.094	.282		.54	-1.04	72	.28	.35	.37	1.82	4.43	5.29
2	.094	.282		1.51	-	80	.22	.41	.37	2.31	3.75	5.33
3	.094	.282		1.45	-.18	88	.22	.43	.35	2.28	3.56	5.71
4	.094	.282		1.424	-.118	66	.24	.38	.38	2.15	4.03	5.16
C80-4-1	.076	.300		.45	-.94	74	.17	.39	.44	2.37	4.22	4.49
2	.076	.300		1.53	.13	78	.16	.41	.43	2.65	3.96	4.57
3	.076	.300		1.55	.11	87	.15	.44	.41	2.75	3.74	4.78
4	.076	.300		1.365	.025	67	.16	.38	.46	2.55	4.29	4.32
C85-4-1	.056	.32		.52	-.86	76	.13	.44	.43	2.43	3.99	4.50
2	.056	.32		1.36	.09	76	.11	.39	.50	2.87	4.47	3.92
3	.056	.32		1.36	-.14	86	.11	.50	.4	2.72	3.46	5.12
4	.056	.32		1.351	-.04	68	.13	.44	.43	2.32	3.99	4.57
C90-4-1	.038	.34		.39	-.92	78	.09	.45	.46	2.37	4.09	4.29
2	.038	.34		1.16	-.1	75	.07	.45	.48	2.99	4.09	4.13
3	.038	.34		1.213	-.04	86	.08	.55	.37	2.75	3.35	5.29
4	.038	.34		1.213	-.04	70	.08	.44	.48	2.75	4.18	4.09

C. THREE PHASE PRESSURE LOSS AND VOID TEST (Continued)

Run	Q_w	Q_o	Q_a	ΔP_T	ΔP_f	T	α_w	α_o	α_a	$\tilde{v}_w$	$\tilde{v}_o$	$\tilde{v}_a$
C95-4-1	.019	.36		1.43	-.35	99	.03	.72	.25	4.13	2.73	7.66
2	.019	.36		1.93	.31	75	.04	.63	.33	2.35	3.11	6.05
3	.019	.36		2.11	.45	86	.03	.67	.30	4.13	2.92	6.48
4	.019	.36		1.529	.175	71	.04	.53	.43	2.79	3.72	4.52
C100-4-1	0	.376		2.622	.48	70	0	.75	.25	-	2.71	8.04
2	0	.376		2.475	.69	70	0	.75	.25	-	2.73	7.85
3	0	.376		2.475	.69	71	0	.75	.25	-	2.73	7.85
4	0	.376	.364	2.626	.83	71	0	.75	.25	-	2.71	8.04

Run	Q_w	Q_o	Q_a	ΔP_T	ΔP_f	T	α_w	α_o	α_a	$\tilde{v}_w$	$\tilde{v}_o$	$\tilde{v}_a$
C0-8-1	.376	0	1.092	1.509	.389	64	.42	0	.58	4.90	-	10.17
2	.376	0		1.455	.235	73	.46	0	.54	4.49	-	10.88
3	.376	0		1.476	.416	80	.40	0	.60	5.17	-	9.80
C25-8-1	.282	.094		.785	-.32	64	.41	.04	.55	3.78	13.8	10.63
2	.282	.094		1.176	.026	73	.37	.06	.56	4.10	8.24	10.52
3	.282	.094		1.194	.254	80	.31	.05	.64	5.02	9.63	9.24
C50-8-1	.188	.188		.025	-.665	66	.25	.09	.66	4.60	10.98	9.01
2	.188	.188		1.244	.114	74	.29	.15	.56	3.52	16.99	10.52
3	.188	.188		1.353	.173	80	.29	.17	.54	3.52	5.97	11.07
C75-8-1	.094	.282		.107	-.813	68	.17	.20	.63	3.04	7.70	9.37
2	.094	.282		1.261	.111	75	.18	.28	.54	2.82	5.47	11.01
3	.094	.282		1.426	.196	80	.17	.32	.51	2.93	4.77	11.75
C80-8-1	.076	.300		.094	-1.086	70	.16	.31	.53	2.55	5.22	11.28
2	.076	.300		1.257	.197	77	.13	.30	.57	3.23	5.40	10.41
3	.076	.300		1.273	.413	82	.09	.26	.65	4.75	5.43	9.11
C85-8-1	.056	.32		-.18	-1.24	70	.10	.33	.57	3.04	5.27	10.41
2	.056	.32		.915	.085	78	.06	.28	.66	4.91	6.21	9.01
3	.056	.32		1.108	.068	83	.05	.38	.57	5.74	4.61	10.41
C90-8-1	.038	.34		-.195	-1.135	71	.06	.33	.61	3.69	5.60	9.68
2	.038	.34		1.115	-.145	78	.04	.48	.48	4.69	3.87	12.38
3	.038	.34		1.274	.144	83	.04	.42	.53	4.69	4.36	11.15
C95-8-1	.019	.36		1.121	-.049	72	.1	.48	.51	8.60	4.10	11.61
2	.019	.36		2.663	1.423	79	.1	.51	.48	8.60	3.87	12.28
3	.019	.36		2.535	1.215	83	.1	.54	.45	8.60	3.61	13.30
C100-8-1	0	.376		1.962	.502	72	0	.61	.39	-	3.35	15.21
2	0	.376		3.187	1.657	79	0	.64	.36	-	3.18	16.57
3	0	.376	1.092	2.983	1.543	84	0	.60	.40	-	3.38	14.98

(Continued)

Run	Q_w	Q_o	Q_a	ΔP_T	ΔP_f	T	α_w	α_o	α_a	$\tilde{v}_w$	$\tilde{v}_o$	$\tilde{v}_a$
C0-16-1	.376	0	2.548	1.544	.968	85	.22	0	.78	9.50	0	17.63
2	.376	0		1.534	.850	88	.26	0	.74	8.01	0	18.58
3	.376	0		1.536	.794	.76	.28	0	.72	7.37	0	19.14
C25-16-1	.282	.094		1.405	.738	85	.22	.03	.75	6.84	18.24	18.50
2	.282	.094		1.440	.802	88	.20	.04	.76	7.70	11.60	18.28
3	.882	.094		1.313	.825	76	.20	.03	.77	7.70	20.4	17.84
C50-16-1	.188	.188		1.404	.597	85	.19	.12	.69	5.29	8.37	20.21
2	.188	.188		1.494	.727	88	.18	.12	.70	5.64	8.65	19.74
	.188	.188		1.28	.709	76	.17	.11	.72	5.97	9.63	19.14
C75-16-1	.094	.282		1.747	.774	85	.10	.30	.60	5.11	5.18	22.92
2	.094	.282		1.794	.775	88	.13	.29	.58	4.08	7.44	19.94
3	.094	.282		1.5	.892	77	.10	.21	.69	5.11	7.44	19.94
C80-16-1	.076	.30		1.281	1544	87	.08	.22	.70	5.10	7.48	19.74
2	.076	.30		1.391	.482	90	.05	.32	.63	7.79	5.08	22.11
3	.076	.30		1.61	1.01	78	.07	.23	.70	5.73	6.96	19.94
C85-16-1	.056	.32		1.356	.421	88	.04	.34	.62	6.91	5.07	22.58
2	.056	.32		1.518	.824	90	.04	.25	.71	7.60	7.07	19.38
3	.056	.32		1.316	.71	80	.04	.27	.69	8.22	6.34	20.09
C90-16-1	.038	.34		1.647	.658	88	.03	.39	.59	8.26	4.78	23.50
2	.038	.34		2.035	1.274	80	.03	.39	.58	8.26	4.70	23.78
3	.038	.34		1.72	1.12	80	.03	.29	.68	8.26	6.44	20.12
C95-16-1	.019	.36		2.828	1.769	88	.01	.43	.56	8.60	4.54	24.80
2	.019	.36		3.047	1.809	90	.01	.51	.48	8.60	3.87	28.66
3	.019	.36		2.783	1.636	80	.01	.59	.40	8.60	3.34	34.43
C100-16-1	0	.376		3.031	1.223	88	-	.55	.45	-	3.73	30.62
2	0	.376		3.201	2.062	90	-	.48	.52	-	4.28	26.46
3	0	.376	2.548	3.306	2.231	80	-	.56	.44	-	3.64	31.53

(Continued)

Run	Q_w	Q_o	Q_a	ΔP_T	ΔP_f	T	α_w	α_o	α_a	$\tilde{v}_w$	$\tilde{v}_o$	$\tilde{v}_a$
C0-12-1	.376	0	1.82	1.470	.768	73	.26	0	.74	7.8	-	13.4
2	.376	0		1.379	.677	74	.26	0	.74	7.8	-	13.4
3	.376	0		1.430	.428	84	.37	0	.63	5.46	-	15.79
C25-12-1	.282	.094		1.352	.395	74	.32	.04	.64	4.73	13.8	15.47
2	.282	.094		1.411	.543	75	.32	.03	.65	4.73	16.47	15.33
3	.282	.094		1.403	.588	84	.25	.06	.69	6.15	8.24	14.35
C50-12-1	.188	.188		1.449	.455	75	.27	.11	.62	3.73	9.37	16.02
2	.188	.188		1.499	.451	76	.27	.13	.60	3.73	7.80	16.62
3	.188	.188		1.465	.409	84	.26	.16	.58	4.00	6.55	16.78
C75-12-1	.094	.282		1.522	.471	78	.19	.23	.58	2.73	6.63	16.99
2	.094	.282		1.208	.598	76	.19	.26	.56	2.73	6.01	17.72
3	.094	.282		1.618	.522	85	.14	.30	.56	3.65	5.87	17.72
C80-12-1	.076	.30		1.484	.718	80	.08	.23	.69	5.10	7.05	14.37
2	.076	.30		1.630	.609	78	.08	.37	.55	5.10	4.39	18.38
3	.076	.30		1.276	.335	85	.12	.26	.62	3.50	6.22	15.95
C85-12-1	.056	.32		1.137	.502	81	.04	.22	.74	8.22	7.76	13.38
2	.056	.32		1.200	.441	80	.04	.27	.69	8.22	6.34	14.35
3	.056	.32		1.302	.281	86	.04	.39	.57	8.22	4.50	17.13
C90-12-1	.038	.34		1.392	.722	82	.03	.22	.75	8.26	8.25	13.62
2	.038	.34		1.332	.539	80	.03	.28	.69	8.26	6.67	14.67
3	.038	.34		1.639	.607	86	.03	.38	.59	8.26	4.86	17.28
C95-12-1	.019	.36		2.572	1.238	82	.01	.54	.45	8.60	3.61	22.17
2	.019	.36		2.645	1.254	81	.01	.56	.43	8.60	3.49	23.15
3	.019	.36		2.745	1.466	86	.01	.52	.47	8.60	3.74	21.26
C100-12-1	0	.376		3.040	1.820	82	0	.51	.49	-	4.00	20.22
2	0	.376		3.161	1.869	81	0	.54	.46	-	3.77	21.59
3	0	.376	1.82	3.089	1.810	86	0	.54	.46	-	3.81	21.30

(Continued)

Run	Q_w	Q_o	Q_a	ΔP_T	ΔP_f	T	α_w	α_o	α_a	$\tilde{v}_w$	$\tilde{v}_o$	$\tilde{v}_a$
C0-20-1	.376	0	3.276	1.654	1.000	74	.23	0	.77	8.73	-	23.23
2	.376	0		1.166	.590	72	.22	0	.78	9.50	-	22.67
3	.376	0		1.682	1.149	78	.20	0	.80	10.26	-	22.22
C25-20-1	.282	.094		1.437	.577	74	.29	.03	.88	5.23	16.47	26.32
2	.282	.094		1.514	.731	73	.26	.03	.71	5.85	15.02	25.28
3	.282	.094		1.408	.682	78	.24	.03	.73	6.30	16.47	24.51
C50-20-1	.188	.188		1.365	.601	75	.20	.10	.70	5.13	10.53	25.28
2	.188	.188		1.488	.638	74	.21	.12	.67	4.82	8.65	26.56
3	.188	.188		1.546	1.050	78	.12	.07	.81	8.44	13.99	22.05
C75-20-1	.094	.282		1.494	.843	76	.09	.17	.74	5.49	9.12	24.08
2	.094	.282		1.663	1.020	76	.11	.15	.74	4.82	10.21	23.92
3	.094	.282		1.763	1.063	80	.09	.20	.71	5.87	7.82	24.82
C80-20-1	.076	.30		1.437	.585	76	.09	.26	.65	4.75	6.29	27.21
2	.076	.30		1.454	.583	77	.08	.27	.65	5.10	5.95	27.59
3	.076	.30		1.543	.763	80	.08	.24	.68	5.50	6.71	26.09
C80-20-1	.076	.30		1.437	.585	76	.09	.26	.65	4.75	6.29	27.21
2	.076	.30		1.454	.583	77	.08	.27	.65	5.10	5.95	27.59
3	.076	.30		1.543	.763	80	.08	.24	.68	5.50	6.71	26.09
C85-20-1	.056	.32		1.189	.642	78	.04	.18	.78	7.60	9.45	22.93
2	.056	.32		1.412	.204	78	.05	.24	.71	5.74	7.33	25.06
3	.056	.32		1.510	.900	82	.04	.23	.73	6.91	7.52	24.55
C90-20-1	.038	.34		1.691	.697	78	.03	.39	.58	8.26	4.75	30.37
2	.038	.34		2.058	1.171	78	.04	.33	.63	5.58	5.60	28.11
3	.038	.34		2.134	1.279	82	.03	.33	.64	8.26	5.60	27.59
C95-20-1	.019	.36		3.108	2.095	79	.01	.41	.58	8.60	4.76	30.84
2	.019	.36		3.430	2.237	78	.01	.49	.50	8.60	4.02	35.45
3	.019	.36		3.283	1.885	82	.01	.51	.42	8.60	3.41	42.88

(Continued)

Run	Q_w	Q_o	Q_a	ΔP_T	ΔP_f	T	α_w	α_o	α_a	$\tilde{v}_w$	$\tilde{v}_o$	$\tilde{v}_a$
C100-20-1	0	.376	3.276	3.324	2.126	79	0	.50	.50	0	4.07	35.73
2	0	.376		3.527	2.281	79	0	.52	.48	0	3.91	37.31
3	0	.376	3.276	3.595	2.408	82	0	.50	.50	0	4.10	35.45